2014

A Novel Microgrid Demand-Side Management System for Manufacturing Facilities

Terance J. Harper
Purdue University, harper18@purdue.edu

William J. Hutzel
Purdue University, hutzelw@purdue.edu

James C. Foreman
Purdue University, foremanj@purdue.edu

Aaron L. Adams
Alabama A & M University, aaron.adams@aamu.edu

Athula Kulatunga
Purdue University, nkulatun@purdue.edu

A NOVEL MICROGRID DEMAND-SIDE MANAGEMENT SYSTEM FOR MANUFACTURING FACILITIES

A Thesis

Submitted to the Faculty

of

Purdue University

by

Terance J. Harper

In Partial Fulfillment of the

Requirements for the Degree

of

Master of Science

August 2014

Purdue University

West Lafayette, Indiana

To my parents, brother, family, and friends— thank you for supporting and keeping me on a straight path down my academic & professional road.

TABLE OF CONTENTS

Page

Page

Page

Page

LIST OF TABLES

Table Page

LIST OF FIGURES

Figure Page

Figure Page

Figure Page

ABSTRACT

Harper, Terance J. M.S., Purdue University, August 2014. Microgrids for Improving Manufacturing Energy Efficiency. Major Professor: William J. Hutzel

Thirty-one percent of annual energy consumption in the United States occurs within the industrial sector, where manufacturing processes account for the largest amount of energy consumption and carbon emissions. For this reason, energy efficiency in manufacturing facilities is increasingly important for reducing operating costs and improving profits. Using microgrids to generate local sustainable power should reduce energy consumption from the main utility grid along with energy costs and carbon emissions. Also, microgrids have the potential to serve as reliable energy generators in international locations where the utility grid is often unstable.

For this research, a manufacturing process that had approximately 20 kW of peak demand was matched with a solar photovoltaic array that had a peak output of approximately 3 KW. An innovative Demand-Side Management (DSM) strategy was developed to manage the process loads as part of this smart microgrid system. The DSM algorithm managed the intermittent nature of the microgrid and the instantaneous demand of the manufacturing process. The control algorithm required three input signals; one from the microgrid indicating the availability of renewable energy, another from the manufacturing process indicating energy use as a percent of peak production, and historical data for renewable sources and facility demand. Based on these inputs the algorithm had three modes of operation: normal (business as usual), curtailment (shutting off non-critical loads), and energy storage.

The results show that a real-time management of a manufacturing process with a microgrid will reduce electrical consumption and peak demand. The renewable energy system for this research was rated to provide up to 13% of the total manufacturing capacity. With actively managing the process loads with the DSM program alone, electrical consumption from the utility grid was reduced by 17% on average. An additional 24% reduction was accomplished when the microgrid and DSM program was enabled together, resulting in a total reduction of 37%. On average, peak demand was reduced by 6%, but due to the intermittency of the renewable source and the billing structure for peak demand, only a 1% reduction was obtained. During a billing period, it only takes one day when solar irradiance is poor to affect the demand reduction capabilities. To achieve further demand reduction, energy storage should be introduced and integrated.

CHAPTER 1. INTRODUCTION

This chapter is an overview of research that was conducted for the Purdue Center for Technology Development (CTD) by the Applied Energy Laboratory (AEL) in the Department of Mechanical Engineering Technology (MET) at Purdue University. The research focused on the implementation and evaluation of a microgrid for manufacturing facilities to improve energy efficiency and reliability. This chapter establishes the relevance of the project and describes the research objective. Finally, this chapter contains a list of keywords, design parameters, and experimental processes that were essential for data acquisition.

1.1 Scope

The manufacturing industry, through multiple manufacturing processes, consumes large amounts of energy annually. During a regular workday, any one manufacturing facility will consume energy at a significantly higher rate than average energy supplied to residential and commercial office spaces. In the United States, thirty-one percent of annual energy consumption is from the industrial sector. Within the industrial sector, manufacturing processes accounts for the largest amount of energy consumption. As one example, Figure 1.1 shows the percentage breakdown of energy consumption within a metal manufacturing facility in the U.S.

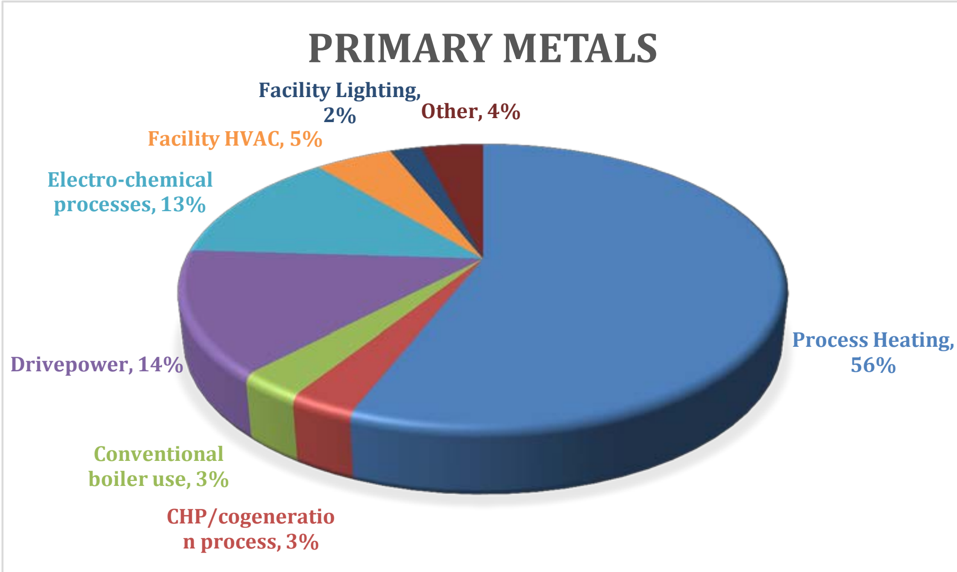

Figure 1.1 Percentage Breakdown of Energy Consumption for Metal Manufacturers (“Managing Energy Costs in Manufacturing Facilities esource.com,” 2012)

It is not surprising that this chart shows that the heating process accounts for more than half of the consumption of a typical metal manufacturing facility. This immense amount of consumption can contribute to peak demand or peak load on national and local utility companies. Due to this peak demand, utility companies charge manufacturers an extra surcharge based on their highest level of energy usage monthly. Subsequently, manufacturers are charged their regular rate plus the surcharge, which increases the overall utility cost.

Through a partnership with Purdue University’s CTD, manufacturers are investigating ways to deploy microgrid technology to improve energy utilization through load management to potentially reduce electrical consumption and peak demand. By obtaining data from corporate manufacturers about their energy consumption, experimental processes were developed to begin to understand and address the problem.

For this research, a microgrid system and Demand-Side Management (DSM) program was developed and investigated as an innovative load management strategy to demonstrate energy cost savings. Microgrids generate electricity from multiple renewable energy generators and/or conventional energy generators. Solar Photovoltaic (PV) energy systems were chosen as the renewable component for offsetting the peak demand (load). By providing another power source outside of the local utility, opportunities for reducing utility electrical consumption were achieved. A solar PV energy system was selected due to the ease of installation, ease of monitoring, ability to generate local electricity, and overall eco-friendliness for a sustainable future.

1.2 Significance

The manufacturing process is the core of many manufacturing enterprises (Zhou, 2011, p. 316), "in which operations such as machining, inspection, transportation, and assembly consume large amounts of energy." For this reason, energy efficiency in manufacturing facilities is increasingly important for reducing operating costs and improving profits. According to Zhou (2011), "the energy consumption level in manufacturing is higher than that of other commercial enterprises, and the potential for energy savings is large" (p.316). Energy consumption and pollutants in these sectors also account for 60-80% of all mechanical industries (Shan, Qin, Liu, & Liu, 2012, p. 1095).

With the rise in electrical energy costs, an awareness of high-energy consumption at manufacturing facilities is important to offset time-of-day and tariff rates. Peak demand surcharges billed by utility companies are a significant part of a typical manufacturer's total electric bill. "To investigate and correct peak demand, DSM was developed and practiced by industries to become more energy efficient" (York, Kushler, & Witte, 2007, p.1). York *et al.* (2007) states that the "very premise of DSM is that there are benefits to both utilities and their customers to change energy use patterns, whether by shifting demand to different periods, reducing demand at specific times, or reducing overall energy use through energy-efficient technologies" (p.1). This is where integrating microgrids to the energy plan of a manufacturing plant has potential, due to" utility system peak loads coinciding with long, hot sunny days during the summer when high solar insolation is also available for a solar PV energy system associated with a microgrid" (Byrne, Hegedus, & Wang, 1994, p.235).

"PV cells are a viable energy technology as they allow consumers of all sizes to produce carbon and emission-free energy from the sun" (Schleicher-Tappeser, 2012, p.65). Currently in the United States," commercial solar energy technologies represents one third of the total installed capacity for solar PV and it has grown faster as the price has fallen more rapidly than for residential solar" (Farrell, 2012, p.1). Figure 1.2 shows the decline of installed PV solar prices ($\$/W_{DC}$) for residential and commercial installs from 1998 to 2012, in the United States. The y-axis is the dollar amount ($) per watt DC ($W_{DC}$) and the x-axis is the years. The data was split into three system size group, ≤ 10 kW, 10-100 kW, and > 100 kW. From this graph, it is evident that for the residential & commercial sector, there is, on average, a steady decline in installed costs annually. Barbose, Darghouth, Weaver, & Wiser, (2013) stated that "from 2011 to 2012, installed prices fell by $0.9/W (14%) for systems ≤10 kW, $0.8/W (13%) for systems 10-100 kW, and $0.3/W (6%) for systems >100 kW" (p.2).

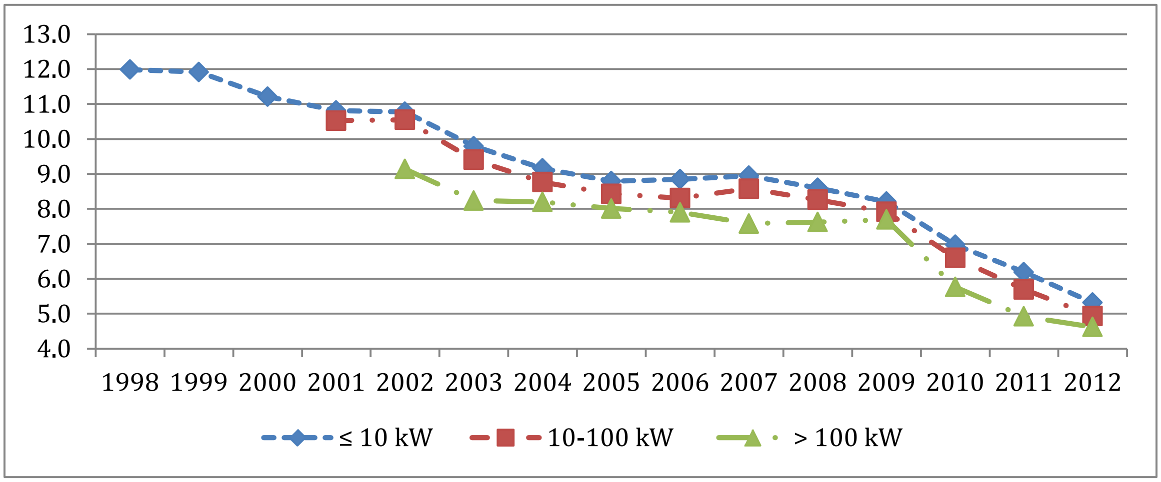

Figure 1.2 Declining Prices of Installed PV Solar Systems (Barbose et al., 2013)

Table 1.1 shows a more concise representation of the projected future decline in the price to purchase and install solar PV (Hall, 2013). As seen in Table 1.1, it is projected that commercial distributed PV energy systems will decline by $1.80 per watt, which will decrease overall installation cost. With projected decline in installation cost, solar PV energy systems will become more economically viable against cheaper conventional energy generators. According to Singh & Alapatt, 2012, “both grid-tied and stand-alone PV energy systems have the distinct advantages of economic predictability, low maintenance and downtime expenses, zero refueling costs, and fast construction time” (p.53).

Recently, governmental agencies and congress have begun focusing global economic and industry policies on renewable energies (Schleicher-Tappeser, 2012). With growing awareness of cleaner alternatives to fossil fueled power generation plants, renewable energy systems are becoming more attractive and sustainable for the future of companies. In 2010, “energy consumed globally was 16.8 Terawatts, and is expected to grow to 28 Terawatts by 2050, the solar energy received on earth per year is 23,000 Terawatts" (Singh & Alapatt, 2012, p.54). Based on this difference, there is potential to significantly increase utilization of the sun's energy. Therefore, "offsetting energy consumption with "green power" has advantages for manufacturers, not only in terms of reduced operating costs, but also in terms of the positive corporate image resulting from actively engaging in sustainable business practices" (Lunt & Levers, 2011, p.1).

Table 1.1 Projected 2020 Solar Prices of Department of Energy SunShot Initiative by (Hall, 2013)

Projected 2020 Solar Prices (2010$/W)		
Market	Benchmark 2010 Price ($/W)	Reference 2020 Price ($/$W_{DC}$)
Utility-Scale PV	3.40	2.51
Commercial distributed PV	5.15	3.36
Residential distributed PV	6.5	3.78

Robert Dohn (2011) from Siemens states "that end users who place a high value on continuous access to reliable, secure power and want a high level of control over their energy supply and demand should look closely at a microgrid solution and its potential to secure energy independence" (p.9). Current implementers of solar PV energy systems are able to estimate the contribution of solar energy to their overall energy consumption "by comparing average energy use from pre-installation data to post-installation data" (York et al., 2007, p.9).

1.3 Statement of Purpose

Microgrids are not widely deployed in manufacturing facilities at this time. This project investigates the potential for using microgrids to improve energy utilization by reducing utility electrical consumption and peak through DSM. In addition to shaving peak demand, microgrids have the potential to serve as reliable energy generators in unstable grid conditions. Therefore, using microgrids to generate renewable energy for manufacturing facilities has both domestic and foreign implications, and should be appealing to many industries.

1.4 Research Questions

The following is the research question for this project:

1. Can a microgrid, along with an optimal active demand-side control strategy, create opportunities for reducing electrical consumption and peak demand from the utility grid at manufacturing facilities?

1.5 Assumptions

The following are assumptions that are inherent to the pursuit of this study:

1. The microgrid test bed was built from a 3 kW photovoltaic array that is already operational on the roof of the Knoy Hall of Technology.

2. The PV arrays and process loads were monitored and controlled by a web-based direct digital control platform.
3. Phase 1 microgrid does not have energy storage capabilities.
4. Phase 1 microgrid does not have islanding capabilities.

1.6 Limitations

The following are factors that are not controllable in pursuit of this study:

1. The weather patterns of Northern Indiana cannot be controlled.
2. The amount of sunlight in a standard day varied with the transition of seasons (spring, summer, fall, winter).
3. The research is limited to the Applied Energy Laboratory in Knoy Hall.

1.7 Delimitations

The following are factors that are controllable in pursuit of this study:

1. A laboratory scale process heating and cooling system simulated the electric loads at a manufacturing facility.
2. Energy storage was not investigated in this study.
3. Real-time utility data was not investigated in this study.
4. Control modes were operated between 9:00a.m. and 5:00p.m. to replicate a single shift at manufacturing facilities.

1.8 Definition of Key Terms

Demand (utility)—"the rate or level at which electricity or natural gas is delivered to users at a given point in time. Electric demand is expressed in kilowatts (kW). Demand should not be confused with load, which is the amount of power delivered or required at any specified point or points on a system" (York et al., 2007, p.39).

Demand-side management (DSM)—"the methods used to manage energy demand including energy efficiency, load management, fuel substitution, and load building" (York et al., 2007, p.39).

Energy savings—"the reduction in use of energy from the pre-retrofit baseline to the post- retrofit energy use, once independent variables (such as weather or occupancy) have been accounted for. For new construction, energy savings are usually calculated by comparing a "baseline" design with an alternative building plan" (York et al., 2007, p.39).

Load—"the amount of electric power supplied to meet one or more end-user's needs. The amount of electric power delivered or required at any specified point or points on a system" (York et al., 2007, p.40).

Load diversity—"the condition that exists when the peak demands of a variety of electric customers occur at different times. The difference between the peak of coincident and non- coincident demands of two or more individual loads" (York et al., 2007, p.40).

Load factor—“the ratio of the amount of electricity a consumer used during a given time span and the amount that would have been used if the usage had stayed at the consumer’s highest demand level during the whole time. Also used as the ratio of the average load to peak load during a specified time interval” (York et al., 2007, p.40).

Load impact—“changes in electric energy use or electric peak demand” (York et al., 2007, p.40).

Load management—“steps taken to reduce power demand at peak load times or to shift some power demand to off-peak times to better meet the utility system capability for a given hour, day, week, season, or year” (York et al., 2007, p.40).

Load shape—“the time-of-use pattern of customer or equipment energy use. Typically used patterns are over a day (24 hours) or an entire year (8,760 hours)” (York et al., 2007, p.40).

Load shape impacts—“changes in load shape induced by a program” (York et al., 2007, p.40).

Metered data—“data collected at customer premises over time through a meter for a specific end-use or energy-using system (e.g., lighting and HVAC) or location (e.g., floors of a building or a whole premise). Metered data may be collected over a variety of time intervals” (York et al., 2007, p.40).

Metering—"the collection of energy consumption data over time at customer premises through the use of meters. These meters may collect information about kWh, kW, or thermos with respect to an end-use, a circuit, a piece of equipment, or a whole building (or facility). End- use metering refers specifically to separate data collection for one or more end-uses in a building, such as lighting, air conditioning, or refrigeration. What is called "spot metering" is not metering in this sense, but is an instantaneous measurement (rather than over time) of volts, amps, watts, or power factor to determine equipment size and/or power draw" (York et al., 2007, p.40).

Model—"a mathematical representation or calculation procedure that is used to predict the energy use and demand in a building or facility or to estimate efficiency program savings estimates. Models may be based on equations that specifically represent the physical processes or may be the result of statistical analysis of energy use data" (York et al., 2007, p.41).

Monitoring (equipment or system)—"gathering of relevant measurement data over time to evaluate equipment or system performance, e.g., chiller electric demand, inlet evaporator temperature and flow, outlet evaporator temperature, condenser inlet temperature, and ambient dry-bulb temperature and relative humidity or wet-bulb temperature, for use in developing a chiller performance map (e.g., kW/ton vs. cooling load and vs. condenser water temperature)" (York et al., 2007, p.41).

Peak demand—"the maximum level of metered demand during a specified period, such as a billing month or during a specified peak demand period" (York et al., 2007).

Peak demand period—"Example: Noon to 7 p.m. Monday through Friday, June, July, August and September" (York et al., 2007, p.41).

Peak load—"the highest electrical demand within a particular period. Daily electric peaks on weekdays occur in late afternoon and early evening. Annual peaks occur on hot summer days" (York et al., 2007, p.41).

1.9 Summary

Although the hardware for microgrids is well understood, there are significant opportunities for innovation to develop new technologies and methods to improve the current technology. As clean energy technologies continue to grow, it is important to introduce the possibilities of utilizing these systems for manufacturing facilities. This research developed a comprehensive strategy that accounted for both supply side and demand side in order to achieve energy reduction and cost savings.

CHAPTER 2. REVIEW OF LITERATURE

2.1 Sustainable Practices in Manufacturing

Currently, large manufacturing facilities are using "300-400 MWh of electricity to sustain their daily production activities" (Taboada, Xiong, Jin, & Jimenez, 2012, p.40). According to Taboada et al., (2012), "to meet the high consumption of electricity, everyday a fossil fuel-fired power plant discharges 180-360 metric tons of CO_2 into the atmosphere, which adversely affects the environment" (p.40). Figure 2.1 shows a Venn diagram of the effects of decreasing energy usage and how it affects people, profit, and the planet.

With this, Lunt & Levers (2011) states that "reducing energy consumption clearly has advantages for manufacturers, not only in terms of reduced operating costs, but also in terms of the positive corporate image resulting from actively engaging in sustainable energy practices" (p.1).

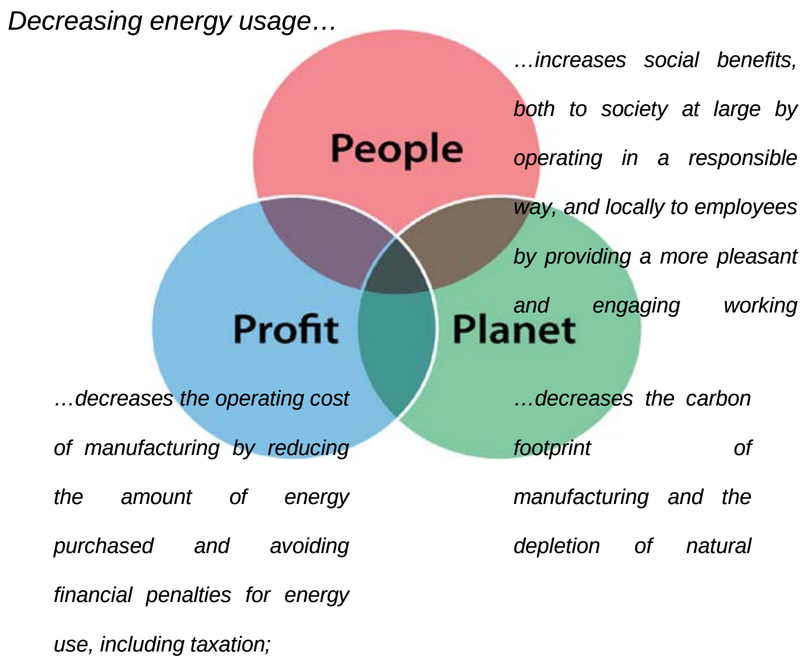

Figure 2.1 Energy and the Triple Bottom Line, (Lunt & Levers, 2011)

Chun & Bidanda (2013) investigated the broad range of literature related to sustainable manufacturing published over the past 50 years in the International Journal of Production Research. This investigation was motivated by growing concern for the environmental impact of pollution and waste, and the ensuing interest in sustainable manufacturing and efficient resource utilization, over the last decade. Previous published publications on manufacturing sustainability were focused on safety, workplace design and process improvements. Current publications are focused on ergonomics, intelligence, global manufacturing, environmental challenges, design for sustainability, product life cycle management, and green supply chain management. For example, current publications in the International Journal of Production indicate current needs, suggest guidelines, and propose potential solutions for sustainability in the manufacturing sector.

It was discovered that conventional manufacturing and operations research principles have been utilized for implementing sustainable manufacturing, but the impact of implementing these concepts and assessing the performance in the real world still remains to be unresolved.

Zhi (2011) stated “manufacturing is a major source of pollution in the current environment” (p.1332). He argued that the increasing demand of electricity for manufacturing facilities has led to an increase in consumption of fossil-based resources, and ultimately an increase in environmental pollution. To solve this problem, he proposed the concept of sustainable development that not only meets the current needs, but also meets the needs of future generations. Zhi (2011) states, “green manufacturing has characteristics of energy savings, reduced consumption, and little to no environmental pollution, which embodies the idea of sustainable development in modern manufacturing” (p.1333). Zhi suggests that phasing out high energy and outdated machinery and equipment, as well as optimizing energy-saving work standards, will promote green manufacturing. Applying these green manufacturing strategies will strengthen green education, improve governmental regulation of sustainable practices, and strengthen legislation and related economic policies.

Similar to Zhi (2011), Leahu-Aluas & Burstein (2010) discussed that “sustainable manufacturing is part of the larger concept of sustainable development” (p.13). This emerged in the early 1980’s in response to increased awareness of the environmental impact of economic growth and global expansion of business and trade. Leahu-Aluas & Burstein found that sustainable manufacturing influences all company processes and decisions, thereby impacting the social and natural environment in which it operates.

However, the investigators stressed the importance of advancing technological and economic performance while reducing or eliminating any negative impacts. The researchers also highlighted several significant drivers for adopting sustainable manufacturing as a core component of any company's strategic initiatives.

Additionally, Ding, Qiu, Mullineux, & Matthews (2010) predicted that sustainable manufacturing will be the dominant factor in designing the future factory. They stated that "any manufacturing operation within factories would affect the environment, be it through the waste it creates, the resources it uses, or the energy it consumes"(Ding, Qiu, Mullineux, & Matthews, 2010, p.767). Ding et al. (2010) investigated issues related to subtractive machining and evaluated research findings in order to assess the current waste hierarchy. Ding et al. discussed the government's desire to determine the factors that contribute to waste in industry that need to change in order to improve sustainable waste practices. With these governmental findings, industry is concerned about how these changes might affect them, and how they can minimize the effect of these changes on their profits. With the design of future sustainable factories, the researchers suggested using the labels of prevention, reduction, reuse, and disposal as the major components of the proposed waste hierarchy. Figure 2.2 shows a diagram of the waste hierarchy, leading with prevention and resorting to disposal.

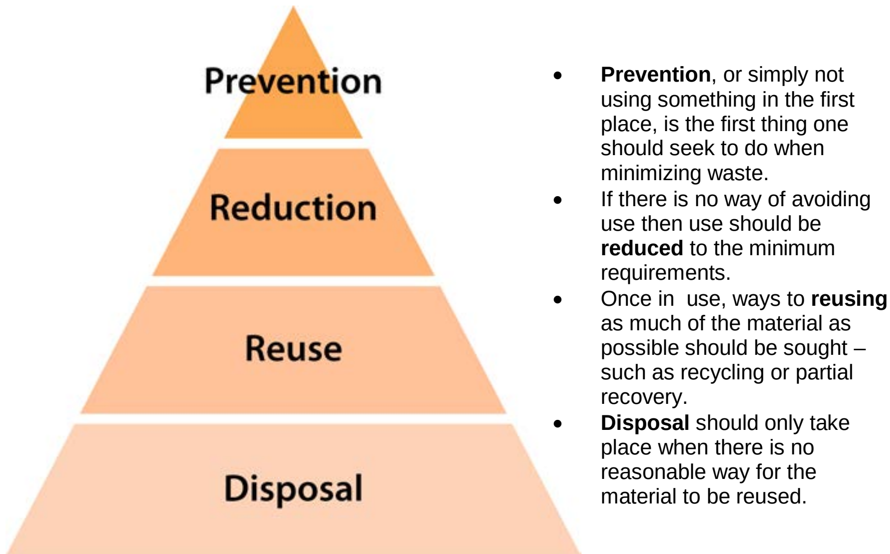

Figure 2.2 Description of Top Down Waste Hierarchy, (Lunt & Levers, 2011)

Carter (2011) mentions that "energy management and sustainability decisions were less complicated for most facility managers not long ago; decisions included switching to fluorescent lighting, installing a more efficient HVAC system, or upgrading to more integrated process controls architecture to streamline production" (p.1). With the advancement of manufacturing, energy management and sustainability decisions have become more complex. To solve this problem, Carter (2011) devises "a fully integrated energy master plan that will facilitate the integration of energy and sustainability projects, and assets in large industrial, manufacturing, and institutional facilities" (p.1). Carter continues to state "that a long-term, broad-scoped plan should be integrated into a company's strategy to optimize all facets of energy efficiency and sustainability" (p.2). Although energy master plans are not entirely new, putting them into integrated packages is a new approach and allows energy managers to recognize opportunities for conservation, sustainable design, and renewable energy. Carter (2011) implemented the energy master plan in a cement plant that used discrete control automation systems and processed functions into a centralized controls architecture. He found that it significantly reduced process cycle times and production per labor hour, as well as improved throughput, energy usage, and equipment return on investment (ROI). “Energy master plans are individualized for each company and have a four-stage approach: investigation, visioning, analysis, and deliverables” (Carter, 2011, p.2).

Lastly, Lunt & Levers, (2011) describes how a number of sustainable manufacturing approaches have been combined, enhanced and applied to the shop floor of a manufacturing facility in the United Kingdom that is responsible for the production of large component assemblies for the aerospace industry. He finds that there is little evidence in the sustainability literature for a systematic approach to energy savings in manufacturing, and for the continued savings such an approach could produce. The researchers did a case study of an aircraft component drying process and found that the process is the largest consumer of electricity. They found that the main fan was running for a large amount of time without the enclosure being occupied. Upon this discovery, they altered the controller logic on the drying process in order to modify the load profile. This study showed that adopting an appropriate approach, which combines best practices in sustainable manufacturing with a suitable improvement and change methodology, leads to visible potential gains and encourages investment into energy savings. The initial project resulted in savings of 70%, applying this approach to similar processes resulted in comparable savings.

2.2 Energy Recovery Methods within Manufacturing

This project used a laboratory scale heating/cooling system to generate the process loads that are common in manufacturing. Boilers that operate by burning fossil fuels like natural gas, coal, diesel fuel, or #2 fuel oil, frequently generate this heating energy. Process cooling is generally accomplished with a chiller that operates on an electrically drive vapor compression cycle. By using energy recovery methods, the process energy can be re-claimed as a by-product of the manufacturing process itself.

There are three main intended uses of waste heat recovery methods; waste heat to heat, waste heat to cooling and refrigeration, and waste heat to power. Plants that use waste heat recovery systems may benefit from significant energy savings potential from a wide variety of industrial process heating and steam system equipment sources (including boilers, furnaces, ovens, dryers, heaters, air-cooled heat exchangers, and kilns), reduced energy costs (from decreased fuel and/or electricity use), lower associated carbon dioxide emissions, reduced capacity and size requirements for plant thermal, and improved productivity by debottlenecking industrial processes, (Orthwein, 2012, p.1).

Despite using renewable energy technologies, “the least expensive energy is the energy that does not have to be produced in the first place” (Andrews & Pearce, 2011, p.1446). Companies who are able to more efficiently utilize energy would be better positioned to succeed during times of increased fuel costs. Therefore, Andrews & Pearce, (2011) devised a technical and economic method of determining the viability of creating waste heat greenhouses using the waste heat from industrial processes in northern climates of Canada. The study took place between a flat glass manufacturer and a commercial tomato greenhouse. The large amount of flue gas heat and CO_2 emissions from burning natural gas for the manufacturing of the glass was used to grow the tomato plants. There are, however, “many additional industries with which a greenhouse could be coupled, including pulp and paper, aluminum smelting, and combined heat and power operations” (Andrews & Pearce, 2011, p.1447). From the methodology that was developed, Andrews and Pearce (2011) showed that a flat glass plant with a revenue production of 500 metric tons/day and a usage of 1.25 PJ of natural gas can support a 3.9 acre greenhouse with a $1.3 million annual revenue, and can offset from 1042 to 2125 metric tons of CO_2 annually (p.1448). Again, the methodologies proved that it could be implemented to any manufacturing process that has a large amount of waste heat.

In a study by Bhattacharjee (2010), case studies of multiple plants in Canada were evaluated for waste heat recovery opportunities using energy audits and feasibility studies. These opportunities included compressed air waste heat recovery, condensing economizer for heating boiler make-up water, waste heat recovery from coffee rosters, waste heat recovery from chemical reactor exhaust to preheat combustion air, and a steam boiler blow down heat recovery. The author suggested “manufacturing industries that have air compressors can generate heat that can be used for space heating; but this would require the installation of heat exchangers, ducting, and other accessories” (Bhattacharjee, 2010, p.7) .The implementation of the heat recovery system would save $12,733 annually in natural gas costs. He suggested that within the food and beverage industry, the recovered waste heat from the boiler blow down process may be used to preheat the make-up water. For manufacturers that utilize furnaces that have combustion air preheating and exhaust air that recovering the exhaust air is beneficial and cost effective. From one study, a chemical plant used a furnace with combustion air preheating capabilities that maintained an exhaust temperature of 1500 °F. With the installation it "reduced the consumption of natural gas by 76,816 m^3 annually with a yearly savings of $36,872, and upfront cost of $150,000, and a 4.07-year payback period" (Bhattacharjee, 2010, p.10).

Lastly, 3M Company (2003) did a technical and economic evaluation of existing energy systems and operations that could benefit from heat recovery and cogeneration opportunities. From four different energy recovery methods, 3M chose a package that was based on a relative aggregate payback period. This package included projects for "chiller consolidation, air compressor cooling improvements, a steam turbine used for cogeneration, and a heat recovery boiler for two of the plant's thermal oxidizers" (3M Company & United States Department of Energy, 2003, p.2). From the assessment of the plant, "staff found that the energy-efficiency measures affecting electric consumption and steam production would provide the greatest potential benefit to plant operations" (3M Company & United States Department of Energy, 2003, p.2). 3M was able to consolidate its chiller capacity of both plants by interconnecting their individual chilled water distribution systems, saving 1.5 million kWh/yr. To cool the air compressors, they used the cooling towers from the chilled water system, saving 1,002,750 kWh/yr. For heat recovery of the thermal oxidizer, they installed a heat recovery boiler that was able to provide steam to loads throughout the plant, saving an estimated 210,000 MMBTU/yr due to reduction of natural gas and fuel oil. Lastly, they installed a steam turbine and electric generator to use the pressure drops for cogeneration in place of a pressure-reducing valve. The steam turbine was estimated to save 3 million kWh/yr. They estimated that this package would save 5.7 million kWh/yr in electricity and 214,499 million British thermal units per year (MMBTU/yr) in natural gas and fuel oil. Through a sponsorship from the DOE Industrial Technologies Program, the total assessment cost of $97,161 was offset by $48,580 from the DOE, with a total project capital cost of $2,045,970. Within the first year, the methods proved to have savings in energy costs of $1 million and a 2-year payback period for all equipment. The assessment done at 3M may be replicated at other manufacturing facilities that use thermal oxidizers for VOC elimination.

2.3 Commercial Microgrids

"Distributed Energy Resources (DERs) have attracted much attention to provide a reliable, efficient, economic, and sustainable energy supply in the Smart Grid initiatives all around the world", (Bozchalui & Sharma, 2012, p.1). "DERs, including distributed generation (DG) and distributed storage (DS), are sources of energy located near local loads and can provide a variety of benefits, including improved reliability, if they are properly operated in the electrical distribution system" (Kroposki et al., 2008, p.41). DG is typically supplied from Solar PV energy systems, wind turbines, fuel cells, and waste heat for combined heat and power (CHP) or microturbines, while DS is typically batteries, supercapacitors, and flywheels used as storage to provide a bridge in meeting the power and energy requirements of the microgrid, (Kroposki et al., 2008, p.42). Kroposki et al. (2008) state "within microgrids, loads and energy sources can be disconnected from and reconnected to the area or local electric power system with minimal disruption to the local loads; however any time a microgrid is implemented in an electrical distribution system, it needs to be well planned to avoid causing problems" (p.41). Bozchalui & Sharma (2012) acknowledged the United States Department of Energy 2020 targets for commercial scale microgrid developments. Targets included over "20% reduction in Greenhouse Gas (GHG) emissions, more than 20% improvement in system energy efficiencies, and reduction outage time to required loads by 98% compared to non- integrated baseline solutions, limiting that commercial scale microgrids have capacities less than 10 MW" (Bozchalui & Sharma, 2012, p.1). Figure 2.3 shows a schematic of the microgrid with the supply side (or DG), energy storage components (or DS), demand-side, and the utilities.

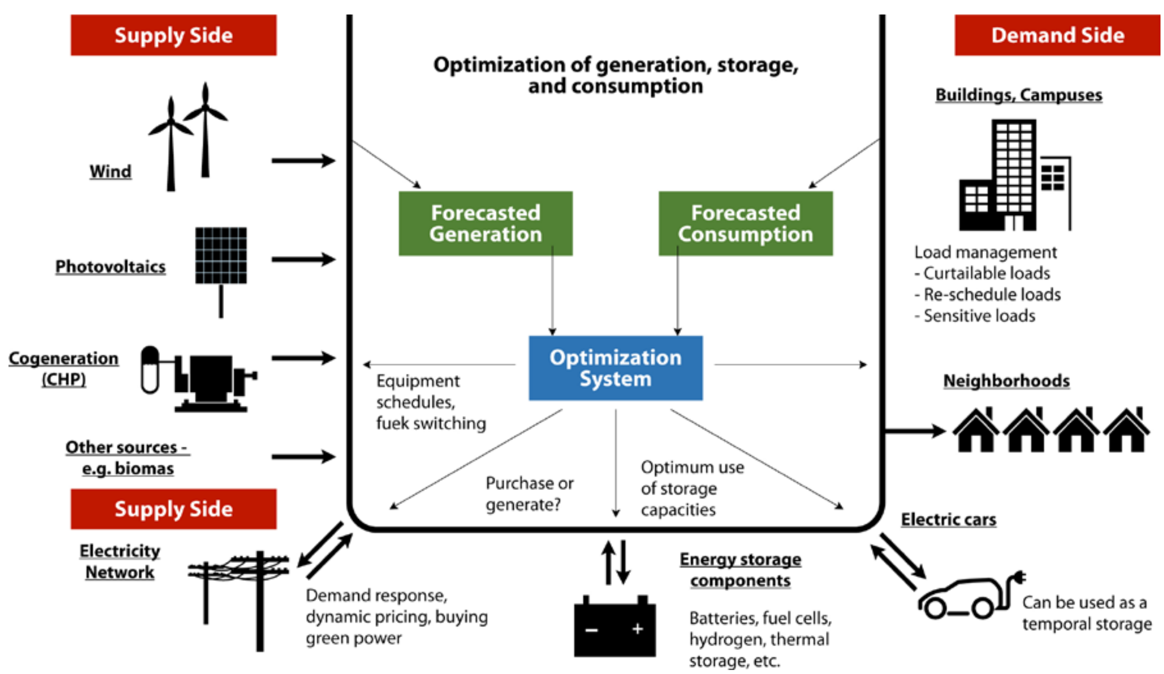

Figure 2.3 Schematic Representation of the Microgrid, (Stluka, Godbole, & Samad, 2011)

2.3.1 Distributed Generation (DG)

In their study, Li, Zhang, & Li, (2009) bring to light the primary difficulty of designing DC microgrids due to various DC voltage ratings in different systems. To solve this problem, the researchers suggested a voltage selection guideline and proposed an efficient wind-PV hybrid generation system for DC microgrids, which would make the system independent from day to night. Li et al., (2009) mentioned “wind and PV power individually suffer from intermittence in nature” (p.1). “Fortunately, wind power and PV power are complementary to some extent, because strong wind usually occurs at nighttime and on cloudy days, whereas sunny days are often calm and weak-winded, making a wind-PV hybrid generation system more reliable for maintaining continuous power than any other individual renewable sources” (Li et al., 2009, p.1). They recognized that “important loads like electric welding machines, arc furnaces, and steel rolling mill are very sensitive to the quality of the electricity supplied, and that these loads typically cause voltage dips and sags” (Li et al., 2009, p.1) . Li et al., (2009) support the use of a “wind-PV hybrid system due to its decreased voltage, the increased power transmission capability of DC cables compared to AC systems, and the absence of reactive current, which ultimately leads to better utilization of the whole system and reduces the total loss when connected to public grid” (p.1). For the system, a DC bus was installed with the energy storage to help with larger voltage dips and outages from the variety of loads.

Taboada et al., (2012) proposed a solar photovoltaic-based co-generation system to accommodate the electricity needs of semiconductor wafer fabricators. They used a “stochastic programming model to minimize the system cost related to the loss of load probability constraint" (Taboada et al., 2012, p.40). Based on their program that was tested at five different United States wafer fabricators, they found that "solar-based energy was economically competitive in regions where the overcast days were less than 35% of the year, with tax incentives or equipment subsidies" (Taboada et al., 2012, p.45). The researchers used a DG system with solar panels, net metering module, and a standard substation. With this setup, additional electricity was generated from the substation to fill the energy gap if the solar power wasn't sufficient enough to power the wafer fabrication. But if excess energy was generated by the solar system then the excess was fed to the main grid, creating a revenue stream for the fabrication. Figure 2.4 is a schematic of the system setup with net metering Taboada et al utilized.

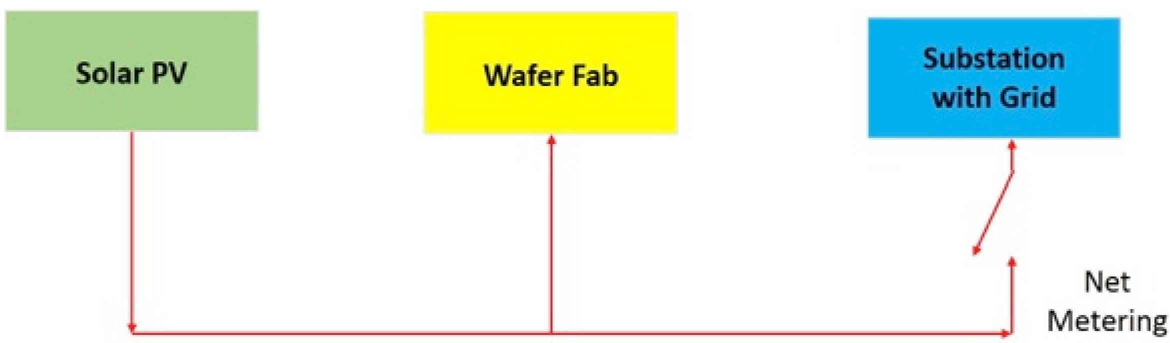

Figure 2.4 Schematic of Solar PV with Grid Integration, (Taboada et al., 2012)

Based on the results, the researchers concluded that "with the reduction of PV costs and the growth of the conversion efficiency, PV is becoming a favorable distributed green energy to power large industry facilities" (Taboada et al., 2012, p.45). A stochastic decision-making model that was formulated to optimize the DG capacity and minimize system costs supported these findings.

Robert Dohn (2011) wrote a white paper, sponsored by Siemens, to exploit "automated microgrid technologies connected seamlessly with the main grid" (p.2). With this, he was able to find a solution that “enhanced reliability, efficiency, security, quality, and sustainability for energy consumers and producers alike” (Dohn, 2011, p.2). Dohn (2011) defines a microgrid as a “discrete energy system consisting of distributed energy sources (e.g. renewables, conventional, storage) and loads capable of operating in parallel with, or independently from, the main grid, and with the primary purpose of ensuring reliable, affordable energy security for commercial, industrial and federal government consumers” (p.2). In his research, Dohn (2011) stated that a “microgrid is the end state of an energy modernization effort that will take two to five years to implement at an installation (corporate park, military base, university campus, etc.)” (p.9). He noted that the appropriate team of software, hardware, systems integration and consulting partners would ease the difficulty of the design and implementation of a successful microgrid. He also noted that the execution of microgrids is the real challenge, but the end user will accrue overall benefits from utilities and the public. Lastly, Dohn (2011) acknowledged that a “fully developed microgrid, with demand reduction, on-site generation and storage, advanced controls and grid independence capabilities, will likely be reserved for large energy consumers with a critical need for reliability and who can afford for a longer payback period” (p.5).

2.3.2 Distributed Storage (DS)

Many DS techniques are being coupled with DG systems to enhance and stabilize the system connection to loads. In a paper titled Making Microgrids Work, researchers state the advantages of DS techniques:

“Distributed storage enhances the overall performance of microgrid systems in

> three ways. First, it stabilizes and permits DG units to run at a constant and stable output, despite load fluctuations. Second, it provides the ride-through capability when there are dynamic variations of primary energy (such as those of sun, wind, and hydropower sources). Third, it permits DG to seamlessly operate as a dispatchable unit. Moreover, energy storage can benefit power systems by damping peak surges in electricity demand, countering momentary power disturbances, providing outage ride-through while backup generators respond, and reserving energy for future demand." (Kroposki et al., 2008, p.42)

"Energy storage technologies provide the opportunity for energy generation to meet the level of power quality and reliability required by energy demand, while also providing emergency power and peak shaving opportunity" (Zahedi, 2011, p.869). In practice, "the electrical power is fed to the storage when there is a lot of sunshine or strong wind and the energy is injected to the utility grid when there is additional power left" (Li et al., 2009,p.2). Typical storage methods that are being practiced include battery storage, thermal energy storage, compressed air storage, flywheel energy storage, super-capacitors, electrolyser and fuel cell. There are two applications of energy storage according to Zahedi (2011), "for low to medium power, energy is stored as kinetic energy, chemical energy, compressed air, hydrogen, or in super-capacitors and for large scale power, energy is stored as potential energy, thermal energy, chemical energy (batteries) or compressed air" (p.69).

2.4 Energy Management

A methodology for planning and operating energy-efficient production systems was devised in an article by Weinert, Chiotellis, & Seliger, (2011). Their research introduced a novel energy monitoring and management protocol to be established within manufacturing processes. Weinert et al., (2011) stated “that there is a lack of decision support when procuring, distributing, and accounting for energy in production systems, which leads to high-energy cost with low energy efficiencies” (p.41). To reverse these problems, the authors devised a methodology that to system-wide prediction of energy consumption and the introduction of analytical energy management methods.

In their research, Weinert et al., (2011) introduced “EnergyBlocks to integrate criteria of energy efficiency and effectiveness in manufacturing planning and scheduling of processes” (p.42). In order to effectively use the EnergyBlocks methodology, the authors had to “identify the power profile of each type of equipment and the time and energy consumption of each operating state, which became an EnergyBlock” (p.42). The EnergyBlocks were then modeled in sequences to plan production processes and investigate the energy consumption profile. Results from a case study showed “that when using the EnergyBlocks as a system-wide approach, energy management could be assessed analytically” (Weinert et al., 2011, p.44).

Stluka et al. (2011) suggested “energy management and control for facilities could be viewed as a large-scale optimization problem” (p.5150). In order to achieve desired optimization, the authors proposed “optimizing the supply-side, integrating of renewable sources, optimizing energy storage, optimizing demand-side, forecasting loads, forecasting renewable generation, modeling equipment, pricing data, and characterizing loads" (Stluka et al., 2011, p.5150). Two problems were formulated for the optimization; the supply-side problem and the demand-side formula. From the optimized formulas, the researchers created an energy management software solution named Versatile Energy Resource Allocation (VERA). According to Stluka et al. (2011), "the VERA system can solve a combination of problems including unit commitment, economic dispatch, fuel switching, balancing of local generation with utility purchases and optimal utilization of the capacity of storage devices" (p.5155). To insure the validity of the VERA system, the researchers executed the system in a hospital in the Netherlands over an eight-year period. VERA proved to decrease the gas and electrical consumption with an annual savings in utility costs ranging between 6% and 12%. Future work included "synchronizing the VERA system with building controls that will insure smooth operation of building systems" (Stluka et al., 2011, p.5157).

An optimization model for optimal energy management of commercial building microgrid systems was introduced by Bozchalui & Sharma, (2012). Bozchalui & Sharma, (2012) aimed to "increase efficiency of energy utilization, minimize operational costs and reduce environmental impacts of energy utilization in commercial buildings" (p.1). Bozchalui & Sharma, (2012) recognized that "commercial buildings with multi-carrier energy systems, namely electricity and natural gas, with hybrid AC/DC electric systems" (p.1), could integrate a microgrid system. So the researchers developed a multi-objective optimization model to optimally operate the systems. The results of the optimization showed "total daily energy costs and GHG emissions were reduced significantly compared to other non-integrated baseline systems by using their optimization method"

(Bozchalui & Sharma, 2012, p.7). The model was proven to “lower GHG emissions, improve the energy system efficiency, and minimize daily total cost of energy using a microgrid” (Bozchalui & Sharma, 2012, p.8).

2.4.1 Communication Protocols

With the transition from traditional grid systems to smarter grid capabilities, smart metering has been gradually introduced to allow for two-way communication from the meter (consumer-side) to the utility (provider-side) and vice versa. Smart meter systems use Advanced Metering Infrastructure (AMI) to collect, measure, analyze, and communicate energy usage among a variety of meters. This communications protocol allows for the sending of messages to homes of consumers about service disconnects, time-of-use pricing, or demand response.

BACnet is a communications protocol used for commercial building automation and controls. It is a standard protocol used by American Society of Heating, Refrigerating and Air-conditioning Engineers (ASHRAE). The ability to communicate human to machine commands gives the consumer the flexibility to control all processes and consumption of energy within facilities. Open Automated Demand Response (OpenADR) is another standard and communication protocol developed at Lawrence Berkeley National Laboratory. In 2009, “OpenADR was released and tested in commercial facilities to allow for automated energy management, by sending information and signals for demand shifts to and from electronic devices” (Holmberg, Ghatikar, Koch, & Boch, 2012, p.B17).

The use of BACnet and OpenADR has led to research into automated demand response that is “a part of a vision for smart grid to allow facilities to respond dynamically to electric grid price and demand response (DR) signals”, (Holmberg et al., 2012, B16). In their article, Holmberg et al. (2012) recognized the importance of “communicating DR events, usage, and electricity prices, along with allowing end users with intermittent renewables the opportunity to better manage energy” (B.16).

Communication protocols for energy monitoring are highly dependent on the use of the Internet and wireless networks. Liyanage et al., (2011) addressed operational challenges of small-scale renewable generation into the grid due to the fluctuations and intermittent nature of renewables. To address this shortcoming, “they proposed an approach to solve the problem using real-time demand management by controlling system elements” (Liyanage et al., 2011, p.198). Information was exchanged using “User Datagram Protocol (UDP) and Transmission Control Protocol (TCP) communication networks, where UDP communicated general information between individual devices and local controllers, while TCP gave information on system’s electrical status in real-time” (Liyanage et al., 2011, p. 201). The experiment used Matlab software to simulate the transfer of data between renewable generation and conventional loads over the networks. In a laboratory setting, “results of the experiment suggested that a control strategy over a public network could work successfully and reduce power fluctuations substantially compared to when the control strategy was not implemented from the communication protocol used” (Liyanage et al., 2011, p.203). Also, the algorithms and simulations confirmed that the local controller unit harnessed the maximum energy from the renewable sources, as expected.

2.4.2 Energy Monitoring

The need for and importance of smart integrated energy monitoring was discussed in an article by Abou-Elnour, Murad, Al-Tayasna, & Abo-Elnor, (2013). The researchers were able to design and implement their own monitoring and management system that monitored real-time data continuously from a PV system and loads. The use of a "hierarchical self-adaptive algorithm" (p.2), allowed Abou-Elnour et al., (2013) to automatically control and optimize the consumption of different loads. Abou-Elnour et al., (2013) also investigated the use of wireless technologies that are required to remotely monitor system variables and control system operation. To collect the data, "sensors were used at loads sent signals over wireless transmitters to a data acquisition card, which then displayed information through software" (Abou-Elnour et al., 2013, p.2). According to Abou-Elnour et al., (2013), "the main function of the monitoring and management system is to accurately control the energy consumption from the solar PV energy system based on accurate determination of the periods of times at which the loads are required to be operated" (p.2). This is achieved by monitoring the system performance by continuously calculating and recording the consumed and generated power from the PV system.

Spertino & Corona (2013) reported on a 1-year monitoring stage of thirteen PV plants in Europe. The work was a part of a joint European research effort named PERSIL. The use of weather stations and pyranometers were important to the PV monitoring, because it allowed the researchers to obtain twenty years' worth of irradiation history. After the year-long period of monitoring, Spertino & Corona, (2013) were able to do 2-year analyses, and they created a prediction model for future energy production of the systems using historical data. With the results, guidelines for designing Solar PV energy systems, installing Solar PV energy systems, and maintaining the systems were developed. The study used a variety of each type of equipment, including PV modules, inverters, and mounting options. At one of the locations, a tracker system was used, but it "required higher maintenance than fixed mounted Solar PV energy systems due to the mechanical maintenance on motors" (Spertino & Corona, 2013, p.732). Also, locations that experienced shading problems showed results that were subpar compared to the predictions for the location. Overall, the researchers were able to show that newer PV plants with monitoring had energy availability values at about 99%, allowing for peak performance.

2.5 Cost Analysis and Case Studies

A report by Farrell (2012), "identified the year when businesses, schools, hospitals, and other entities with available roofs and high electric bills could shift to solar PV energy systems to save money" (p.21). He examined incentives and regulations for solar power that would make solar generation less expensive or costly utility electricity. The report, stated "in places like Hawaii, unsubsidized solar is already less costly than retail electric prices, and in several parts of the United States, grid parity with electric companies is closer to be achieved" (Farrell, 2012, p.2). Figure 2.5 shows a chart of Unsubsidized Solar Electricity Price versus Commercial Retail Electricity Price (Nominal).

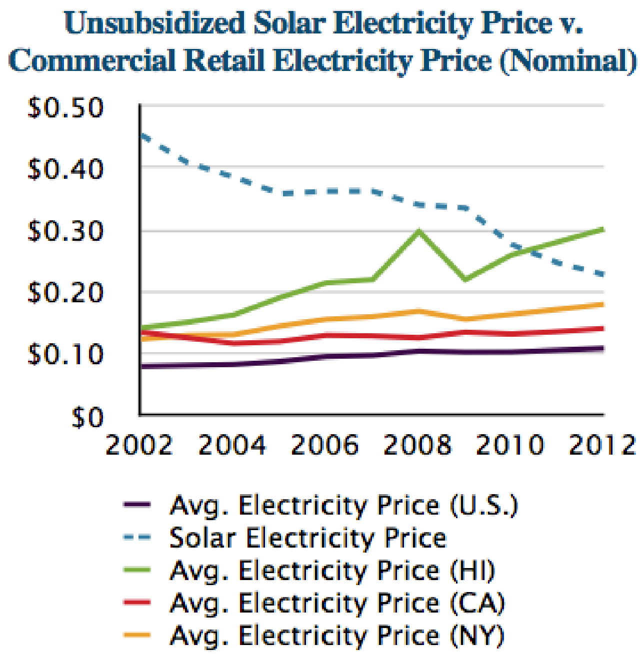

Figure 2.5 Chart of Unsubsidized Solar Price versus Retail Electricity Price, (Farrell, 2012)

As shown in Figure 2.5, Farrell (2012) illustrated the steady decline in solar prices and the gradual increase of utility energy prices. Through his study, he found that even when limiting solar to 20% of utility load, in the next decade 10% of commercial electricity demand could be met by cheaper-than-grid, unsubsidized solar electricity. He mentioned that policies and regulations have to be addressed to allow for grid parity and monitoring of net metering limits.

Case studies of hybrid renewable energy systems around the world in Japan, Hawaii, Norway, and other areas, including the National Renewable Energy Laboratory (NREL), were investigated by (Aki, 2010). Each of the systems discussed in the study were designed for their local conditions and unique or individual purpose of application.

The first hybrid system studied, located on Utsira Island in Norway, demonstrated a system equipped with wind turbines, a proton exchange membrane fuel cell (PEMFC) stack, a hydrogen engine, and more components that are seen in Table 2.1 (Aki, 2010, p.2). In this system, “the wind turbines supplied the primary energy for ten households on the island” (Aki, 2010, p.2). When wind was not sufficient, “the excess energy that was converted to hydrogen by an electrolyser was then supplied to a hydrogen engine or the PEMFC to support the shortage” (Aki, 2010, p.2). The system was “primarily operated in independent mode, but electricity can also be supplied from the main grid of the island in case of emergency” (Aki, 2010, p.2). The next system investigated was a hybrid wind-PV-electrolyser-FC energy system located at Kahua Ranch on Big Island Hawaii. As shown in Figure 2.6 the system is currently “being used as a test bed, where various experimentation can be conducted, such as testing performance of flow batteries, ultra capacitors, bio-gas fuel, etc” (Aki, 2010, p.2). In Osaka, Japan, “about 5,000 PEMFCs were installed at households in 2009” (Aki, 2010, p.3). After initial installation, “the systems were adversely affected by fluctuations in load demand from residents” (Aki, 2010, p.3). To solve this problem the “Osaka group interconnected the apartments with an energy network involving hydrogen pipes and FC-based electricity and heat (hot water) production” (Aki, 2010, p.3). In this system, “techniques for utilizing waste heat recovery from the FC exhaust allowed for heat waste recovery to heat the water supplied to the apartment tenants” (Aki, 2010, p.3).

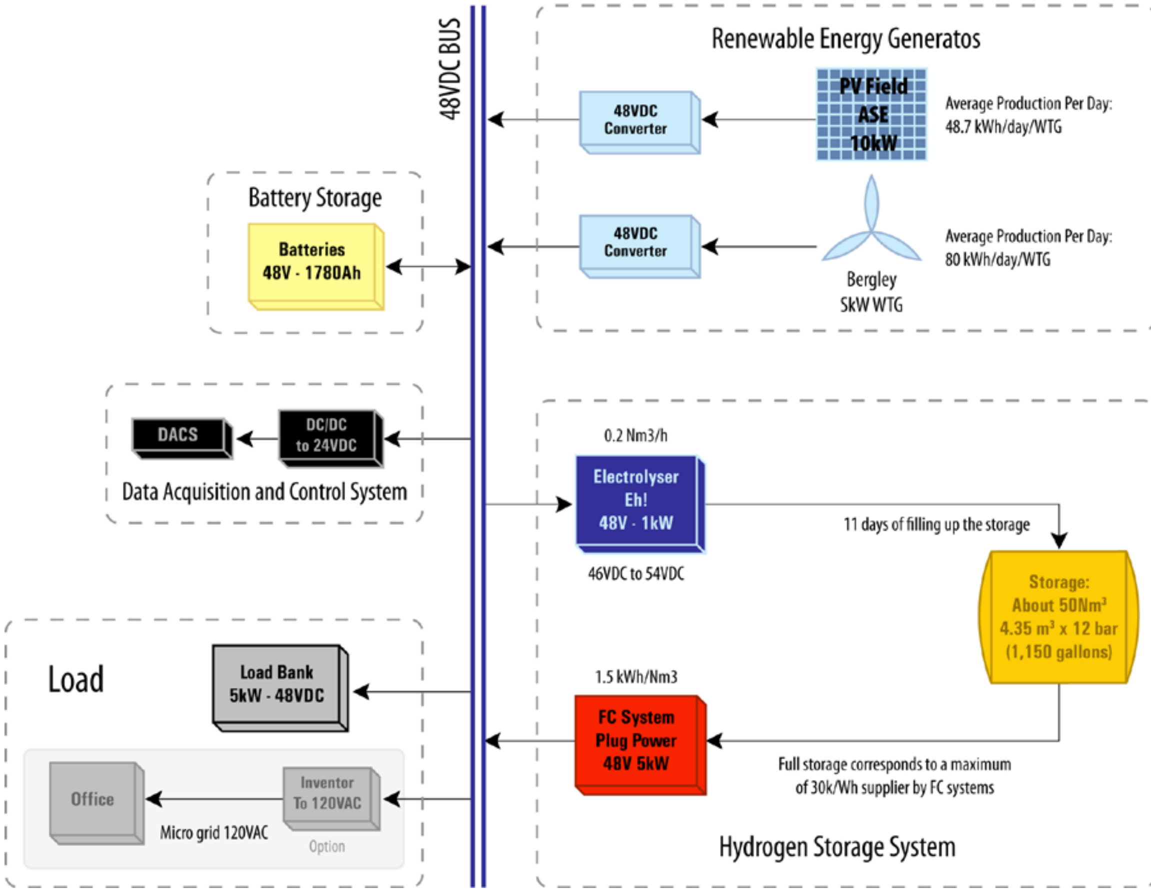

Figure 2.6 Hawaii Hybrid System Schematic, (Aki, 2010)

Table 2.1 Application of Hybrid Systems in Locations around the World, (Aki, 2010)

Equipment	Utsira Island	Hawaii Island	NEXT21, Osaka	Kythnos Island	Hichinohe	NWTC, NREL
Wind turbine	600 kW x 2	7.5 kW			8 kW x 2, 2 kW x 2	100 kW
Photovoltaic generation		10 kW		10 kW + 2 kW (I&C)	50 kW x 2, 10 kW x 3	
Battery	35kWh	85 kWh		53 kWh + 32 kW (I&C)	100 kW	
Flywheel	5Kwh					
Fuel cell	10kW	5 kW	0.7 kW x 3			40 kW
Electrolyser	10 Nm^3/h, 48kW	0.2 Nm^3/h (PEM)				
H_2 production			1.5 Nm^3 x 1			
Hydrogen tank	2400 Nm^3	50 Nm^3 at 1.2 Mpa				1294 Nm^3
Engine	55 kW			5 kVA (diesel)	170 kW (bio-gas) x 3	50 kW
Inverter		3.6 kW				
Compressor	5.5 kW					
Hotwater tanks			370 L x 1, 200 L x 2			
Load bank		5 kW				
Brief description	On/off-grid modes are available. Power is supplied to approx. 10 houses.	Test facility. Operated in off-grid mode. Power is supplied to office, and hydrogen tank.	Demonstration of networks of electricity, heat, and hydrogen in an apartment building.	The system is operated in off-grid mode. Power is supplied to houses.	On/off-grid modes are available. Power is supplied to a city hall, schools.	Test facility. Power is supplied to grid and hydrogen can be supplied to a hydrogen station.

Currently, Solar PV energy systems have been implemented in many commercial facets. Pacific Alloy Casting Co. INC. in California completed the installation of “1,190 solar panels on its roof in July 2011, an addition that is now providing the company nearly 10% of its total electricity consumed” (Gibbs, 2012, p.35). The energy costs in California are “amongst the highest in the country and new regulations are being implemented to increase the amount of electricity coming from renewables to 33% by 2020” (Gibbs, 2012, p.35) . From the savings that Pacific Alloy are witnessing, Gibbs, (2012) felt that as “solar energy becomes increasingly economical, more metal casting companies may join in the solar market” (p.36). The company received federal and state incentives to finance the project that was just over $1 million dollars. The federal government issued a 30% cash grant and the state of California granted $0.20 per kW for power generated by the solar panels for five years. Also, the system that Pacific Alloy utilizes is net metered, meaning they are paid for excess energy at the same rate that is charged at the time of day of solar generation.

Sharp has also been a leader of providing Solar PV energy systems for commercial industries. A few examples are Google headquarters in California, AT&T Park in San Diego California, Denver International Airport, and FedEx’s Oakland International Airport hub. According to Sharp, (2008a), Google has set an example for other corporations by utilizing the tremendous environmental and financial benefits of solar energy. In 2007 when the system was installed, Google held the largest commercial solar system at 1.6-megawatts. Their system is roof-mounted on eight of their office buildings and on two carports for employees to charge their hybrid vehicles. This system is capable of providing 30% of Google’s peak electricity demand and prevents an estimated

3,637,627 pounds of greenhouse gases. In San Diego, the Giants are the first to have a solar energy system in the Major League Baseball. Sharp (2008b) was able to install a 122-kilowatt system at the AT&T Park to promote energy-efficient operations. Their system also feeds back into the grid to provide electricity to residential homes in north and central California. In the middle of the country, “the Denver International Airport has the nation’s most visible solar photovoltaic system plant”, (Sharp, 2009). Sharp (2009) noted that the system spans seven-and-a-half acres at the entrance of the main terminal and is a 2-megawatt solar electric system. With this the Denver International Airport can generate 3 million kilowatt hours of clean electricity annually. Their systems are pole mounted and uses a single-axis tracking system, which maximizes the generation of energy due to following the suns path. Denver’s commitment to environmental sustainability has resulted in reducing carbon emissions by more than 6.3 million pounds each year.

2.6 Summary

In this chapter the idea of using microgrids for manufacturing practices was introduced. While there are various variations of microgrids, the usage of these technologies show promise of promoting sustainable manufacturing practices. Also, evidence showed that stand-alone systems of just wind or PV are currently being used by commercial entities, but there is a slow adoption of the combination of the two intermittent sources with other energy generators, as well as with storage, to make more reliable systems for integration with the smart grid by 2020.

CHAPTER 3. METHODOLOGY

This chapter presents the experimental methodology for developing and evaluating a prototype microgrid and optimal DSM control strategies. Techniques were developed in a laboratory that includes solar PV, facility-scale HVAC equipment, and a web-based automated building control platform. The Statement of Work shown in Appendix A describes the timeline for this research.

3.1 Microgrid Prototype

For the last 10 years, the AEL has maintained a 3 kW solar PV array mounted at 45° with respect to latitude and at an azimuth angle of 180°, as shown in Figure 3.1a. The array consists of 24 Kyocera 120-watt solar panels that were originally designed to be grid independent battery-based; meaning that the electricity was stored in batteries. The solar power was used for running several local pumps and fans in the laboratory, but did not have access to the electric grid. To fully enable the microgrid research, several electrical infrastructure upgrades were needed. The specific tasks included electric work to grid-tie the existing solar PV array to Purdue University's electrical grid. An interactive three-phase grid-tie inverter was installed, in place of an old single-phase inverter, to replicate industrial facilities receiving AC power from three circuit conductors at 480 or 120/208 volts, as shown in Figure 3.1b.

These technologies mimic equipment that is found in commercial buildings and form the core of a microgrid.

a) b) c)

Figure 3.1 Prototype Microgrid and Process Load

Unlike traditional microgrid solutions, the microgrid for this study did not have islanding or energy storage capabilities. All of the systems are monitored and controlled by a web-based building automation control platform, which was programmed and monitored to collect the data for the research. Figure 3.1c shows a process heating and cooling system used as the demand-side loads for this research. The system housed four pumps (A, B, C, and D), one electric heating unit, and an external air-cooled chiller. Each pump is rated at 250W for a total of 1kW dispatchable electric demand. The heating unit has a steady demand of 9kW when heating was enabled. The chiller has a range of 500W - 4,000W of electric demand when enabled.

The system was intelligently controlled through a building automation platform. For the DSM research, Pump B, C, and D were chosen as the loads that would be curtailed when curtailment schemes were enabled. To simulate an energy storage scheme, either the process heating or cooling could be operated in an energy storage mode using 40-gallon tanks integrated within the hydronic system. Again, for the DSM research, Pump B, C, and D were chosen as the loads that would be curtailed when curtailment schemes were enabled.

3.1.1 Electrical Upgrade

The main component of power conditioning equipment is the inverter, which converts the DC input from a PV array to an AC output that is used for traditional AC loads. There are multiple types of inverters for different applications; stand-alone, interactive (grid-tie), and battery based. For thus research, an interactive three-phase grid-tie inverter was installed to replicate industrial facilities receiving AC power from three circuit conductors. Three-phase inverters output an AC frequency of 60 Hz at 120/208 or 480 volts to the main utility grid. This avoids creating power fluctuations or balance issues when interconnecting the inverter to the host facility.

Before upgrading the power conditioning equipment, decommissioning of the previous battery-based electrical infrastructure was necessary to allow for grid interactive conditions. Figure 3.2 presents an electrical schematic that was constructed for safety approvals from Purdue University Facility engineers, and also to comply with policies and regulations for interconnecting PV energy systems to the main grid. The electric schematic shown in Figure 3.2 was constructed per National Electric Code (NEC) article 690.

To achieve optimal voltage and amperage for the three-phase inverter, the 3 kW solar PV array was separated into two sub-arrays with 12 panels wired in series for each sub-array as seen in Figure 3.2 and Appendix B. Each sub-array was then connected to individual DC disconnects that are rated for 600VDC at 60A, to allow for external disconnecting of DC power flow to the inverter. From the DC disconnects, the DC power was then wired into the inverter where the electricity is converted into AC power for AC loads.

To allow for interconnection to Knoy Hall, three-phase conductors and a neutral were wired into a smart meter located in the AEL, for wireless monitoring for the SMIL lab. From the smart meter, an AC disconnect rated at 250VAC and 60A was installed, per NEC article 690, to allow for external disconnection from the inverter within the AEL. After wiring into the AC disconnect, the three-phases and neutral were wired to an open circuit breaker furthest from the main bus bar within the electrical panel allowed interconnection to Knoy Hall. For over-current protection purposes, 60A fuses were installed in the AC disconnect and the electrical panel disconnect. All solar panels, disconnects, and the inverter on the DC-side were grounded by bonding a bare copper wire to the building steel of the building. This allowed the DC side to be earth grounded per NEC article 690. On the AC side, each component between the inverter and main electrical panel was bonded and grounded to the AC electrical panel within Knoy Hall.

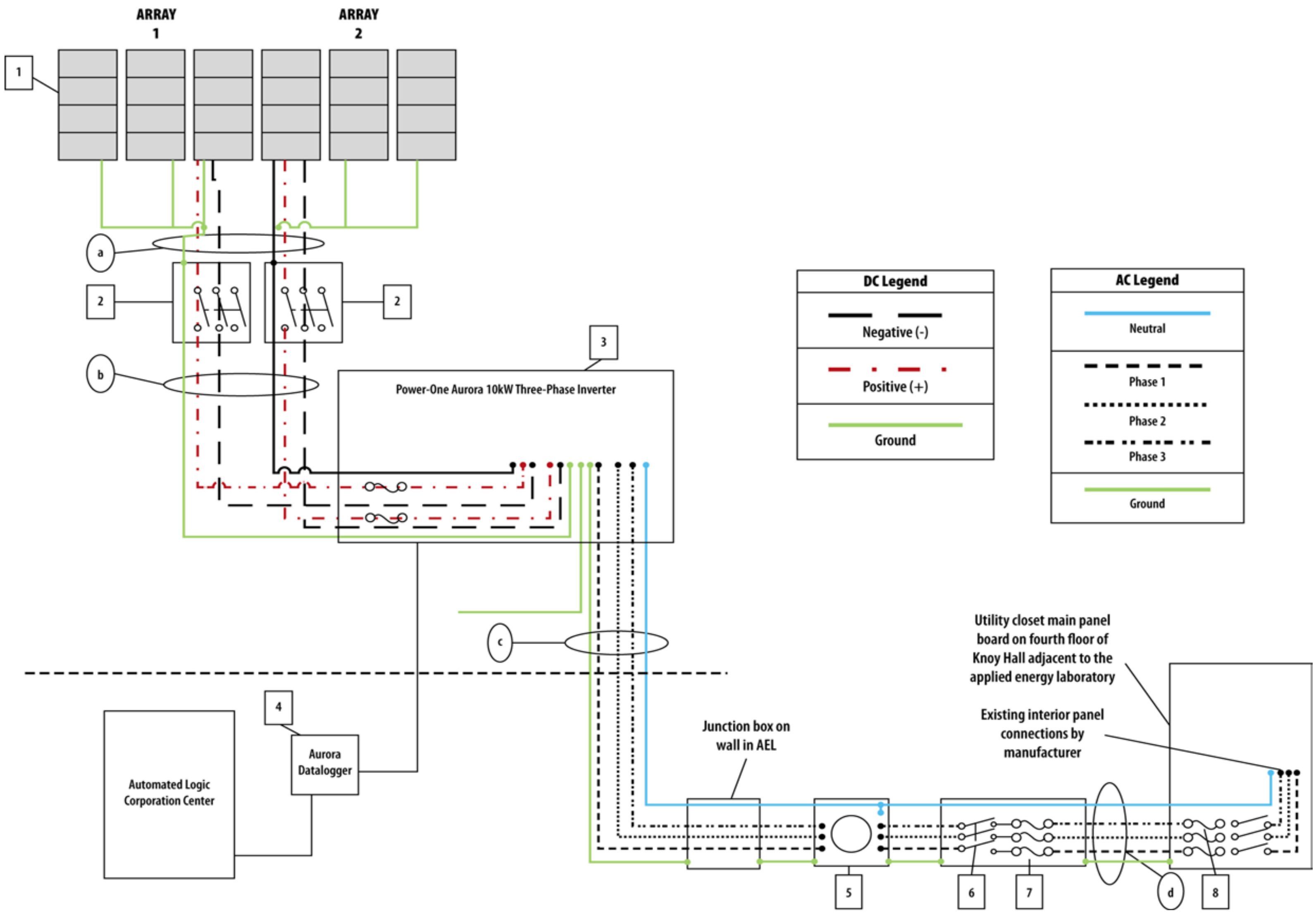

Figure 3.2 Three-Line Electrical Schematic of Grid-Tied Energy System Weather Station

A weather station was installed along with the three-phase inverter to enable monitoring of outside conditions. Figure 3.3 shows a Power-One aurora environmental entry weather station. The weather station is mounted directly above sub-array 2 in a way that it does not contribute to shading effects. The weather station has sensors that measure the global solar irradiance, plane of array irradiance, ambient air temperature, and PV panel temperature. These measurements are critical for forecasting and using historical data to optimally monitor the solar PV output.

Figure 3.3 Power-One Aurora Environmental Entry Weather Station

3.2 Data Acquisition

As shown in Figure 2.4, microgrids have very different types of equipment to monitor and control. To perform optimally, the supply side and demand side must have a common communication platform or at least some way of collecting and sharing data. The ability to coordinate data from multiple sources into one platform was essential to this research.

On the supply side, the three phase interactive inverter used for this research read and wrote real-time data to the manufacturer's proprietary data acquisition platform. The real time information included measurements of power and energy for each sub-array.

The data acquisition platform was also connected to an external weather station so that temperature, humidity, and solar intensity were tracked in real time. All of this information was transmitted via Ethernet using Modbus TCP/IP so that data could be viewed on the inverter manufacturer's website or transferred to a third-party SCADA platform over a network. The common communication protocol is what enabled the communication between the supply side to the demand side of the microgrid.

On the demand side, the simulated manufacturing process was monitored and controlled using a building automation platform called WebCTRL from Automated Logic Corporation. As seen in Appendix E, logic was developed in WebCTRL that monitored and controlled the process loads. This building automation platform allowed scheduling of the process loads to mimic a single shift of production at a manufacturing enterprise. This system also had sensors that monitored electrical energy use of the pumps, heater, and chiller used for process loads.

WebCTRL was also the SCADA system that linked the supply side and demand side of the microgrid. Using its network Modbus interface, WebCTRL collected real-time data on renewable energy production and weather conditions. With the supply side and demand side information on the same SCADA platform, developing process control strategies became relatively easy. The web-based platform also made it easy to manage this process from remote locations without direct access to the process loads in the laboratory or the solar panels on the roof.

3.2.1 Data Acquisition Setup

A Power-One AuroraVision Datalogger Max was installed to enable accurate data collection from the inverter and weather station proprietary protocol. Both the inverter and weather station transfer proprietary data through protocol Modbus RS-485, then the Datalogger modifies the protocol to be compliant to SunSpec standards so that it can be communicated through protocol Modbus TCP/IP. SunSpec Alliance is an organization that aims to “specify de facto standards – information models, data formats, communication protocols, systems interfaces, and other artifacts – that enable Distributed Energy power plants to interoperate transparently with system components, software applications, financial systems, and the Smart Grid”, (Sunspec.org, 2013) Using EIKON LogicBuilder, Modbus TCP/IP communication logic was written to monitor the output data from the inverter and weather station through AutomatedLogic WebCTRL. Figure 3.4 and 3.5 show graphic views for WebCTRL that were constructed so that end-users could have ease in reading measured data. The PV monitoring logic was used to create optimal DSM control strategies for the hydronic system.

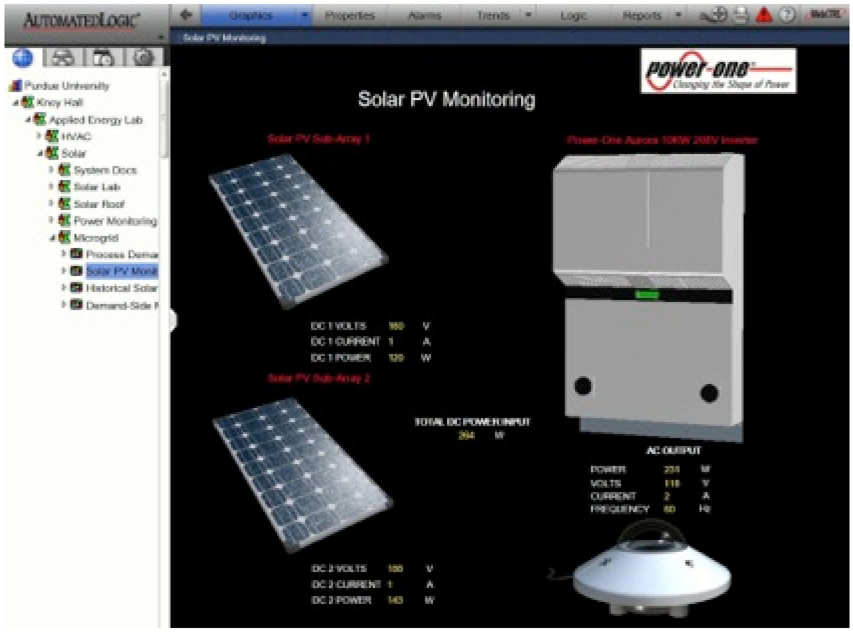

Figure 3.4 WebCTRL Graphic View of Solar PV Monitoring

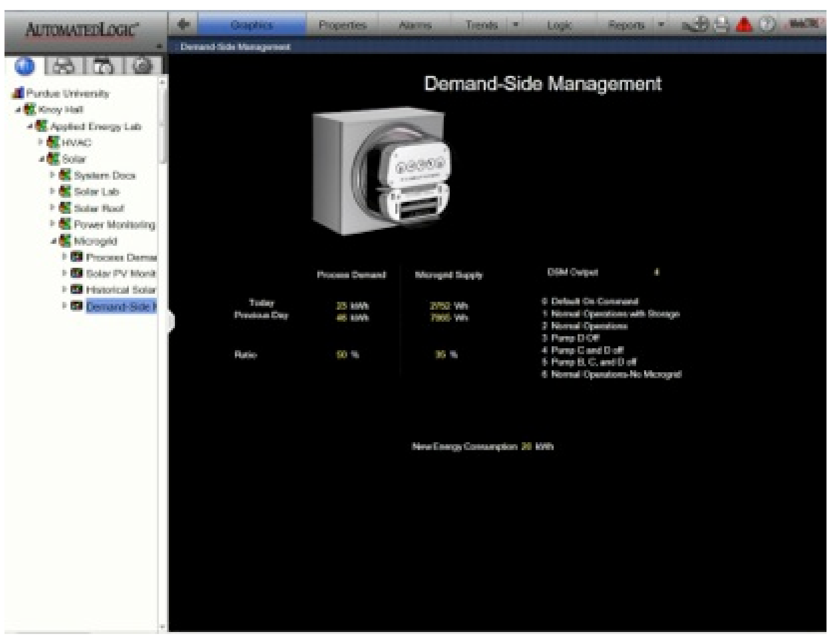

Figure 3.5 WebCTRL Graphic View of Demand-Side Management Monitoring

3.3 Hypothesis

The research component of this project was developed and evaluated with hypothesis analyses. This research should determine if microgrid technologies have the potential to reduce peak demand and electrical consumption for manufacturing facilities by using DSM programs based from microgrid generation and process demand. Table 3.1 summarizes performance objectives that tested the hypothesis.

Table 3.1 Performance Objectives for Microgrid Research

	Performance Objective	**Metric**	**Data Requirements**	**Success Criteria**
1.	Manufacturing Process Output	Instantaneous Demand vs. Power Generated	Power Sensor(s)	Maintain 70% of full capacity
2.	Peak Demand Reduction	Peak Demand (kW)	Power Sensor(s)	Reduce Peak Demand 5%
3.	Electrical Consumption Reduction	Electrical Consumption (kWh)	Power Sensor(s)	Supply 15% capacity

Performance objective one targets manufacturing process output and aims to show that renewable energy and improved controls have the potential to maintain 70% of manufacturing full capacity during peak time periods. A threshold of 70% was selected after analyzing daily utility usage for a manufacturing facility where energy usage ranged between 36% and 100% of full capacity. The manufacturing output percentage was computed from the ratio of overall consumption for one day with the DSM algorithm and microgrid in operation as compared to manufacturing demand with no controls in place.

Maintaining 70% of full capacity from a microgrid should be of interest for facilities around the world that are forced to shut down due to poor electrical grid systems and result in 0% of manufacturing output.

The goal of the second performance objective is to show that beyond maintaining a designated capacity, renewable energy can reduce peak demand by 5%. Peak demand often results in higher overall utility cost due to utilities charging manufacturers for the highest peak achieved in a monthly bill period. Do to peak demand being charged differently than electrical consumption, a 5% reduction should result in substantial cost savings.

Lastly, the third performance objective aims to show that overall electrical consumption from the utility grid is being reduced. The solar PV energy system is rated to supply 13% of the thermal process demand. This percentage was derived by the ratio of estimated kWh generation per year and baseline annual kWh consumption. For this objective a success criteria was targeted to reduce electrical consumption by 15%. This reduction in electrical consumption will further reduce energy cost resulting in more cost savings.

3.4 Demand-Side Management Model

Figure 3.6 shows a diagram of the DSM model that was developed to manage the intermittent nature of the microgrid and process loads and to determine optimal control outputs. The model used an algorithm that required an input from the microgrid, an input of energy demand from manufacturing processes, and historical data to actively determine optimal control strategies.

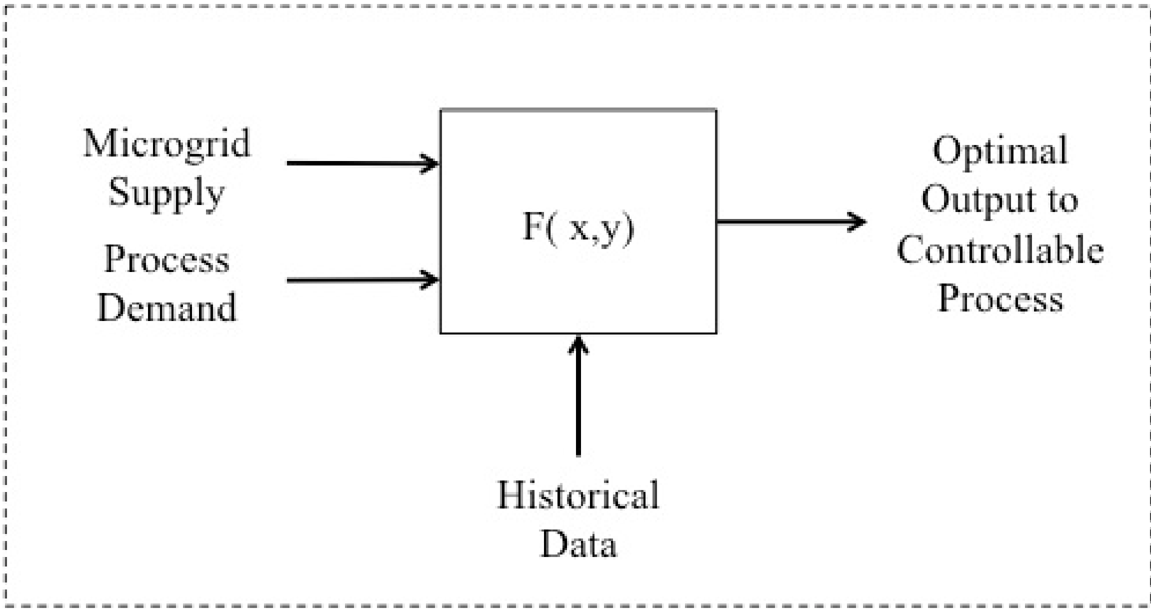

Figure 3.6 DSM Model for Optimal Control Strategies

3.4.1 Microgrid Supply

The microgrid supply is a variety of distributed generation and storage technologies used to generate locally accessible electricity. These technologies include, but are not limited to, solar, wind, cogeneration units (CHP), battery storage, and fuel cells configured in complex or stand-alone setups. For this study, only the solar output was investigated as the microgrid supply. Depending on technologies that are used to represent a functional microgrid, the sum of instantaneous power generation (kWh) was used as the microgrid supply input.

3.4.2 Demand Energy

Process demand is the total electricity from all energy consuming processes. This includes critical processes, curtailable processes, and re-schedulable processes, as determined by facility engineers. Critical processes are loads that cannot be interrupted and need a steady, reliable supply of electrical energy. Curtailable processes are loads that can be cycled, switched, or shut down to maintain processes but reduce energy consumption. Re-schedulable processes are loads that can be rescheduled for use during off-peak hours when electrical costs are cheaper. For this study, the four dispatchable pumps served as curtailable loads, for the DSM program.

3.4.3 Historical Data

Past generation data for all renewable energy technologies and historical energy usage were needed for the model to optimally control the processes. Figure 3.7 is historical renewable energy data that was obtained from databases managed by the National Renewable Energy Laboratory (NREL). NREL maintains the web-based software tool called PVWatts that provided historical hourly and monthly solar irradiance levels. The data obtained from PVWatts takes into account geographic locale, angle of PV array to respect to azimuth angle, and system size.

The other historical data is the energy usage at a given facility, which is obtained by metering the overall consumption of the facility on a daily, weekly, or monthly basis. Based on how the facility is metered, the historical demand can be scaled hourly to correlate with the work shifts for a given facility to output process demand.

West Lafayette, Indiana Average AC System Ouput Hourly (Wh)						
	January	***February***	***March***	***April***	***May***	***June***
8:00:00 AM	-	-	22	187	171	236
9:00:00 AM	0.6	127	456	734	686	814
10:00:00 AM	406	691	1,347	1,575	1,592	1,699
11:00:00 AM	1,069	1,614	2,490	2,689	2,708	2,853
12:00:00 PM	2,149	2,725	3,843	3,898	3,821	4,118
1:00:00 PM	3,017	4,011	5,248	5,377	5,064	5,435
2:00:00 PM	3,860	5,251	6,686	6,705	6,249	6,653
3:00:00 PM	4,849	6,430	7,878	7,866	7,363	7,928
4:00:00 PM	5,705	7,359	9,019	8,851	8,302	8,899
5:00:00 PM	6,240	7,771	9,774	9,538	8,998	9,625
6:00:00 PM	6,278	7,903	10,108	9,878	9,347	10,024
7:00:00 PM	6,278	7,903	10,110	9,885	9,370	10,084
8:00:00 PM	6,278	7,903	10,110	9,885	9,370	10,085
	July	***August***	***September***	***October***	***November***	***December***
8:00:00 AM	199	195	134	19	-	-
9:00:00 AM	793	827	718	427	236	-
10:00:00 AM	1,777	1,860	1,679	1,147	781	444
11:00:00 AM	3,075	3,240	2,950	2,177	1,554	1,066
12:00:00 PM	4,520	4,929	4,449	3,304	2,554	1,864
1:00:00 PM	6,034	6,569	5,920	4,476	3,656	2,570
2:00:00 PM	7,463	8,154	7,265	5,667	4,719	3,052
3:00:00 PM	8,786	9,495	8,582	6,722	5,496	3,472
4:00:00 PM	9,837	10,720	9,664	7,549	6,091	3,924
5:00:00 PM	10,650	11,622	10,423	7,974	6,349	4,171
6:00:00 PM	11,116	12,088	10,744	8,012	6,350	4,171
7:00:00 PM	11,181	12,118	10,745	8,012	6,350	4,171
8:00:00 PM	11,182	12,118	10,745	8,012	6,350	4,171

Figure 3.7 Historical Hourly and Monthly Solar Irradiance for West Lafayette, IN

3.4.4 Output to Process

An algorithm determined the output signal to the controllable process that analyzed ratios from the microgrid supply and process demand. The ratio of microgrid power generation to historical generation is computed and converted to an equivalent percentage that provides parameters for the DSM algorithm to determine an optimal control strategy. Similar to the microgrid supply, the ratio for process demand is hourly process usage to hourly historical usage and is converted to an equivalent percentage. Depending on the ratios, the algorithm made decisions once an hour to optimally control processes.

3.5 Demand-Side Management Control Program

Figure 3.8 is the DSM algorithm flowchart that was developed based from the DSM model. As previously mentioned, the algorithm required three primary inputs in order to output a single control strategy. Using the inputs, two-parameter ratios were calculated, a solar ratio and a demand ratio. The solar ratio calculated a percentage between actual solar generation and expected solar generation hourly when the microgrid/DSM was enabled. Similar to the solar parameter, the demand parameter calculated a percentage between actual process demand and historical demand on an hourly basis. After calculating the solar ratio and demand ratio, the algorithm determined ideal operating conditions based on the demand and the generated energy. Appendix D shows a sequence of operations that was used to create and develop the algorithm for AutomatedLogic. Appendix E is the Pseudocode to decide the optimal control output for the process dependent on the microgrid and demand parameters. To allow for customizable setups for different facilities and facility engineers, a separate Pseudocode was developed to control electric loads. Appendix F is the Pseudocode to control the processes decided by the facility engineers.

The algorithm for this study prioritized five optimal control strategies that operated between 9:00a.m. and 5:00p.m. to replicate a single shift in manufacturing. The process heating and cooling system served as the simulated manufacturing process since pumps are typical loads found in manufacturing facilities. The DSM model investigated four control programs.

- All pumps run on continuous cycle with storage (Normal Operations with Storage),
- All pumps run on continuous cycle (Normal Operations),
- Pumps B, C, and D run on Curtailment Schemes
- No microgrid (Normal Operations).

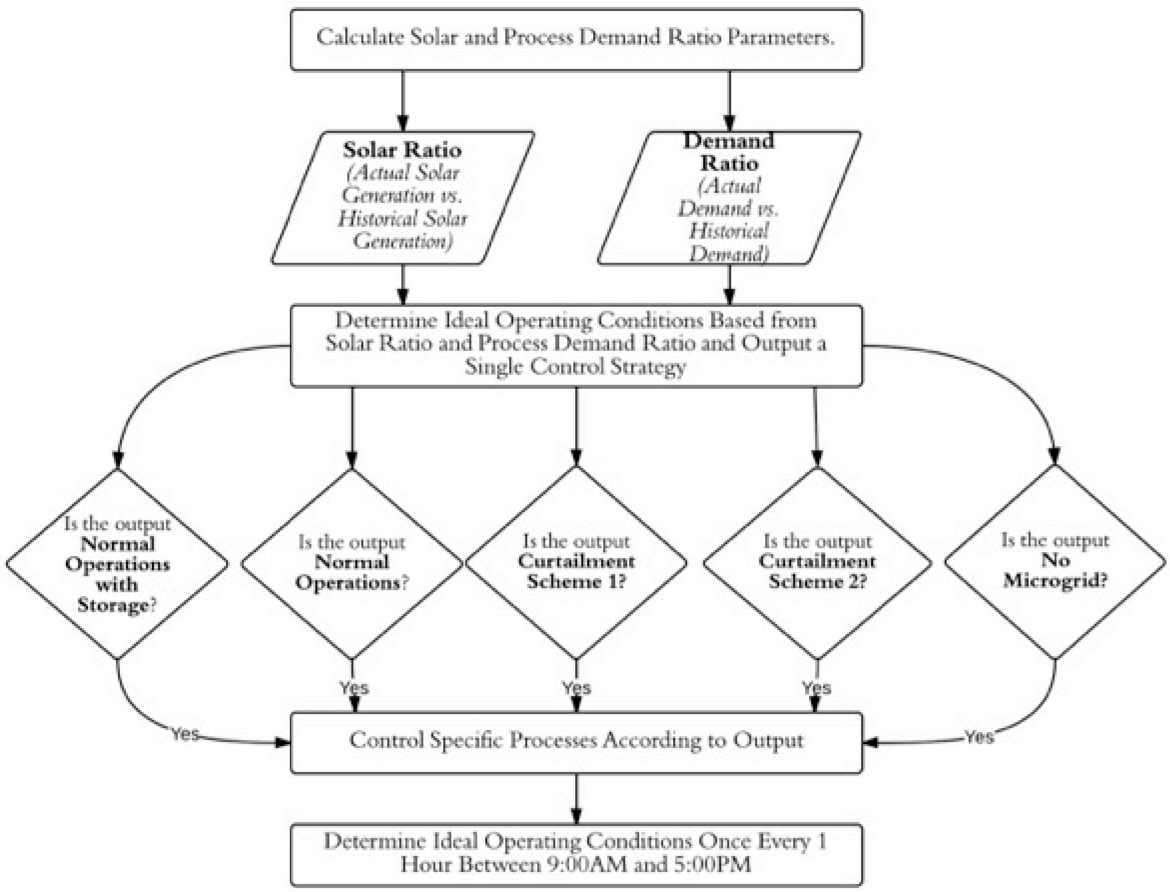

Figure 3.8 DSM Control Algorithm

CHAPTER 4. RESULTS

4.1 Electrical Consumption Reduction

To analyze the impact of the DSM program and microgrid on electrical consumption, data was measured and recorded using web-based monitoring interface WebCTRL. Load status, load energy consumption, microgrid instantaneous power, and microgrid instantaneous generation were used to evaluate the DSM program and the impact toward reducing energy consumption. A default start at 9:00a.m. was chosen to allow the DSM program to calculate the demand ratio for the first hour of operation. This default start assisted with optimally controlling the simulated processes throughout the day. The DSM program was evaluated based on three microgrid generation supplies: 80% or higher of maximum (11 kWh or greater), between 25% to 75% of maximum (between 5 and 10 kWh), and 25% or lower in relation to maximum (lower than 5 kWh).

4.1.1 Ideal Supply Generation and DSM Performance

Excellent supply generation was categorized as ideal days when solar irradiance levels were 80% of the maximum energy generation, which translates to greater than 11 kWh. During days of excellent generation from the microgrid, the DSM optimally controlled the simulated process depending on microgrid generation and process demand.

On days when morning cloud cover was in the area, the DSM algorithm curtailed one or two pumps, but as the day progressed and improved, normal operations was decided and enabled.

Figure 4.1 summarizes the DSM algorithm in operation for one day. This trend is taken from WebCTRL and there are three sections to the figure. The first section is the on/off status of Pumps A, B, C, and D. Wthin this section the end-user can see whether when the pumps are in normal operation or curtailments throughout the day. The second section is the instantaneuos solar power in watts generated over the course of a day. The last section is the cumulative energy generated from the microgrid for the day in kilowatt-hours (kWh).

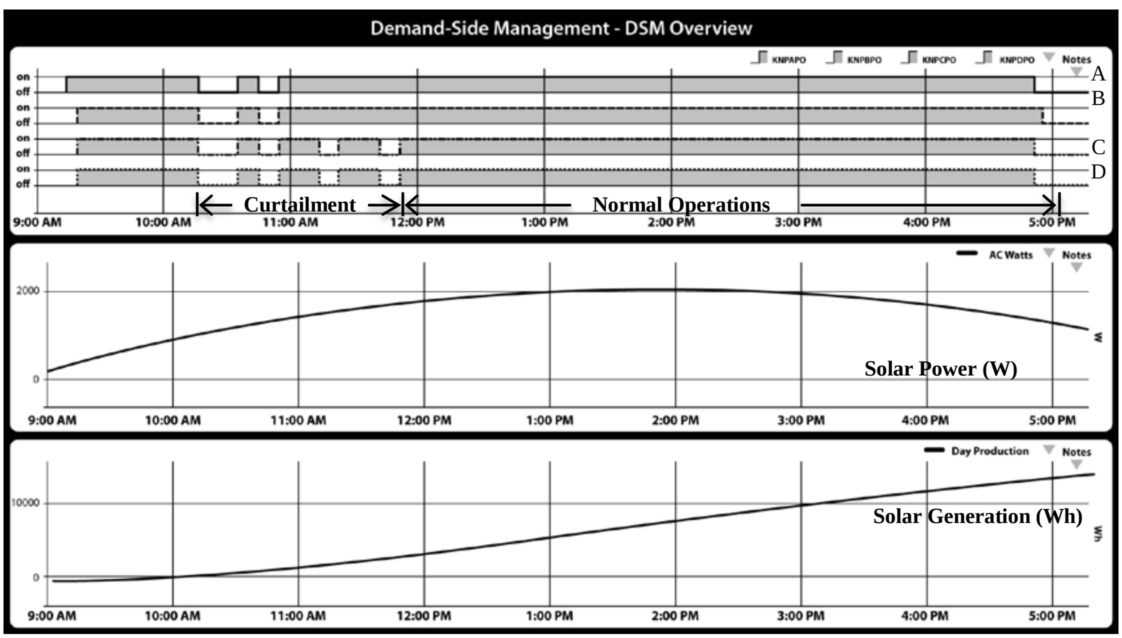

Figure 4.1 DSM Decision Summary for Excellent Generation Day

Figure 4.1 is an example of an excellent day for renewable energy in the DSM algorithm. The microgrid generation for the day totaled at 14 kWh, but between 9:00 a.m. and 11:00 a.m. there was cloud cover and the power generation was low. The DSM algorithm recognized this and intellengently enabled a curtailment scheme for Pump B, C, and D between 10:00 a.m. and 11:00 a.m. As the day progressed, the DSM algorithm intelligently controlled pumps C and D on a curtailment until 12:00 p.m. when sufficient energy generation was measured and the DSM program enabled normal operations for the remainder of the day.

Figure 4.2 presents the consumption levels of the thermal process during the excellent supply generation day as kWh versus time of day. The baseline consumption without the DSM program or microgrid is depicted as the solid line, overall consumption with the DSM program enabled is depicted as the dotted line, and consumption with the DSM and microgrid is depicted as the dashed line. During days of excellent generation from the microgrid, the DSM optimally controlled the simulated process depending on microgrid generation and process demand. With the DSM program enabled, overall energy consumption was reduced from 66 kWh to 58 kWh, a 12% reduction. Microgrid supply for this day was 14 kWh; this reduced average overall consumption even more from 58 to 44 kWh, a 29% reduction from the baseline consumption 66 kWh. Overall total electric reduction from the baseline is 22 kWh for this day.

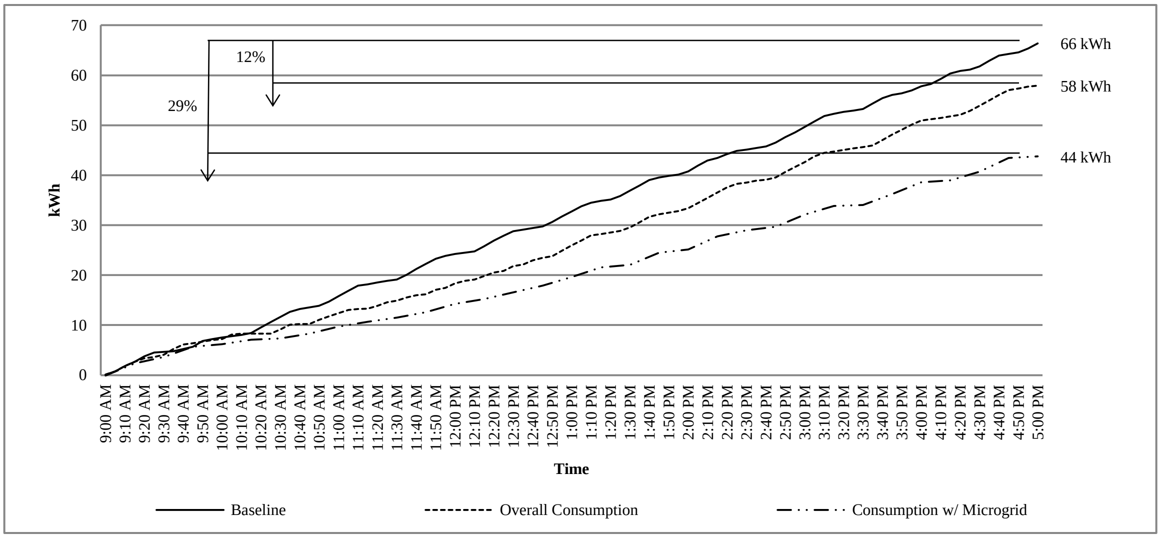

Figure 4.2 Consumption Reduction with Excellent Supply Generation

4.1.2 Optimal Supply Generation and DSM Performance

During days when microgrid generation ranged between 25% and 75% of maximum, weather conditions were partly cloudy or cloudy throughout the day. These days were labeled as “Good” supply generation days. Though weather conditions were not ideal, the DSM algorithm intelligently controlled the simulated processes to reduce energy consumption and enabled curtailments due to lower microgrid generation.

As shown in Figure 4.3, normal oprations were enabled from 9:00 a.m. to 12:00 p.m., due to steady microgrid generation. As the day progressed, the DSM program recognized a change in generation at 12:00 p.m., this is noticed by the dip in solar power generation around 12:00 p.m. The DSM algorithm enabled curtailment strategies for pump A, B, C, and D at 12:00 p.m., but supply was determined to be enough to run pump A at normal operations for the remainder of the day after 1:00 p.m. Pump B, C, and D remained in curtailment until 4:00 p.m. when Pump B was ran at normal operations until 5:00 p.m.

Figure 4.4 presents the consumption levels for the thermal process from Figure 7 above. Despite having lower energy generation than an excellent day, the DSM algortihm continued to optimally control the simulated process and lower energy consumption overall from the utility. With the DSM program enabled, average overall energy consumption was reduced from 66 kWh to 45 kWh. This reduction resulted in a 32% reduction from the baseline. Microgrid supply for the day was 8 kWh, this reduced average overall consumption even more from 45 to 37 kWh, a 44% reduction from the baseline consumption 66 kWh. Overall total electric reduction from the baseline is 29 kWh for this day

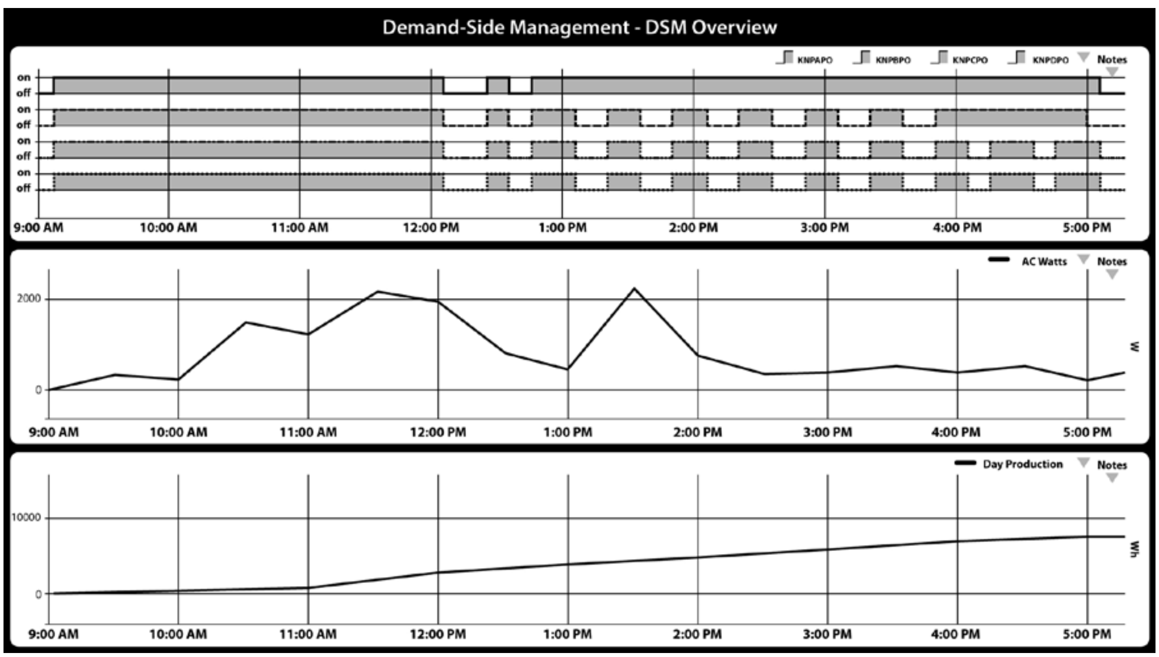

Figure 4.3 DSM Decision for Good Generation Day

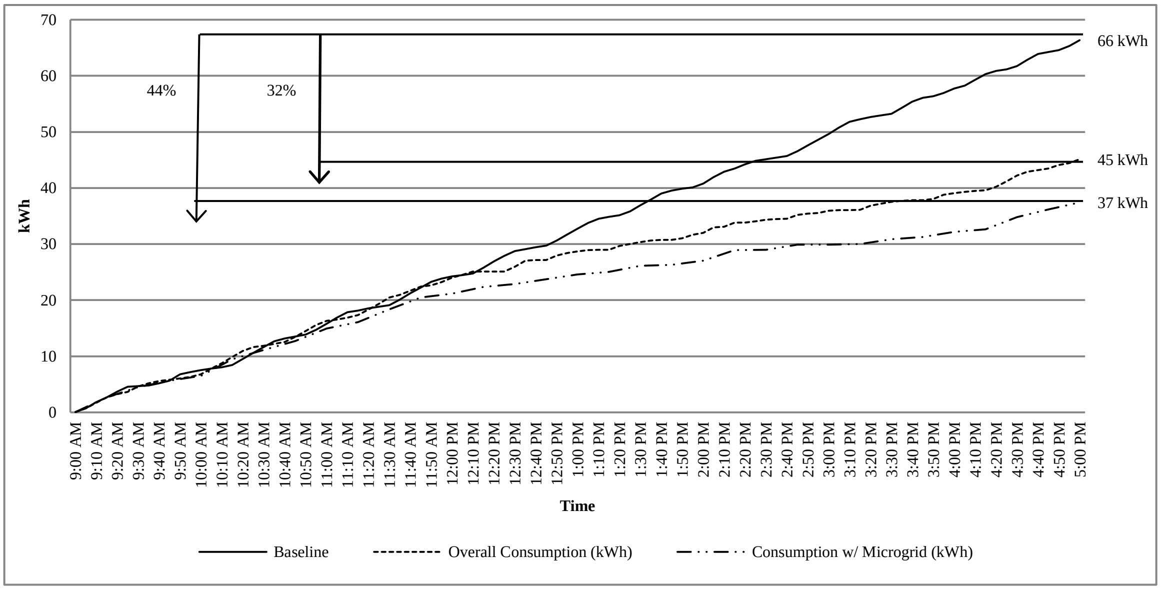

Figure 4.4 Consumption Reduction with Good Supply Generation

4.1.3 Less than Optimal Supply Generation and DSM Performance

During days when microgrid generation supplied less than 25% of maximum, weather conditions were mostly cloudy or raining throughout the day. These days were labeled as "Poor" supply generation days. Figure 4.5 presents the performance of the DSM algorithm during a day with poor generation.

As seen in Figure 4.5, at 10:00 a.m. the DSM program enabled curtailment for all pumps until 1:00 p.m. when pump A was enabled to run at normal operations for the remainder of the day. Pumps B, C, and D continued on a curtailment startegy for the remainder of the day due to the supply not meeting the demand of the process.

Figure 4.6 presents consumption levels for the day used for Figure 9. During this day, the overall electrical consumption using the DSM program was reduced to 28 kWh, a 58% reduction from baseline. Microgrid supply for this day was 2 kWh, this reduced average overall consumption from 28 to 25 kWh, a 61% reduction from the baseline.

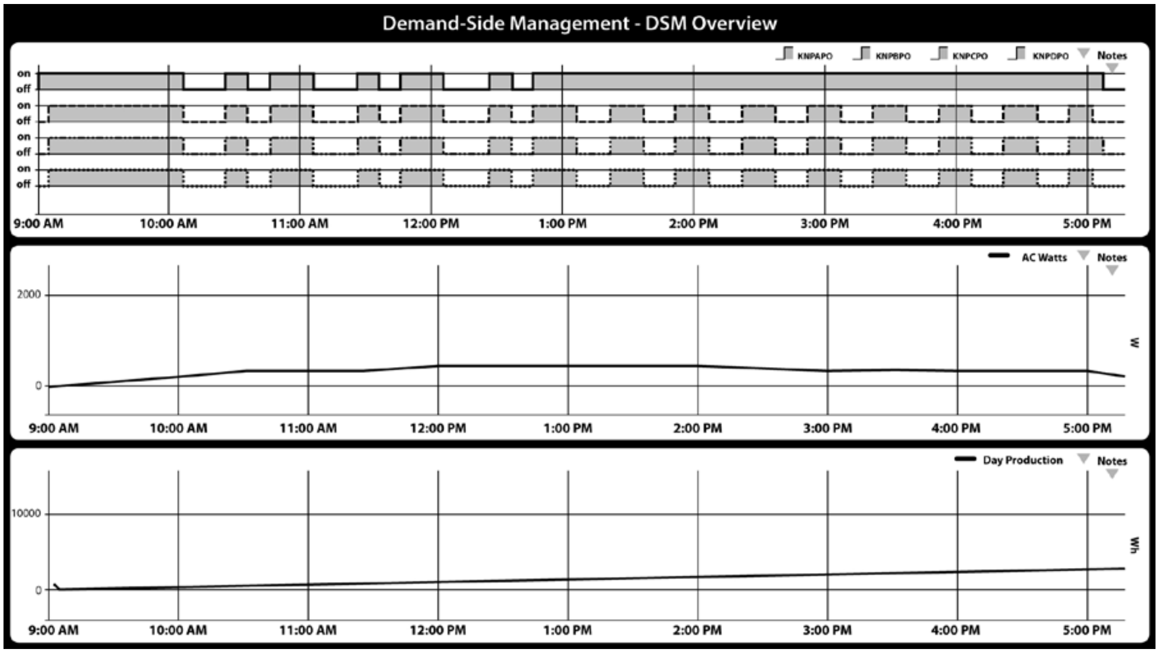

Figure 4.5 DSM Decision for Poor Generation Day

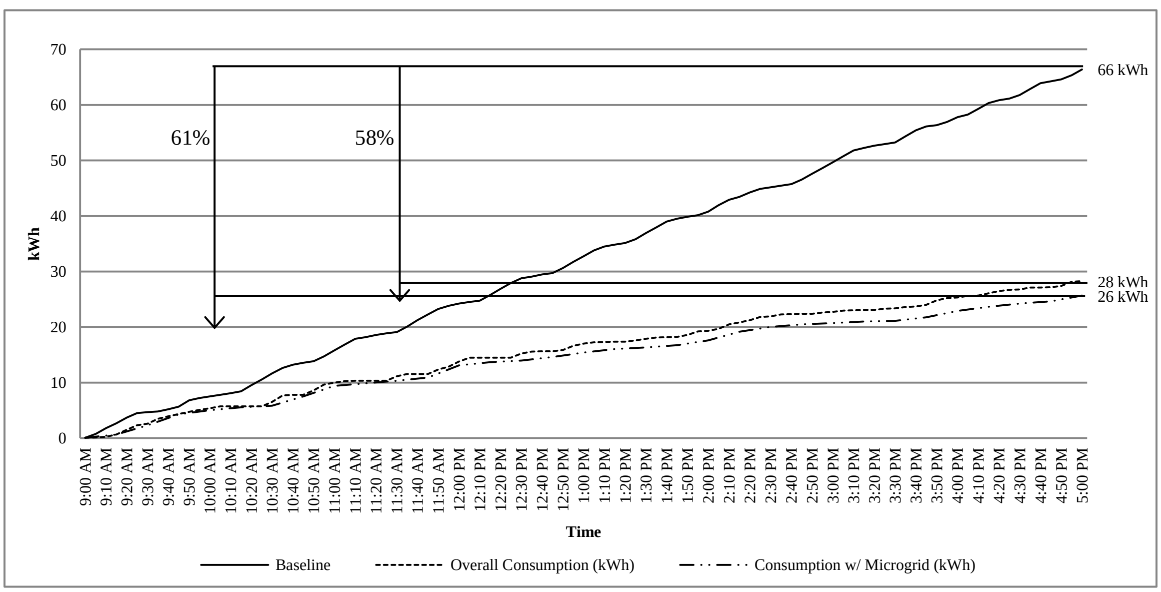

Figure 4.6 Consumption Reduction with Poor Supply Generation

4.2 Peak Demand Reduction

To analyze the impact of the DSM program and microgrid on peak demand, similar data was measured and recorded using web-based monitoring interface WebCTRL. Figure 4.7 presents the baseline peak demand for the thermal process without the DSM and microgrid, the peak demand with only the DSM enabled, and the peak demand with DSM and microgrid enabled. The baseline peak demand is the top solid black line and stays at a constant peak of 20.2 kW without the DSM program and microgrid. The middle dash-dot line is the peak demand using only the DSM program. Due to the algorithm optimally controlling the thermal process, the peak demand fluctuated from day to day. The bottom dashed line is the peak demand using the DSM and the Microgrid.

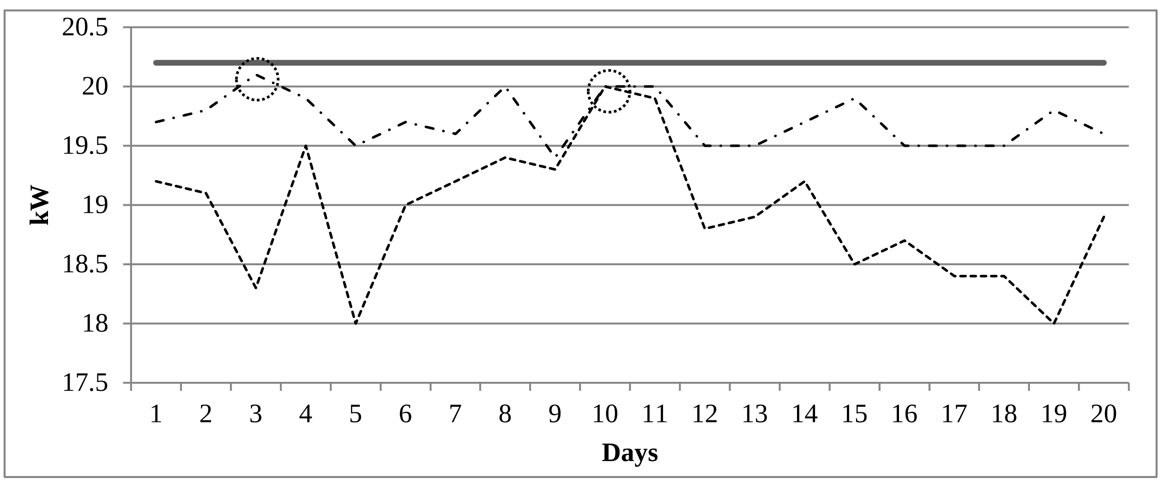

Figure 4.7 Peak Demand Reduction

This data shows the potential of demand reduction with the use of a microgrid and DSM program. Peak demand is the critical parameter because it is a real time variable that has a large impact on the cost of energy at a manufacturing facility. With the DSM program enabled, the highest peak recorded was 20.1 kW on Day 3, resulting in a .5%

reduction from the baseline of 20.2 kW. With the microgrid enabled along with the DSM, the highest peak demand was 20 kW on Day 10, a 1% reduction.

As previously stated, peak demand has a large impact on the cost of energy at a manufacturing facility. With the DSM and microgrid, the peak demand of the thermal process was reduced by 1%. Despite recording days with an 11% reduction, the performance objective of reducing peak demand by 5% was not achieved. During a billing period, it only takes one day when solar irradiance is poor to affect the demand reduction capabilities. To achieve further demand reduction, energy storage should be introduced and integrated. The use of energy storage should assist with managing peak demand during peak-hours. Depending on the peak storage capacity, this should result in further cost reduction, separate from consumption.

4.3 Statistical Analysis: ANOVA *f*-test

Statistical hypothesis tests were performed on the raw data for electrical consumption and peak demand. A one-way analysis of variance (ANOVA) *f*-test was conducted for electrical consumption and peak demand reduction, with three independent groups, Baseline, DSM, and Microgrid. A hypothesis test for regression slope *t*-test was conducted on the relationship between MI vs. MO. SAS Statistical Software was used to test the independent and dependent variables for each analysis.

4.3.1 Electrical Consumption Statistical Analysis

An one-way analysis of variance (ANOVA) test was used to understand whether kWh consumption differed based on consumption total for the day, using three independent groups; Baseline, DSM, & Microgrid. The ANOVA test determines whether there are differences between group's means in the population. This test normalizes the data collected as a sample in a laboratory setting. The null and alternative hypotheses are as follows for this test:

H_o: all group's means are equal

$$H_o:\ \mu_1 = \mu_2 = \mu_3 = \ldots = \mu_k$$

H_a: at least one group mean is different

$$H_a:\ \mu_1 > \mu_2 > \mu_3 = \ldots = \mu_k$$

To insure that the ANOVA test was valid, the dataset was tested for normality and to detect outliers based on statistical assumptions. Assumption 1 is the dependent variable should be continuous; the dependent variable for this test is measured in minutes. Assumption 2 states that the independent variable should have two or more categorical, independent groups. There are three independent groups for the ANOVA test, Baseline Consumption, DSM Consumption, and Microgrid Consumption. Assumption 3 states that there should be no relationship between the observations in each group or between the groups. Figure 4.8 is a boxplot output from SAS that was used to detect outliers for the ANOVA test. The boxplot displays, as horizontal lines from bottom up, the minimum, the 25th percentile, the median, the 75th percentile, and the maximum-recorded consumption, lastly the mean depicted by a diamond symbol. As seen in Figure 4.8, there are no outliers in the data, as assessed by inspection of the boxplot for values greater than 1.5 box-lengths from the edge of the box.

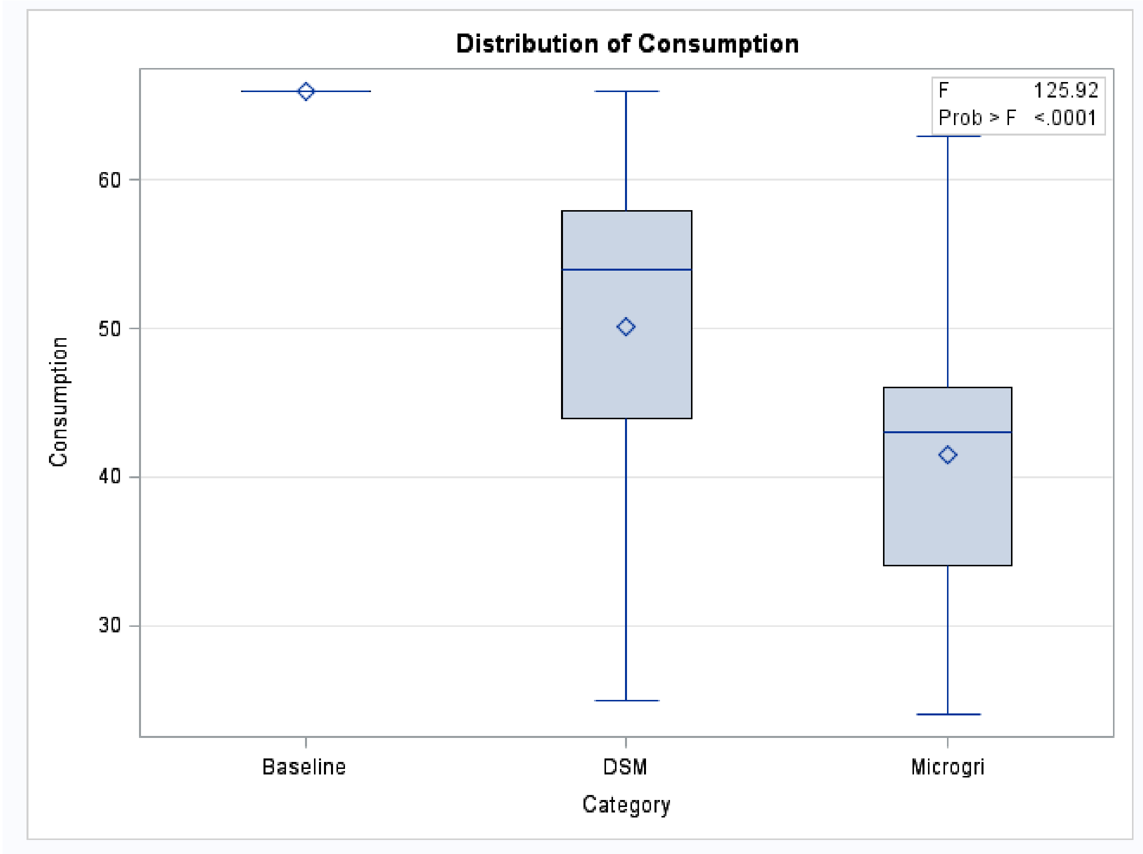

Figure 4.8 SAS Boxplot Graph Output for Electrical Consumption based one Baseline Consumption, DSM Consumption, and Microgrid Consumption

To accurately analyze the differences in means, Table 4.1 presents the descriptive statistics for the Baseline, DSM, and Microgrid consumptions. The means (with standard deviations in parentheses) for Baseline, DSM, and Microgrid consumptions were 66 (0), 50.1 (11.2), and 41.4 (9.7), respectively. Table 4.2 shows the output of the ANOVA analysis used to determine if there is a statistically significant difference between the groups means. The significance level is 0.001 (p = 0.001), which is well below $\alpha = 0.05$. Therefore, there is a statistically significant difference in the mean electrical consumption between Baseline, DSM, and Microgrid.

Table 4.1 Descriptive Statistics for Electrical Consumption

	N	***Mean***	***Std. Deviation***	***Minimum***	***Maximum***
Baseline	59	66	0	66	66
DSM	59	50.1	11.2	25	66
Microgrid	59	41.5	9.7	24	63

Table 4.2 ANOVA Results for Electrical Consumption

	Sum of Squares	***df***	***Mean Square***	***F***	***P-Value***
Between Groups	18286.15	2	9143.07	125.92	<.0001
Within Groups	12634.03	174	72.61		
Total	30920.18	176			

Based on the results, there was a statistically significant difference between groups as determined by one-way ANOVA ($F(2,174) = 125.92$, $p = 0.0001$). A Bonferroni correction revealed that the electrical consumption statistically lowered after using the DSM program (50.1 ±11.2, $p<0.05$) and DSM/Microgrid program (41.5 ±9.7, $p<0.05$) compared to the baseline program (66 ±0), as shown in Table 4.3.

Table 4.3 Bonferroni Correction Multiple Comparisons for Electrical Consumption ANOVA

Consumption(A)	***Consumption(B)***	***Mean***	***LCI***	***UCI***	***Sig.***
Baseline	DSM	15.9	12.11	19.69	Yes
	Microgrid	24.54	20.75	28.34	Yes
DSM	Baseline	-15.898	-19.69	-12.11	Yes
	Microgrid	8.64	4.85	12.44	Yes
Microgrid	Baseline	-24.54	-28.34	-20.75	Yes
	DSM	-8.64	-12.44	-4.85	Yes

4.3.2 Peak Demand Statistical Analysis

An one-way analysis of variance (ANOVA) test was used to understand whether peak demand differed based on demand peak for the day, using three independent groups; Baseline, DSM, & Microgrid. Appendix I present the raw data input into SAS Statistic software. The null and alternative hypotheses are as follows:

H_o: all group's means are equal

$$H_o: \mu_1 = \mu_2 = \mu_3 = \ldots = \mu_k$$

H_a: at least one group mean is different

$$H_a: \mu_1 > \mu_2 > \mu_3 = \ldots = \mu_k$$

To insure that the ANOVA test was valid, the dataset was tested for normality and to detect outliers based on statistical assumptions. Assumption 1 is the dependent variable should be continuous; the dependent variable is measured in minutes. Assumption 2 states that the independent variable should have two or more categorical, independent groups. There are three independent groups for the ANOVA test, Baseline peak demand, DSM peak demand, and Microgrid peak demand. Assumption 3 states that there should be no relationship between the observations in each group or between the groups Figure 4.9 is a boxplot output from SAS that was used to detect outliers for the ANOVA test. The boxplot displays from bottom to top the minimum, the 25th, the median, the 75th, and the maximum-recorded demand, also depicted by a diamond symbol is the mean. As seen in Figure 4.9, there are no outliers in the data, as assessed by inspection of the boxplot for values greater than 1.5 box-lengths from the edge of the box.

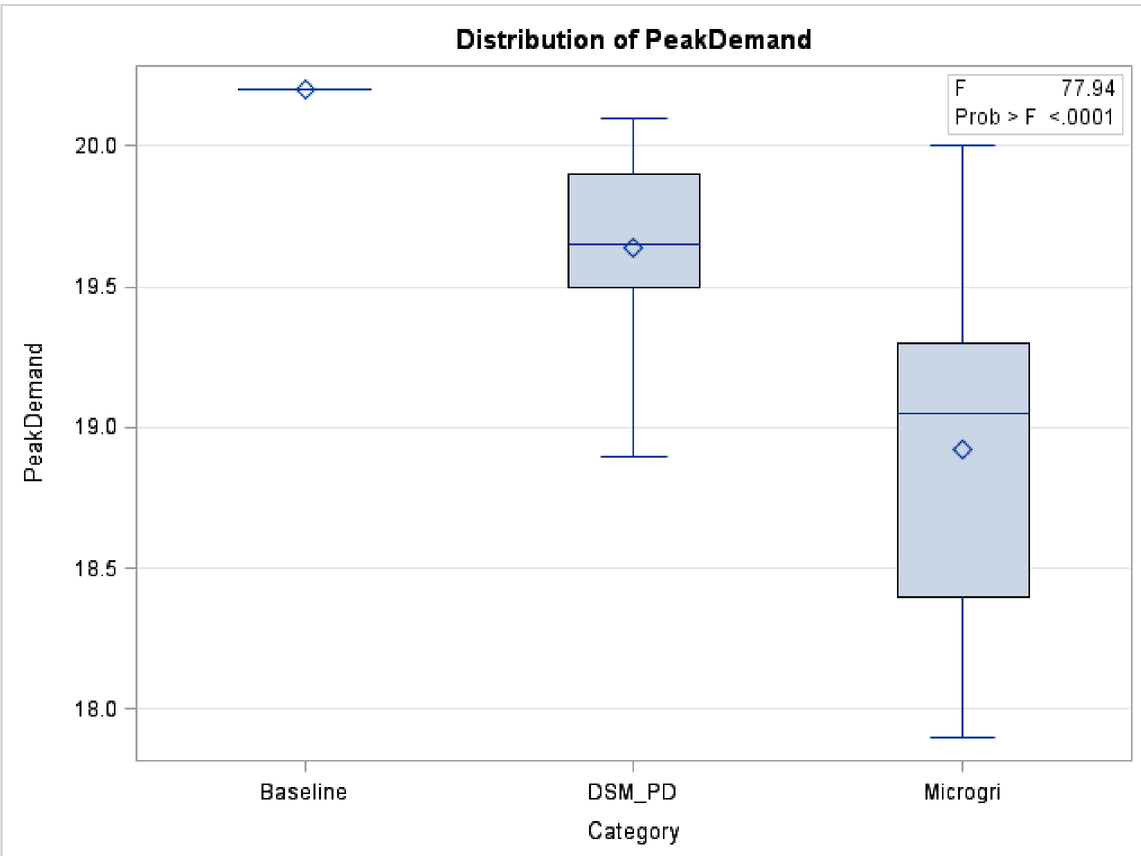

Figure 4.9 SAS Boxplot Graph Output for Peak Demand based one Baseline Consumption, DSM Consumption, and Microgrid Consumption

Similar to the analysis of electrical consumption reduction, Table 4.4 presents the descriptive statistics for the Baseline, DSM, and Microgrid. The means (with standard deviations in parentheses) for Baseline, DSM, and Microgrid were 20.2 (0), 19.6 (.28), and 18.9 (.57), respectively. Table 4.5 shows the output of the ANOVA analysis used to determine if there is statistically significant difference between the groups means. The significance level is 0.001 (P = o.oo1), which is well below α = 0.05. Therefore, there is a statistically significant difference in the mean peak demand between Baseline, DSM, and Microgrid.

Table 4.4 Descriptive Statistics for Peak Demand

	N	***Mean***	***Std. Deviation***	***Minimum***	***Maximum***
Baseline	26	20.2	0	20.2	20.2
DSM	26	19.6	0.28	18.9	20.1
Microgrid	26	18.9	0.57	17.9	20.0

Table 4.5 ANOVA Results for Peak Demand

	Sum of Squares	***df***	***Mean Square***	***F***	***P-Value***
Between Groups	21.30	2	10.64	77.94	<.0001
Within Groups	10.25	75	0.14		
Total	31.55	77			

Based on the results, there was a statistically significant difference between groups as determined by one-way ANOVA (F (2,75) = 77.94, p = 0.0001). A Bonferroni correction revealed that the electrical peak demand statistically lowered after using the DSM program (19.6 ±0.28, p<0.05) and DSM/Microgrid program (18.9 ±0.57, p<0.05) compared to the baseline program (66 ±0), as shown in Table 4.6.

Table 4.6 Bonferroni Correction Multiple Comparisons for Peak Demand ANOVA

PeakDemand(A)	***PeakDemand(B)***	***Mean***	***LCI***	***UCI***	***Sig.***
Baseline	DSM	0.56	.31	.81	Yes
	Microgrid	1.27	1.03	1.53	Yes
DSM	Baseline	-0.56	-0.81	-0.31	Yes
	Microgrid	0.72	0.46	0.97	Yes
Microgrid	Baseline	-1.28	-1.53	-1.03	Yes
	DSM	-0.72	-0.97	-0.46	Yes

4.4 Success Criteria Outcomes

The results show that a real-time management of a manufacturing process with a microgrid will reduce electrical consumption and peak demand. The renewable energy system for this research was rated to provide up to 13% of the total manufacturing capacity. With actively managing the process loads with the DSM program alone, electrical consumption from the utility grid was reduced by 24% on average. An additional 13% reduction was accomplished when the microgrid and DSM program was enabled together, resulting in a total reduction of 37% on average. On average, peak demand was reduced by 6%, but due to the intermittency of the renewable source and the billing structure for peak demand, only a 1% reduction was obtained.

For project objective two the success criteria for peak demand reduction was 5%. For this study results showed that peak demand reduced only 1% but did see days where reduction was at 6%. But due to the nature of how peak demand is recorded, 6% reduction could not be justified. Performance objective three address electrical consumption and has a success criteria of 15%. The microgrid was rated at 13% and during this study a 13% reduction was achieved, not achieving the 15% goal. But, with enabling the DSM an extra 24% of reduction was achieved making a total of 37% reduction. The next chapter will discuss performance objective one and conclude with future opportunities for this research.

CHAPTER 5. DISCUSSION & CONCLUSION

5.1 Impact of DSM/Microgrid on Manufacturing Process

The performance objective for this research was to show that the combination of a microgrid and DSM controls could help maintain manufacturing at close to full capacity. A threshold of 70% was targeted as a reasonable goal, as opposed to facilities around the world that are forced to shut down due to poor electrical grid systems. Figure 5.1 evaluates the impact of the microgrid in terms of achieving the 70% goal for Manufacturing Intensity (MI).

The horizontal axis of Figure 5.1 is the Microgrid Output (MO). This ratio compares the MO for one day as compared to its expected output. The values for MO exceeded 100% due to high irradiance levels that can sometimes exceed the expected generation during the respective month. The vertical axis of Figure 5.1 is MI, which is the ratio of the overall consumption for one day with the demand-limiting algorithm and microgrid in operation as compared to manufacturing demand with no controls in place. By definition, MI varies from 0 to 100%.

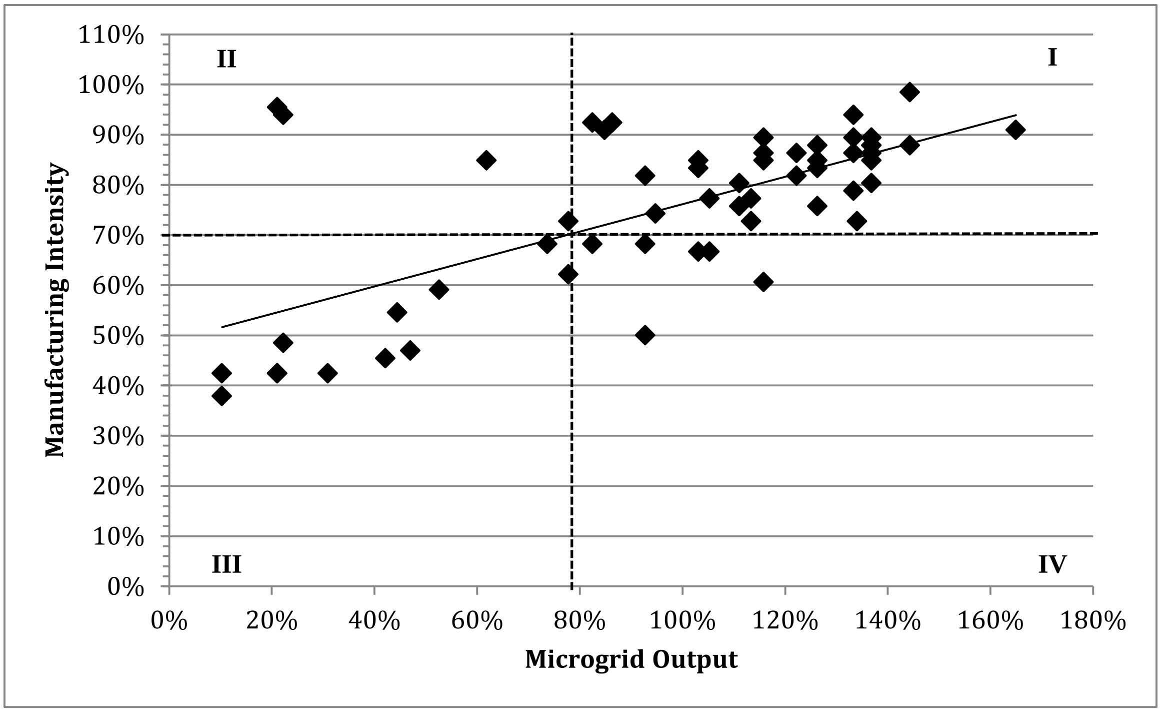

Figure 5.1 Impact of Microgrid and DSM on Manufacturing Process.

Figure 5.1 illustrates that the goal of 70% MI was achieved more frequently when MO was above 80% of its expected output, as shown in quadrant I. Dashed lines were used to annotate the 70% manufacturing intensity goal and the 80% microgrid output. On days when MO was below 80% but the MI was above 70%, as shown in quadrant II, the DSM algorithm intelligently controlled the manufacturing process to run at normal operations due to no generation sufficient enough to supply to the process. As a result we have three days than are below 80% of MO but achieve 70% of MI. Also, on days when MO was below 80%, as shown in quadrant III, the MI was below the target of 70% ranging from 40% to 50%. For days when the forecast called for morning or evening clouds, the DSM would intelligently curtail pumps to result for days when microgrid output was above 80%, but manufacturing intensity was below 70%. Not surprisingly, Figure 5.1 also shows a positive correlation for MI as a function of MO. This simply means that it is easier to meet manufacturing goals when the microgrid contributes substantially to the energy mix.

5.2 Statistical Analysis: Regression Slope *t*-test

A hypothesis test for regression slope was used to analyze the relationships between Manufacturing Intensity and Microgrid Output to answer and validate the relationship between Microgrid Output and Manufacturing Energy Intensity on controlling for the effects of the manufacturing process utilizing the Microgrid/DSM. For this analysis, the significance level was $\alpha = 0.01$. Using the sample data, a linear regression *t*-test was conducted to determine whether the slope of the regression line differs from zero. The null and alternative hypotheses are as follows:

H_o: There is no relationship between Microgrid Output and Manufacturing Intensity on the manufacturing process.

$$H_o: B_1 = 0$$

H_a: There is a relationship between Microgrid Output and Manufacturing Intensity on the manufacturing process.

$$H_a: B_1 > 0$$

Appendix J presents the raw analysis output from SAS for a regression *t*-test. The sample size was 57 observations with degrees of freedom of 55 observations. SAS outputs a slope of 0.27 with a *SE* of 0.04, therefore outputting a *t*-score test statistic of 6.86.

With a df=55, *t*-score of 6.86, and a P-value of .0001, there is evidence to reject H_o and that increased Microgrid Output increases Manufacturing Intensity. There is a

99% confidence that the true change in Manufacturing Intensity per increase in Microgrid Output is between 0.17 and 0.38. So, there is 99% confidence that at 80% of Microgrid Output, the Manufacturing Intensity is predicted to be 70.62% based on equation 1. This resulting percentage is .62% higher than the target Manufacturing Intensity of 70%.

$$y = 48.65 + 0.27x \tag{1}$$

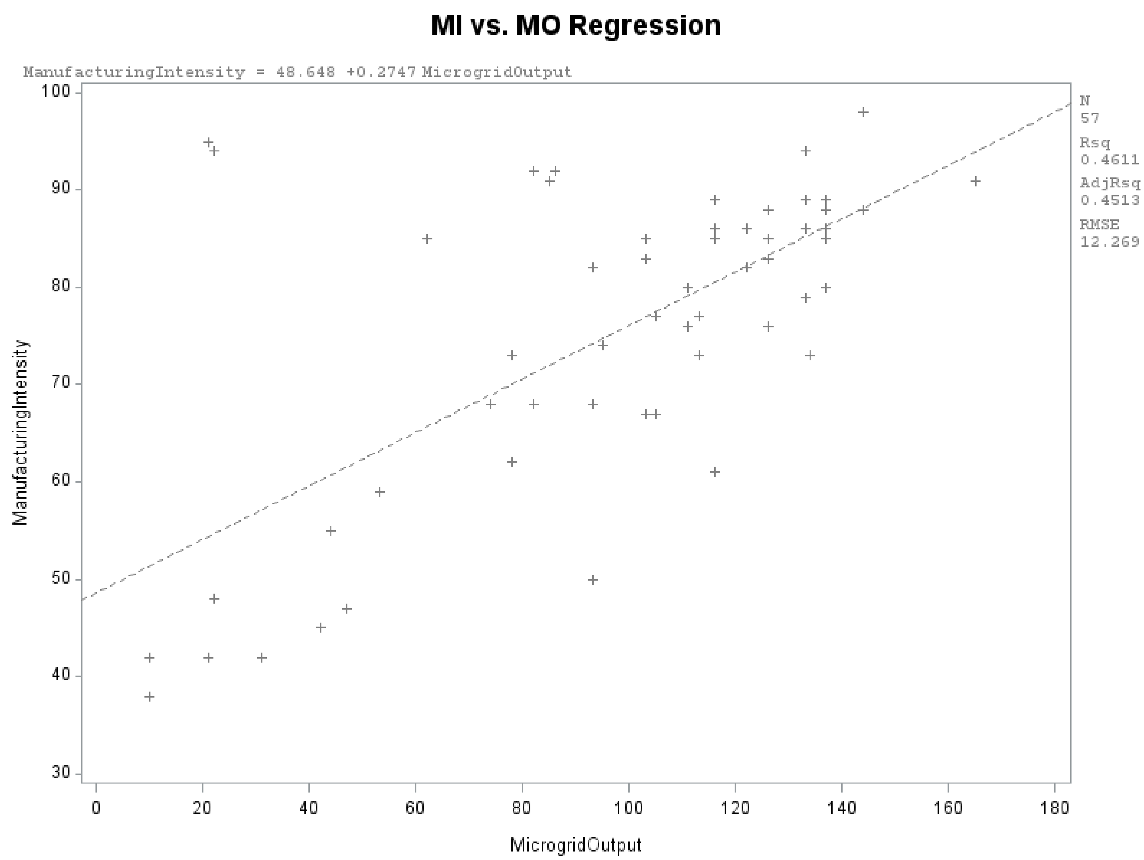

Figure 5.2 SAS Graph Output for Regression Slope Hypothesis Test

5.3 Manufacturing Scale-Up

This research evaluated the potential for using a combination of renewable energy and DSM to reduce overall energy use and also peak demand in manufacturing facilities. A significant concern is the feasibility of scaling up renewables and DSM strategies to a scale that makes sense for a much larger manufacturing enterprise. Although this project was completed in a simulated manufacturing environment, it is believed that the findings have relevance to full scale manufacturing facilities. To scale up to a manufacturing facility, utility data provided for this research was analyzed to determine baseline consumptions. Tables 5.1, 5.2, and 5.3 begin to summarize how a novel microgrid/DSM system might be scaled up in size for a manufacturing enterprise.

Table 5.1 presents the microgrid scale-up from a prototype to a full-scale system suitable for a manufacturing facility. The prototype microgrid was rated at 13% of power required for the process loads. Using this scaling factor, a solar component of a microgrid should be sized to provide 13% of 75,000 MWh. It was calculated that 13% of 75,000 MWh is 9,500 MWh, as seen in Table 5.1. So the solar component of the microgrid has to generate 9,500 MWh for the year.

Table 5.1 Microgrid Scale-Up for Lafayette, IN

Prototype		**Full Scale Projection**	
System Size (kW)	*Annual Electric Generation (kWh)*	*System Size (MW)*	*Annual Electrical Generation (MWh)*
3	3,100	8	9,500

The system size was calculated by dividing annual generation by 365 days to get a daily generation need. Depending on the location of the facility, the daily need is divided by the amount of average sun-hours to obtain the kW AC need from the solar system. Due to different efficiency losses in solar energy systems there is an overall 20% power loss when converting from DC to AC. The kW AC need has to be divided by a derate factor to boost the power output 20% for DC. For this facility an 8 MW solar PV energy system is recommended to provide 13% of the annual need. This system size would need 18 acres of land space for a ground mount system or 780,000 square feet of roof space for a fix mounted roof system. For purposes of comparison, a 1 MW system would cover 9,120 m^2 or 2 acres or 98,000 ft^2.

Table 5.2 shows the impact of the microgrid/DSM on manufacturing in Lafayette, IN. As shown in Table 5.2, there is Prototype setting and a Full Scale Projection for electrical consumption. There was a baseline of 75,000 MWH for the full-scale projection of annual electrical consumption. There is no reduction with the baseline. When the DSM is enabled the annual manufacturing electric consumption was reduced to 57,000 MWh. This was a reduction of 24% from the baseline of 75,000 MWh. Reduction was further reduced when the microgrid was enabled along with the DSM. For this facility, annual electric consumption was reduced to 47,300 MWh, a 37% reduction from the baseline of 75,000 MWh. Therefore resulting in a projected total reduction of 27,750 MWh at a 37% reduction.

Table 5.2 Impact of Microgrids/DSM on Manufacturing in Lafayette, IN

	Prototype		**Full-Scale Projection**	
	Electric Consumption (kWh)	*Annual Electric Consumption (kWh)*	*Reduction (%)*	*Annual Manufacturing Electric Consumption (MWh)*
Baseline	*66.0*	*24,100*	*0%*	*75,000*
DSM	50.1	18,300	24%	57,000
Microgrid	41.5	15,100	37%	47,300
Total Reduction	24.5	8,950	-37%	27,800

The same facility has a peak of 12 MW with no DSM or microgrid enabled. With the DSM enabled the projected annual peak demand reduction is .5% at 11.9 MW. When the DSM and Microgrid were enabled it is projected that the annual peak demand be reduced to 11.8 MW, a 1% reduction from baseline. This results in a projected total reduction of .1 MW at a 1% reduction.

Table 5.3 Impact of Microgrids/DSM on Manufacturing on Peak Demand

	Prototype		**Full-Scale Projection**	
	Peak Demand (kW)	*Annual Peak Demand (kW)*	*Reduction (%)*	*Annual Manufacturing Peak Demand (MW)*
Baseline	20.2	20.2	0%	12.0
DSM	20.1	20.1	0.50%	11.9
Microgrid	20.0	20.0	1%	11.8
Total Reduction	0.2	0.2	-1%	0.1

5.4 Seasonal Variations

Electrical consumption and Manufacturing Intensity should see a difference during seasonal variations. This research began and ended in the spring, and didn't fully explore the affects of seasonal variations. It is expected to have higher electrical consumption and peak demand reduction with higher MI during the summer months when days are longer and solar irradiance is more intense. Figure 5.3 shows daily energy reduction and consumption per bar graph. Starting from the bottom up, the black bar shows the amount power consumed from the utilities in kWh. The green bar is the green power generated by the microgrid in kWh. Lastly, the grey bars are the DSM reduction, from the initial baseline of 66 kWh. There are no generic trends in the data shown in Figure 5.3, but the research is aware that different seasons bring different irradiance intensity levels and length of days. Also, the researcher is aware based on the results of this study that when solar resources increase than manufacturing intensity or process output increase. So during the summer months manufacturing intensity would be in the higher percentage while in the winter months manufacturing intensity will be lower. This leads to the next section of future opportunities to better manage the microgrid and process loads.

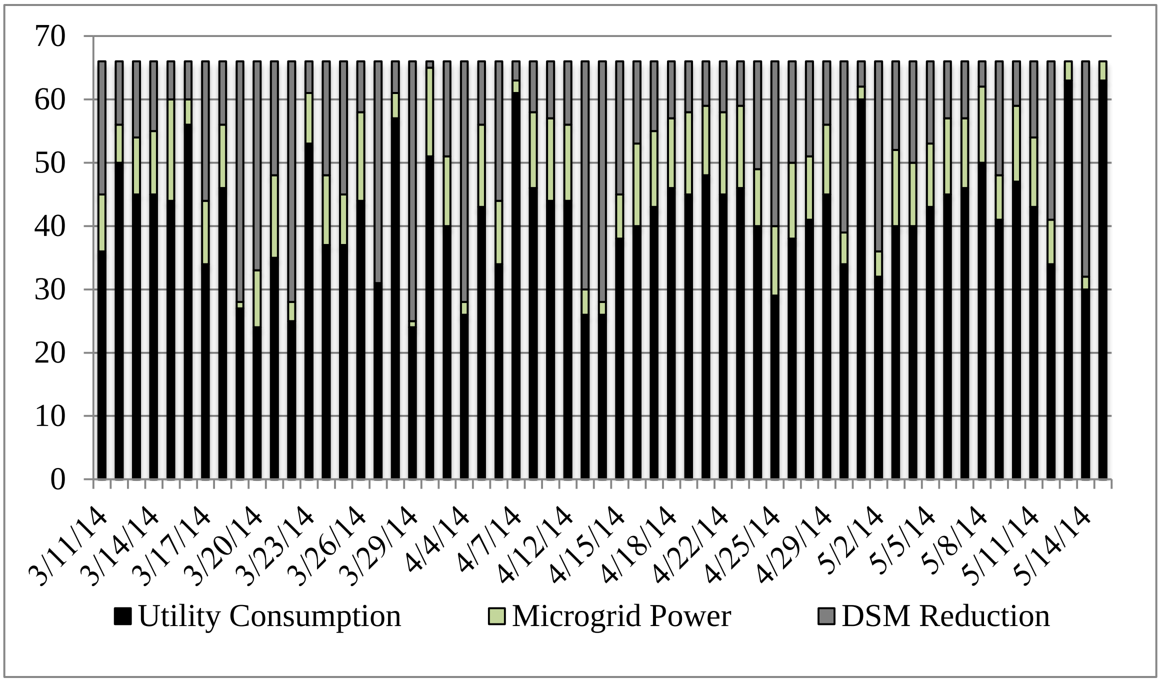

Figure 5.3 Daily Energy Consumption and Reduction

5.5 Future Opportunities

In this case, it was concluded that the DSM algorithm provided an extra buffer to help achieve higher reduction levels, as oppose to using a standalone microgrid system with no management program. Though levels of peak demand reduction were low, opportunities for designing and integrating an energy storage system could address and further enhance the reduction of peak demand.

Figures 5.1 and 5.2 begin to provide insight into the required mix of renewables and DSM to maintain a reasonable level of MI. Equation 1, allows a predictability opportunity with predicting expected Manufacturing Intensity with expected Microgrid Output. It was recognized that when MO was above 80% of expected output, MI would be predicted to be above the threshold of 70% of full capacity. Further refinement of the DSM program should be explored to forecast MO so facility engineers can predict their MI to stay above a designated threshold.

REFERENCES

REFERENCES

3M Company, & U.S. Department of Energy. (2003, June). 3M: Hutchinson Plant Focuses on Heat Recovery and Cogeneration during Plant-Wide Energy Efficiency Assessment. U.S. DOE Industrial Technologies Clearinghouse. Retrieved from https://www1.eere.energy.gov/manufacturing/tech_deployment/pdfs/ch_cs_3m_pwa.pdf

Abou-Elnour, A., Murad, F. S., Al-Tayasna, I. S., & Abo-Elnor, O. (2013). Smart integrated energy monitoring and management system for standalone photovoltaic systems (Vol. 8688, p. 86882Q–86882Q–7). doi:10.1117/12.2009984

Aki, H. (2010). Independent hybrid renewable energy systems: Example applications around the world. In *2010 IEEE Power and Energy Society General Meeting* (pp. 1–4). doi:10.1109/PES.2010.5589565

Andrews, R., & Pearce, J. M. (2011). Environmental and economic assessment of a greenhouse waste heat exchange. *Journal of Cleaner Production*, *19*(13), 1446–1454. doi:10.1016/j.jclepro.2011.04.016

Barbose, G., Darghouth, N., Weaver, S., & Wiser, R. (2013). *Tracking the Sun VI: An Historical Summary of the Installed Price of Photovoltaics in the United States from 1998 to 2012* (No. LBNL-6350E) (p. 70). Berkeley: Lawrence Berkeley National Laboratory. Retrieved from http://emp.lbl.gov/sites/all/files/lbnl-6350e.pdf

Bhattacharjee, K. (2010). Energy Conservation Opportunities in Industrial Waste Heat Recovery Systems. *Energy Engineering*, *107*(6), 7–13.

Bozchalui, M. C., & Sharma, R. (2012). Optimal operation of commercial building microgrids using multi-objective optimization to achieve emissions and efficiency targets. In *2012 IEEE Power and Energy Society General Meeting* (pp. 1 –8). doi:10.1109/PESGM.2012.6345600

Byrne, J., Hegedus, S., & Wang, Y.-D. (1994). Photovoltaics as a demand-side management technology: An analysis of peak-shaving and direct load control options. *Progress in Photovoltaics: Research and Applications*, *2*(3), 235–248. doi:10.1002/pip.4670020308

Carter, J. (2011). Sustainable Engineering: Energy master plan reduces cots. *Plant Engineering*. Retrieved from http://search.proquest.com/docview/1022968770?accountid=13360

Chun, Y., & Bidanda, B. (2013). Sustainable manufacturing and the role of the International Journal of Production Research. *International Journal of Production Research*, 1–8. doi:10.1080/00207543.2012.762135

Ding, L., Qiu, X. L., Mullineux, G., & Matthews, J. (2010). The Development of the Sustainable Manufacturing Processes. *Advanced Materials Research*, *118-120*, 767–774. doi:10.4028/www.scientific.net/AMR.118-120.767

Dohn, R. (2011). *The business case for microgrids White paper: The new face of energy Modernization* (p. 9). Siemens.

Farrell, J. (2012, December). *Commercial Rooftop Revolution*. *Institute for Local Self-Reliance*. Retrieved February 23, 2013, from http://www.ilsr.org/commercial-roofop-revolution/

Gibbs, S. (2012, January). Pacific Alloy Harnesses Sun's Power. *Modern Casting*, 35–37.

Hall, D. (2013). *Webinar Series: Manufacturing Opportunities in Clean Energy Markets*. Retrieved from www.thecemc.org

Holmberg, D., Ghatikar, G., Koch, E., & Boch, J. (2012). OpenADR Advances. *ASHRAE Journal*, B16–B19.

Kroposki, B., Lasseter, R., Ise, T., Morozumi, S., Papatlianassiou, S., & Hatziargyriou, N. (2008). Making microgrids work. *IEEE Power and Energy Magazine*, *6*(3), 40–53. doi:10.1109/MPE.2008.918718

Leahu-Aluas, S., & Burstein, E. P. R. (2010). Sustainable Manufacturing: An Essential Component of the Global "Clean" Economy. *Manufacturing Engineering*, *145*(1), 13–14.

Li, J., Zhang, X., & Li, W. (2009). An efficient wind-photovoltaic hybrid generation system for DC micro-grid. In *8th International Conference on Advances in Power System Control, Operation and Management (APSCOM 2009)* (pp. 1–6). doi:10.1049/cp.2009.1790

Liyanage, K. M., Manaz, M. A. M., Yokoyama, A., Ota, Y., Taniguchi, H., & Nakajima, T. (2011). Impact of communication over a TCP/IP network on the performance of a coordinated control scheme to reduce power fluctuation due to distributed renewable energy generation. In *2011 6th IEEE International Conference on Industrial and Information Systems (ICIIS)* (pp. 198–203). doi:10.1109/ICIINFS.2011.6038066

Lunt, P., & Levers, A. (2011). *Reducing Energy Use in Aircraft Component Manufacture - Applying Best Practice in Sustainable Manufacturing* (No. 2011-01-2739). Warrendale, PA: SAE International. Retrieved from http://digitallibrary.sae.org.ezproxy.lib.purdue.edu/content/2011-01-2739

Managing Energy Costs in Manufacturing Facilities | esource.com. (2012). Retrieved February 28, 2013, from http://www.esource.com/BEA1/CEA/CEA-16

Orthwein, B. (2012, July). Unlock Energy Savings with Waste Heat Recovery. U.S. DOE Advanced Manufacturing Office. Retrieved from http://www1.eere.energy.gov/manufacturing/tech_deployment/pdfs/wasteheatrecovery_factsheet.pdf

Schleicher-Tappeser, R. (2012). How renewables will change electricity markets in the next five years. *Energy Policy*, *48*, 64–75. doi:10.1016/j.enpol.2012.04.042

Shan, Z., Qin, S., Liu, Q., & Liu, F. (2012). Key manufacturing technology & equipment for energy saving and emissions reduction in mechanical equipment industry. *International Journal of Precision Engineering and Manufacturing*, *13*(7), 1095–1100. doi:10.1007/s12541-012-0143-y

Sharp. (2008a). AT&T Park Home of the San Francisco Giants. Sharp Electronics Corporation. Retrieved from http://files.sharpusa.com/Downloads/Solar/CaseStudy/sol_dow_ATTPark_Case_Study.pdf

Sharp. (2008b). Google Installs Sharp Solar Power Systems. Sharp Electronics Corporation. Retrieved from http://files.sharpusa.com/Downloads/Solar/CaseStudy/sol_dow_Google_Case_study.pdf

Sharp. (2009). Denver International Airport. Sharp Electronics Corporation. Retrieved from http://files.sharpusa.com/Downloads/Solar/CaseStudy/sol_dow_Denver_Airport_Case_Study.pdf

Singh, R., & Alapatt, G. F. (2012). Innovative paths for providing green energy for sustainable global economic growth, 848205–848205. doi:10.1117/12.928058

Spertino, F., & Corona, F. (2013). Monitoring and checking of performance in photovoltaic plants: A tool for design, installation and maintenance of grid-connected systems. *Renewable Energy*, *60*, 722–732. doi:10.1016/j.renene.2013.06.011

Stluka, P., Godbole, D., & Samad, T. (2011). Energy management for buildings and microgrids. In *2011 50th IEEE Conference on Decision and Control and European Control Conference (CDC-ECC)* (pp. 5150–5157). doi:10.1109/CDC.2011.6161051

Sunspec.org. (2013, November). Information Standards for Distributed Energy. Retrieved from http://www.sunspec.org/wp-content/uploads/2013/11/SunSpec-Backgrounder-2013.pdf

Taboada, H., Xiong, Z., Jin, T., & Jimenez, J. (2012). Exploring a solar photovoltaic-based energy solution for green manufacturing industry. In *2012 IEEE International Conference on Automation Science and Engineering (CASE)* (pp. 40–45). doi:10.1109/CoASE.2012.6386321

Weinert, N., Chiotellis, S., & Seliger, G. (2011). Methodology for planning and operating energy-efficient production systems. *CIRP Annals - Manufacturing Technology*, *60*(1), 41–44. doi:10.1016/j.cirp.2011.03.015

York, D., Kushler, M., & Witte, P. (2007). *Examining the Peak Demand Impacts of Energy Efficiency: A Review of Program Experience and Industry Practices* (No. U072) (pp. 1–109). American Council for an Energu-Efficient Economy.

Zahedi, A. (2011). Maximizing solar PV energy penetration using energy storage technology. *Renewable and Sustainable Energy Reviews*, *15*(1), 866–870. doi:10.1016/j.rser.2010.09.011

Zhi, B. J. (2011). Green Manufacturing is the only Way to the Sustainable Development. *Advanced Materials Research*, *230-232*, 1332–1334. doi:10.4028/www.scientific.net/AMR.230-232.1332

Zhou, K. (2011). Study on design and implementation of manufacturing process optimization system based on energy consumption. In *2011 3rd International Conference on Advanced Computer Control (ICACC)* (pp. 316 –319). doi:10.1109/ICACC.2011.6016422

APPENDICES

Appendix A: Statement of Work

This research focused on investigating practical applications of microgrids for manufacturing energy efficiency. Table A1 summarizes the six major tasks that guided the research on a monthly basis, starting May 1, 2013 until May 31, 2014. Most tasks were completed in a four-month period except for Task 3 (Data Collection & Analysis), which was not be completed until May of 2014.

Table A1. Time Action Plan

Timeline	2013							2014					
Task Month:	M	J	J	A	S	O	N	D	J	F	M	A	M
1. CTD Partnerships	X	X	X	X									
2. Microgrid Prototype		X	X	X	X	X							
3. Experimental Framework							X	X	X	X			
4. Data Collection & Analysis									X	X	X	X	X
5. Development of findings and conclusion												X	X
6. Reporting	X	X	X	X	X	X	X	X	X	X	X	X	X

Task 1. CTD Partnerships

The first step was to build a team of collaborators in industry and academia with a vested interest in this project. This required visits to various manufacturing facilities of the CTD membership to assess energy use, level of current energy technology, expertise of facilities personnel, and potential for future microgrid deployment.

Task 2. Microgrid Prototype

The second task was to develop a prototype microgrid in a laboratory setting that includes solar photovoltaic and facility-scale HVAC equipment. The solar photovoltaic component was grid-tied to Knoy Hall to allow the use of renewable energy for the process loads. The microgrid performance was monitored and controlled by a comprehensive web-based control platform that allowed for collection of data related to the production of electricity and for adjustment of energy use in response to variable weather or real time energy prices.

Task 3. Experimental Framework

Task 3 is to develop a formal hypothesis related to reduction of energy consumption and peak demand along with energy savings potential. A data collection plan was developed within AutomatedLogic building automation control platform. This task also required elucidation of experimental tasks to complete during data collection (Task 4).

Task 4. Data Collection & Analysis

The fourth task was to investigate how process loads could be operated and controlled to optimize energy efficiency in the context of the microgrid, including the relationship between solar energy generation and process demand, and how this relationship is used to determine optimal outputs to efficiency control a process. Task 4 involved establishing and testing DSM based control strategies based on their impact on building and process controls. Data collection will be used to develop a model that will be scaled-up from prototype to support implementation at manufacturer facilities.

Task 5. Development of Findings and Conclusion

In the month of April and May, all data was compiled and consolidated. Statistical analysis tests were conducted for more accurate results. Data and findings was accurately be conveyed in written form to assist with future phases of the project.

Task 6. Reporting

This task includes several phases of project documentation. The first phase entails comprehensive documentation of all the hardware and controls installed in the Applied Energy Laboratory. Particular emphasis will be given to innovative control strategies and optimization routines that may become intellectual property. The second phase includes monthly and quarterly progress reports to the Center for Technology Development. The third phase involved the development and defense of a thesis in partial fulfillment of the requirements for a Master's of Science degree. The final phase included one or more technical papers submitted to appropriate conferences and/or journals for presentation and publication opportunities, respectively.

Appendix B: Schematics of Grid-Tie System

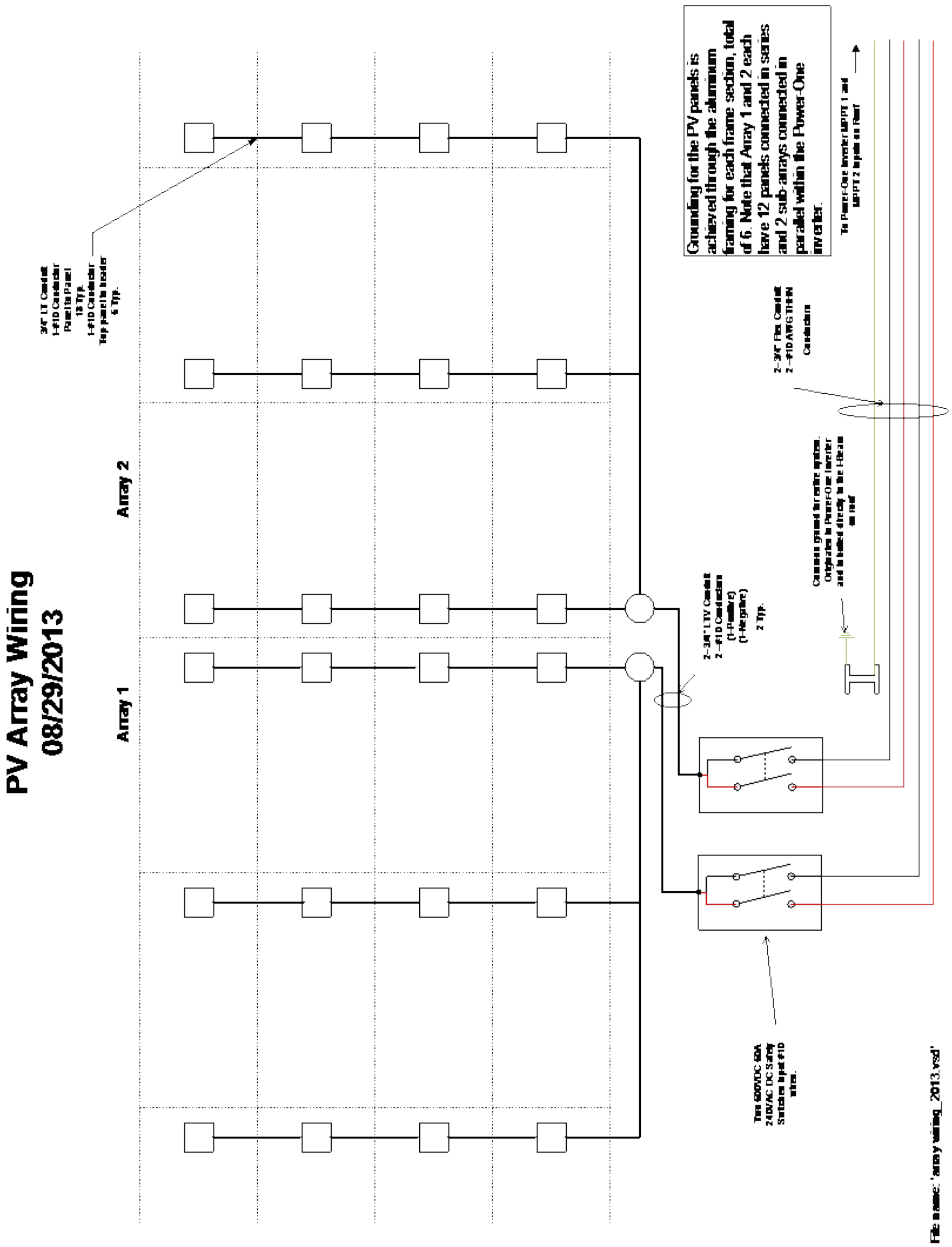

Figure B.1 PV Array Wiring Diagram

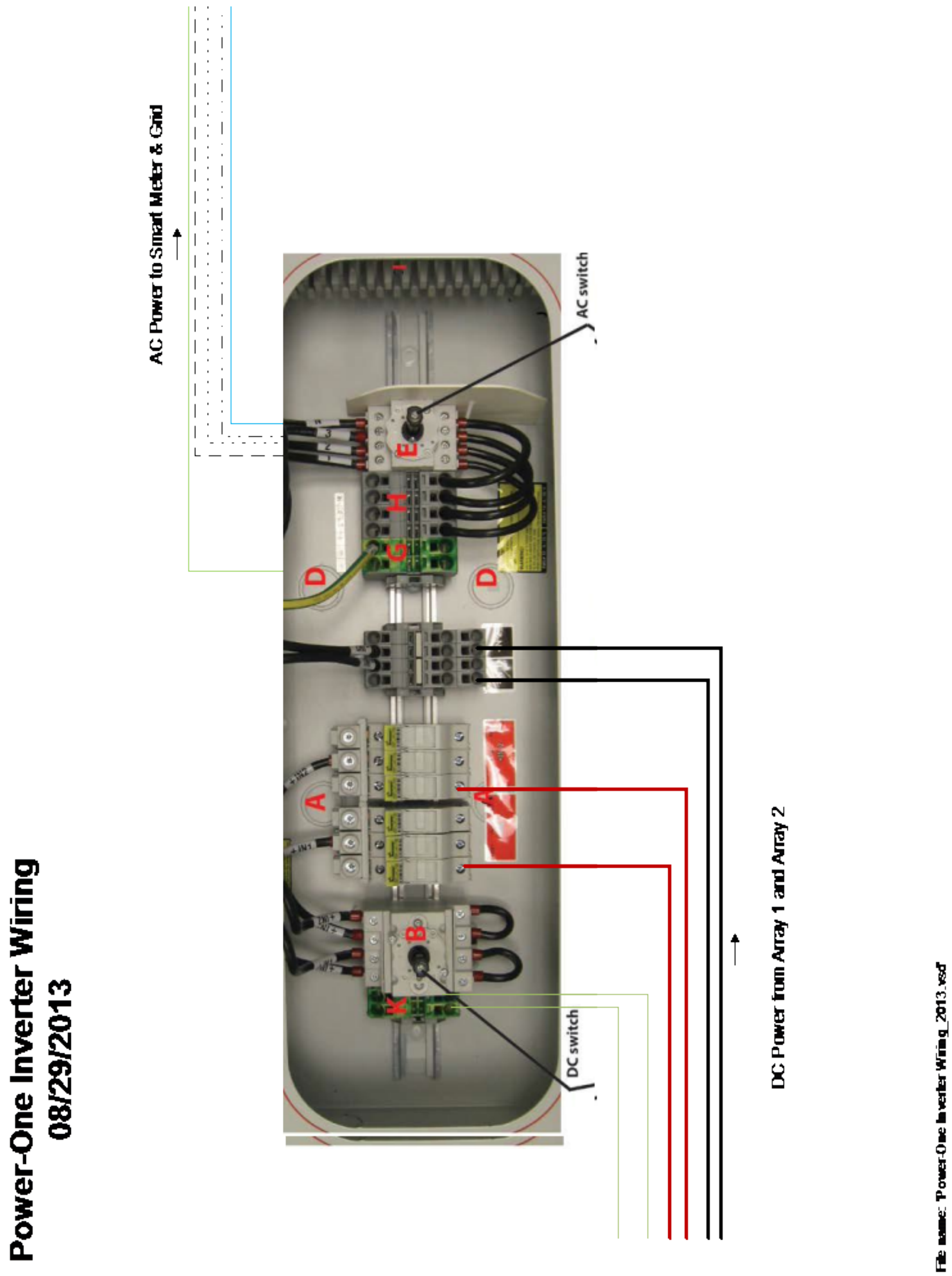

Figure B.2 Schematic of Power-One Inverter Wiring

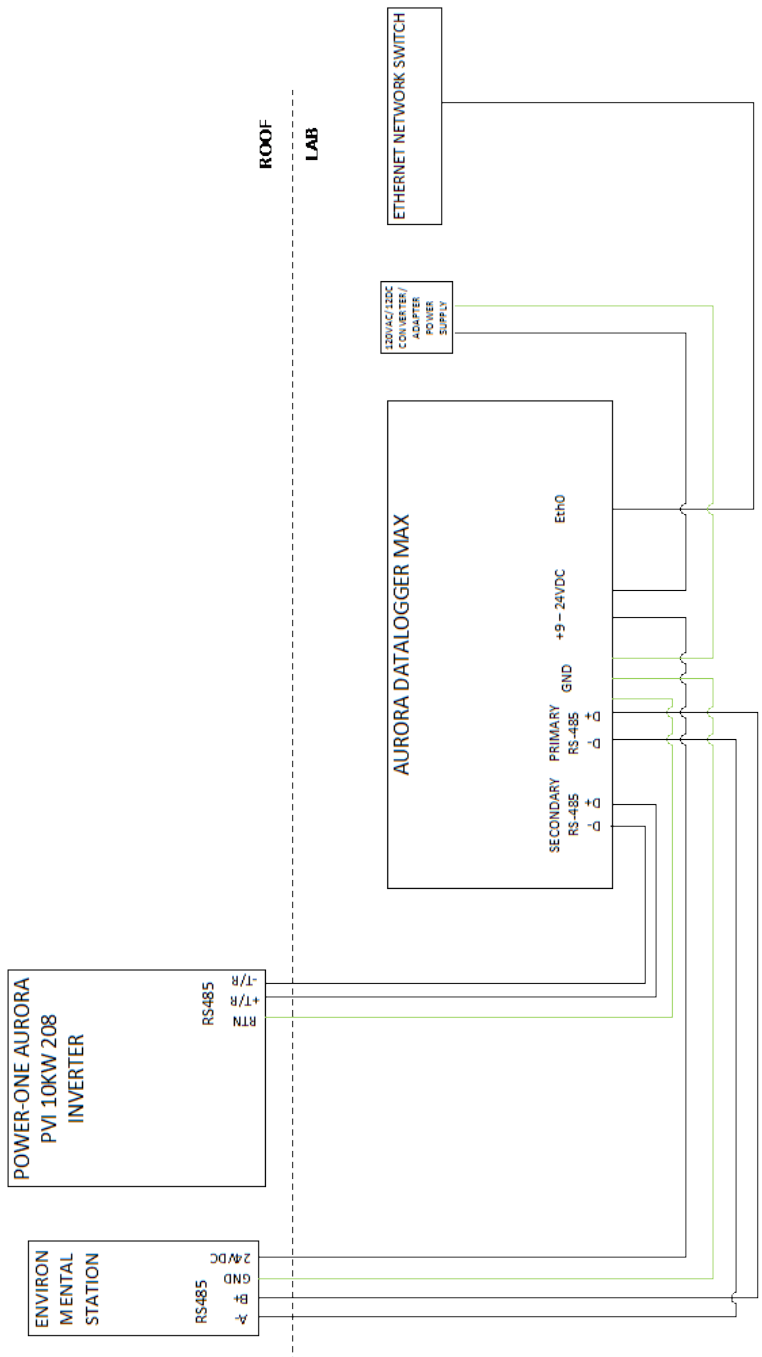

Figure B.3 Wiring Schematic for Data Acquisition

Appendix C: Equipment List

Figure C.4 3 kW Solar PV Array

KYOCERA

MODEL KC120-1

KC120-1

HIGH EFFICIENCY MULTICRYSTAL PHOTOVOLTAIC MODULE

TYPICAL OUTPUT 120 Wp

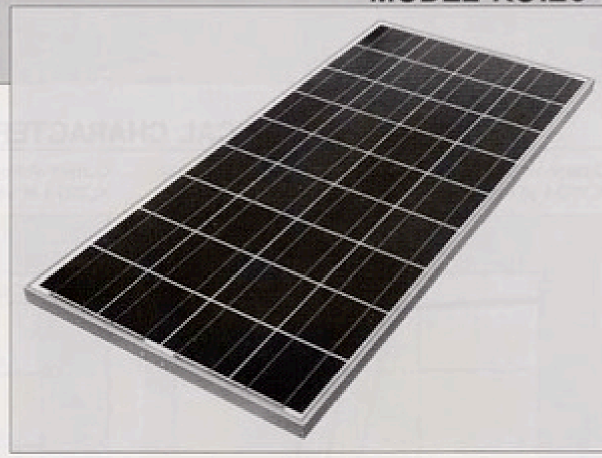

HIGHLIGHTS OF KYOCERA PHOTOVOLTAIC MODULES

Kyocera's advanced cell processing technology and automated production facilities have produced a highly efficient multicrystal photovoltaic modules.
The conversion efficiency of the Kyocera solar cell is over 14%.
These cells are encapsulated between a tempered glass cover and an EVA pottant with PVF back sheet to provide maximum protection from the severest environmental conditions.
The entire laminate is installed in an anodized aluminum frame to provide structural strength and ease of installation.

APPLICATIONS

- Microwave/Radio repeater stations
- Electrification of villages in remote areas
- Medical facilities in rural areas
- Power source for summer vacation homes
- Emergency communication systems
- Water quality and environmental data monitoring systems
- Navigation lighthouses, and ocean buoys
- Pumping systems for irrigation, rural water supplies and livestock watering
- Aviation obstruction lights
- Cathodic protection systems
- Desalination systems
- Recreational vehicles
- Railroad signals
- Sailboat charging systems

SPECIFICATIONS

■ Electrical Specifications

MODEL	KC120-1
Maximum Power	120 Watts
Maximum Power Voltage	16.9 Volts
Maximum Power Current	7.10 Amps
Open Circuit Voltage	21.5 Volts
Short-Circuit Current	7.45 Amps
Length	1425mm (56.1in.)
Width	652mm (25.7in.)
Depth	56mm (2.2in.)
Weight	11.9kg (26.3lbs.)

Note: The electrical specifications are under test conditions of Irradiance of $1kW/m^2$, Spectrum of 1.5 air mass and cell temperature of 25°C

Kyocera reserves the right to modify these specifications without notice.

■ Physical Specifications

(Unit: mm)

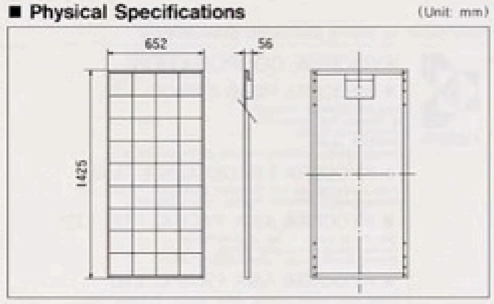

Figure C.5 Kyocera KC120-1 Solar Panel Spec Sheet (http://www.kyocerasolar.com/assets/001/5180.pdf)

Figure C.6 Dual Siemens Heavy Duty 600VDC 60A Non-Fused DC Disconnects

Figure C.7 Power-One PVI-10.0-I-OUTD-US 208V Inverter

TECHNICAL DATA	VALUES	PVI-10.0-I-OUTD-US		PVI-10.0-I-OUTD-CAN		
Nominal Output Power	W	10000	10000	10000	10000	10000
Maximum Output Power	W	11000**	11000**	10000***	10000***	10000***
Rated Grid AC Voltage	V	208	480	208	480	600
Input Side (DC)						
Number of Independent MPPT Channels		2; programmable as a single paralleled input		2; programmable as a single paralleled input		
Maximum Usable Power for Each Channel	W	6800		6800		
Absolute Maximum Voltage (Vmax)	V	520		520		
Start- Up Voltage (Vstart)	V	200 (Adj. 120-350)		200 (Adj. 120-350)		
Full Power MPPT Voltage Range	V	220-470		220-470		
Operating MPPT Voltage Range	V	0.7 x Vstart-520		0.7 x Vstart-520		
Maximum Current (Idcmax) for both MPPT in Parallel	A	48		48		
Maximum Usable Current per Channel	A	24		24		
Maximum Short Circuit Current Limit per Channel	A	29		29		
Number of Wire Landing Terminals per Channel		Standard version: 2; -S1/-S2 version: 3		Standard version: 2; -S1/-S2 version: 3		
Array Wiring Termination Type		Terminal Block, Pressure Clamp, 20AWG-6AWG		Terminal Block, Pressure Clamp, 20AWG-6AWG		
Output Side (AC)						
Grid Connection Type		3Ø/3W or 4W+Ground	3Ø/4W+Ground	3Ø/3W or 4W+Ground	3Ø/4W+Ground	3Ø/3W or 4W+Ground
Adjustable Voltage Range (Vmin-Vmax)	V	183-228	422-528	183-228	422-528	528-660
Grid Frequency	Hz	60		60		
Adjustable Grid Frequency Range	Hz	57-63		57-63		
Maximum Current (Iac max)	A_{RMS}	30.0	14.0	30.0	14.0	10.6
Power Factor		>0.995 (+/-0.9)		>0.995 (+/-0.9)		
Total Harmonic Distortion At Rated Power	%	<2		<2		
Grid Wiring Termination Type		Terminal Block, Pressure Clamp,12AWG-4AWG		Terminal Block, Pressure Clamp, 12AWG-4AWG		
Protection Devices						
Input						
Reverse Polarity Protection		Yes		Yes		
Over-Voltage Protection Type		Varistor, 2 for each channel		Varistor, 2 for each channel		
PV Array Ground Fault Detection		GFDI (GFD fuse) per UL1741/NEC690.5 (A)		GFDI (GFD fuse) per UL1741/NEC690.5 (A)		
Output						
Anti-Islanding Protection		Meets UL1741/IEEE1547 requirements		Meets UL1741/IEEE1547 requirements		
Over-Voltage Protection Type		3 + gas arrester Varistor, One per line + spark gap to Ground		3 + gas arrester Varistor, One per line + spark gap to Ground		
Efficiency						
Maximum Efficiency	%	96.5	97.3	96.5	97.3	97.3
CEC Efficiency	%	96.0	97.0	96.0	97.0	97.0
Operating Parameters						
Feed-In Power Threshold	WRMS	30		30		
Stand-by Consumption	WRMS	< 8		< 8		
Communication						
User-Interface (Display)		16 Characters X 2 lines LCD display		16 Characters X 2 lines LCD display		
Remote Monitoring (1xRS485 incl.)		AURORA-UNIVERSAL (opt.)		AURORA-UNIVERSAL (opt.)		
Wired Local Monitoring (1xRS485 incl.)		PVI-USB-RS485_232 (opt.), PVI-DESKTOP (opt.)		PVI-USB-RS485_232 (opt.), PVI-DESKTOP (opt.)		
Wireless Local Monitoring		PVI-DESKTOP (opt), with PVI-RADIO MODULE (opt)		PVI-DESKTOP (opt), with PVI-RADIO MODULE (opt)		
Environmental						
Ambient Air Operating Temperature Range	F(°C)	-13 to +140 (-25 to +60) Derating above +122 (+50)		-13 to +140 (-25 to +60) Derating above +122 (+50)		-13 to +140 (-25 to +60) Derating above +113 (+45)
Ambient Air Storage Temperature Range	F(°C)	-40 to +176 (-40 to +80)		-40 to +176 (-40 to +80)		
Relative Humidity	%RH	0-100 condensing		0-100 condensing		
Acoustic Noise Emission Level	db (A) @1m	<50		<50		
Maximum Operating Altitude without Derating	ft(m)	6560 (2000)		6560 (2000)		
Mechanical Specifications						
Enclosure rating		NEMA 4X		NEMA 4X		
Cooling		Natural Convection		Natural Convection		
Dimensions (H x W x D)	in//mm	28.2″ x 25.4″ x 8.7″ / 716mm x 645mm x 222mm // 37.7″ x 25.4″ x 8.7″ / 958mm x 645mm x 222mm (-S/-S1/-S2 version)		28.2″ x 25.4″ x 8.7″ / 716mm x 645mm x 222mm // 37.7″ x 25.4″ x 8.7″ / 958mm x 645mm x 222mm (-S/-S1/-S2 version)		
Unit Weight	lb(kg)	101(45.8) (US version); 107(48.5) (S1 version); 114(51.7)(S2 version)		101(45.8) (US version); 107(48.5) (S1 version); 114(51.7)(S2 version)		
Shipping Weight	lbs(kg)	with pallet: 254(<115); without pallet: 143(<65)		with pallet: 254 (<115); without pallet: m143 lb(<65)		
Conduit Connections		Bottom: (1) 1/2″ EKO,(2) 1″ pluggable opening, (4) 1/2″ pluggable openings / Left and Right Side: (1) Concentric EKOs 3/4″, 1″ Back: (2) Concentric EKOs 3/4″, 1″, (2) Concentric EKOs 3/4″, 1″		Bottom: (1) 1/2″ EKO,(2) 1″ pluggable opening, (4) 1/2″ pluggable openings / Left and Right Side: (1) Concentric EKOs 3/4″, 1″ Back: (2) Concentric EKOs 3/4″, 1″, (2) Concentric EKOs 3/4″, 1″		
Mounting System		Wall Brackett		Wall Brackett		
Ground Fault Detector Fuse Size/ Type	A/V / mm	1/600/10x38		1/600/10x38		
Optional String Combiner Fuse Size/Type	A, A/V / mm	12, 15/600/10x38		12, 15/600/10x38		
DC Switch Current Rating (Per Contact)	A	32		32		
Safety						
Isolation Level		Isolated - High Frequency transformer		Isolated - High Frequency transformer		
Safety and EMC Standard		UL1741, CSA22.2 #107.1-01		UL1741, CSA22.2 #107.1-01		
Safety Approval		$_{c}CSA_{us}$		$_{c}CSA_{us}$		
Warranty						
Standard Warranty	Years	10		10		
Extended Warranty	Years	15 & 20		15 & 20		
Available Models						
Standard		PVI-10.0-I-OUTD-US-208-NG	PVI-10.0-I-OUTD-US-480-NG	PVI-10.0-I-OUTD-CAN-208-NG	PVI-10.0-I-OUTD-CAN-480-NG	PVI-10.0-I-OUTD-CAN-480-NG
With DC Switch and DC Fuses		PVI-10.0-I-OUTD-S1-US-208-NG	PVI-10.0-I-OUTD-S1-US-480-NG	PVI-10.0-I-OUTD-S1-CAN-208-NG	PVI-10.0-I-OUTD-S1-CAN-480-NG	PVI-10.0-I-OUTD-S1-CAN-480-NG
With AC and DC Switches and DC Fuses		PVI-10.0-I-OUTD-S2-US-208-NG	PVI-10.0-I-OUTD-S2-US-480-NG	PVI-10.0-I-OUTD-S2-CAN-208-NG	PVI-10.0-I-OUTD-S2-CAN-208-NG	PVI-10.0-I-OUTD-S2-CAN-208-NG

*All data is subject to change without notice

**Capability enabled at power-factor of +/-.995 and with sufficient DC power available.

***Inverter can be field configured to output up to 110% of rated power under certain conditions

AURORA TRIO 3

Figure C.8 Technical Spec Sheet for Power-One Inverter

(http://www.abb.com/solarinverters)

Figure C.9 Landis+Gyr E330 FOCUS AX Polyphase Smart Meter

Figure C.10 Eaton 250VAC 60A Fused AC Disconnect

Figure C.11 Power-One Aurora DataLogger Max

PARAMETER	AURORA LOGGER
Communication Interfaces	
Serial Port Interface	(2) RS-485 + (2) RS-232
Maximum Devices per Serial Port	Physical limitation of 32 (reduced by poll rate, inverter data set size, and logger type)
Fieldbus Cable	RS-485 Shielded twisted pair. Recommend Belden # 1120A cable or # 3106A for 3 conductors
Ethernet Port 0	Firewall protected Ethernet WAN port for internet connection
Ethernet Port 1	Local LAN with static IP address
Ethernet Connections	RJ-45 Ethernet 10/100 base-T (LAN/WAN)
Communication Protocols	
Plant Fieldbus Protocols	Aurora, Modbus RTU, SunSpec
LAN/WAN Protocols	HTTP, DHCP, SSL, SSH, XML
Data Logging Specif cations	
Data Sampling Rate	High frequency data sampling - 1 minute average
Local Storage	Log data for 30 days based on 15-minute intervals. (Days logged reduced by intervals shorter than 15-minute)
Upgradeability	Field upgradable over the Internet or locally via USB memory stick
Power Supply	
DC Power Supply Input	100 - 240 VAC
DC Power Supply Output	12VDC, 1A
Environmental Parameters	
Ambient Temperature Range	0ºC to 40ºC
Environmental Protection Rating	IP20
Relative Humidity	<85% Non-condensing
Mechanical Parameters (per unit)	
Dimensions H x W x D	1" x 5.5" x 5.25" (.03m x .14m x .13m)
Weight	2 lbs (0.91kg)
Mounting System	Screws through f anges
Compliance	
Emission	FCC Part 15 Class B, CISPR 22, EN 55022 Conducted and Radiated Emission
Immunity	EN55024

LOGGER MODEL COMPARISON

	RESIDENTIAL (VSN-MGR-RES-P1-XX)	COMMERCIAL (VSN-MGR-CMML-P1-XX)	MAX (VSN-MGR-MAX-XX)
Logging Real Time Power Values	15-minute intervals only	1 to 7 minute conf gurable intervals	1 to 7 minute conf gurable intervals
Modbus/TCP Server	No	No	YES
Inverter Control Commands	No	No	YES
Devices Supported	5 Power-One	10 Power-One	All Power-One devices
	Single phase (only) string inverters	String inverters	3rd party meters (Consult latest supported list)
		1 Weather station	

ACCESSORIES		
VSN-MGR-DIN	Din Rail Kit to mount logger on a din rail	
VSN-ENVIRO-ENTRY	Weather station with sensor: ambient, panel, global irradiance	
VSN-ENVIRO-CMML	Weather station with sensor: ambient, panel, global irradiance, plane of array irradiance, wind speed & direction	

Figure C.12 Technical Spec Sheet for Aurora DataLogger Max (http://www.abb.com/solarinverters)

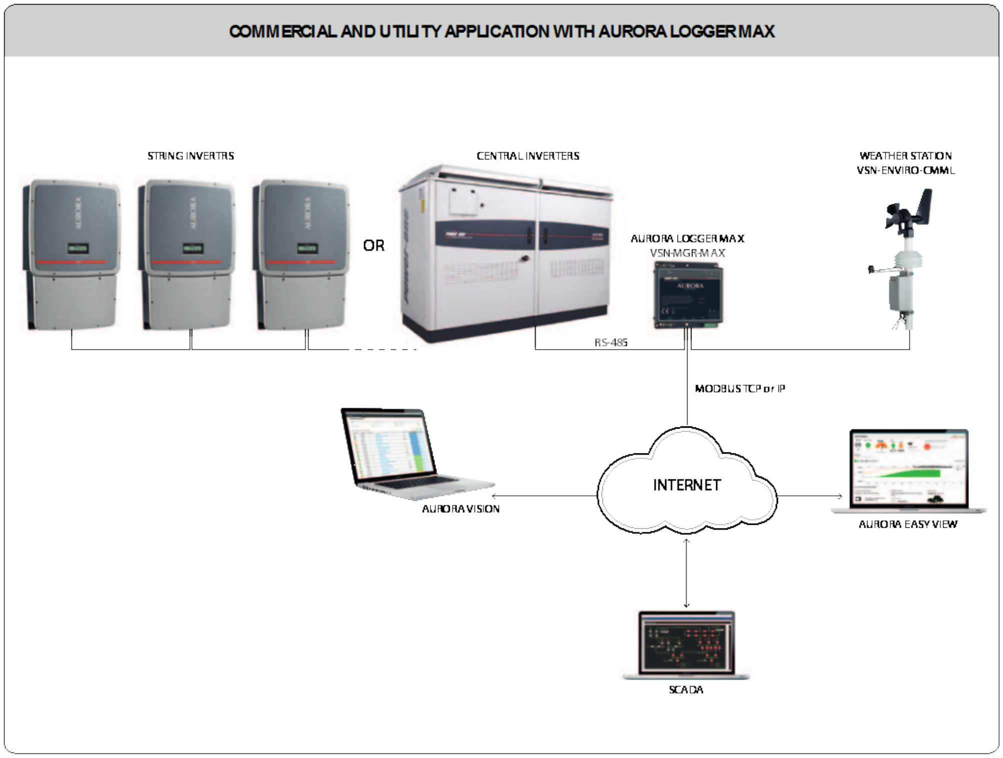

Block Diagram

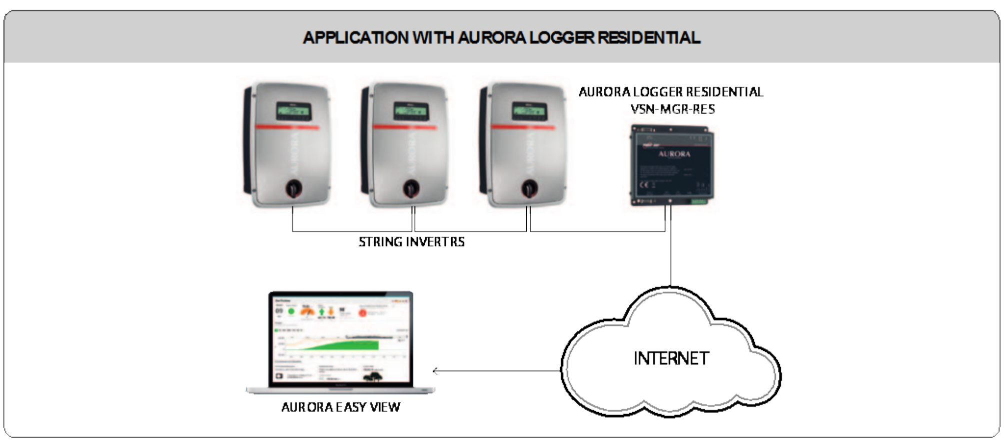

2 AURORA VISION

Figure C.13 Block Diagram of Data Acquisition with Aurora DataLogger Max (http://www.abb.com/solarinverters)

Figure C.14 Wiring Installation for Power-One Inverter

Figure C.15 Wiring Installation into DC Disconnects from Sub-Arrays

Figure C.16 Electrical Panel in Utility Room on Fourth Floor of Knoy Hall

Figure C.17 Interconnection into the Electrical Panel

Appendix D: Demand-Side Management Sequence of Operations

Process Demand Time Activation:

This computation creates a time designation to determine the hourly scaling for subsequent logic.

- The time activation shall be programmed to allow for hourly activation between 8:00am and 8:00pm to be used for analysis in subsequent logic.

- Each activated time shall allow for scaling (6 hour scale, 8 hour scale, 10 hour scale) of expected hourly demand based from historical production usage.

Process Demand Hourly Expected kWh for Scaling Conversion:

This computation simplifies the expected demand scale of each hour to one usable output to be used for calculating demand ratios in subsequent logic.

- 12 inputs (8:00am – 7:00pm) will be used to compute historic demand at 1 hour increments

Solar and Process Demand Ratio Parameters:

This logic will determine the ratio of actual output and expected output from the solar and process demand. The process demand ratio will utilize use the hourly expected kWh demand conversion to calculate its ratio.

- Two parameter ratios shall be written for use in the demand side management algorithm:
  - Solar:
    - Find the ratio between solar generation (kWh) and historical expected generation output (kWh).
    - Convert to percentage.
    - Trend this logic.
  - Process Demand
    - Find the ratio between process demand (kWh) and historical demand usage (kWh).
      - Historical demand shall be the product of previous demand and demand conversion.

        - Convert to percentage.
        - Trend this logic.

Demand Side Management (DSM) Calculation Algorithm:

This logic will determine the ideal operating conditions contingent on solar and demand ratios. Five control strategies will be determined; Normal Operations with Storage, Normal Operations, Curtailment Scheme 1, Curtailment Scheme 2, and No Microgrid Normal Operation.

- The DSM calculation shall be enabled to decide once every 1 hour between the time 9:00am and 5:00pm, 1 of 5 control strategies.

- The optimal demand side management control strategy will be determined based on microgrid and demand ratio parameters.

Demand Side Management Control Algorithm

This logic will control specific processes operation contingent upon the DSM calculation.

- Specific processes will be controlled based on Normal operation with Storage, Normal Operations, Curtailment Scheme 1, Curtailment Scheme 2, and No Microgrid Normal Operation from the DSM calculation.

    - Thermal storage shall be programmed based on user specified temperatures.
    - Curtailment or load shedding schemes shall be programmed based on user definable curtailment or load shedding strategies.

Energy Consumption

This logic will calculate the overall energy consumption based on the demand side management control algorithms.

- This logic shall determine the new energy consumption based from microgrid generation and process usage.

- Trend this logic.

Appendix E: Pseudocode Demand-Side Management Decision

```
Title DSM Decision

AInput Micro
AInput Demand
AOutput DSM

//Default Start = 0
//Normal Operation plus Storage = 1
//Normal Operation = 2
//Pump D Off = 3
//Pump C and D Off = 4
//Pump B, C, and D Off = 5
//No Microgrid = 6

Every 1 H Do

    Begin
//Default Start

    If BETWEEN (Demand,0,25) then DSM = 0

//Extreme Manufacturing Production

    If BETWEEN (Micro, 150,175) and BETWEEN (Demand,175,300) then DSM = 2
    If BETWEEN (Micro, 125,150) and BETWEEN (Demand,175,300) then DSM = 3
    If BETWEEN (Micro, 100,125) and BETWEEN (Demand,175,300) then DSM = 4
    If BETWEEN (Micro, 75,100) and BETWEEN (Demand,175,300) then DSM = 5
    If BETWEEN (Micro, 50,75) and BETWEEN (Demand,175,300) then DSM = 6

//High Manufacturing Production

    If BETWEEN (Micro, 125,150) and BETWEEN (Demand,125,174.9) then DSM = 2
    If BETWEEN (Micro, 100,125) and BETWEEN (Demand,125,174.9) then DSM = 3
    If BETWEEN (Micro, 75,100) and BETWEEN (Demand,125,174.9) then DSM = 4
    If BETWEEN (Micro, 50,75) and BETWEEN (Demand,125,174.9) then DSM = 5
    If BETWEEN (Micro, 0,50) and BETWEEN (Demand,125,174.9) then DSM = 6

//Normal Manufacturing Production

    If BETWEEN (Micro, 125,150) and BETWEEN (Demand,75,124.9) then DSM = 1
    If BETWEEN (Micro, 100,125) and BETWEEN (Demand,75,124.9) then DSM = 2
    If BETWEEN (Micro, 75,100) and BETWEEN (Demand,75,124.9) then DSM = 3
    If BETWEEN (Micro, 50,75) and BETWEEN (Demand,75,124.9) then DSM = 4
```

```
    If BETWEEN (Micro, 0,50) and BETWEEN (Demand,75,124.9) then DSM = 5
//Light Manufacturing Production

    If BETWEEN (Micro, 125,150) and BETWEEN (Demand,25,74.9) then DSM = 1
    If BETWEEN (Micro, 100,125) and BETWEEN (Demand,25,74.9) then DSM = 1
    If BETWEEN (Micro, 75,100) and BETWEEN (Demand,25,74.9) then DSM = 2
    If BETWEEN (Micro, 50,75) and BETWEEN (Demand,25,74.9) then DSM = 3
    If BETWEEN (Micro, 0,50) and BETWEEN (Demand,25,74.9) then DSM = 4
    End

ExitProg
```

Appendix F: Pseudocode Demand-Side Management Control

```
Title DSM Control

AInput DSM
DOutput PumpA, PumpB,  PumpC,  PumpD
DOutput Chill

//Normal Operation plus Storage = 1
//Normal Operation = 2
//Load Shed One Pump = 3
//Load Shed Two Pumps = 4
//Load Shed Three Pump = 5
//Normal Operation No Microgrid = 6

If (dsm=0) then

    Begin
    Start (pumpa,pumpb,pumpc,pumpd)
    End

If (dsm=1) then

    Begin
    Start (pumpa,pumpb,pumpc,pumpd)
    Start (Chill)
    End

If (dsm = 2) then

    Begin
    Start (pumpa, pumpb, pumpc, pumpd)
    Stop (Chill)
    End

If (dsm= 3) then

   Begin
   Start (pumpa, pumpb,pumpc)
   Stop (Chill, pumpd)
   End

If (dsm= 4) then
```

```
    Begin
    Start (pumpa, pumpb)
    Stop (Chill, pumpc, pumpd)
    End
If (dsm= 5) then

    Begin
    Start (pumpa)
    Stop (Chill, pumpb, pumpc, pumpd)
    End

If (dsm= 6) then

    Begin

    Start (pumpa,pumpb,pumpc,pumpd)
    Stop (Chill)
    End

ExitProg
```

Appendix G: Monitoring Interface

Figures H.23 to H.26 present the monitoring interfaces used to monitor and manage the Solar PV Output, Process Demand, and Historical Data. Figure F.1 was used solely to allow visitors of the AEL the opportunity to track the performance of the 3 kW solar energy system at Purdue University.

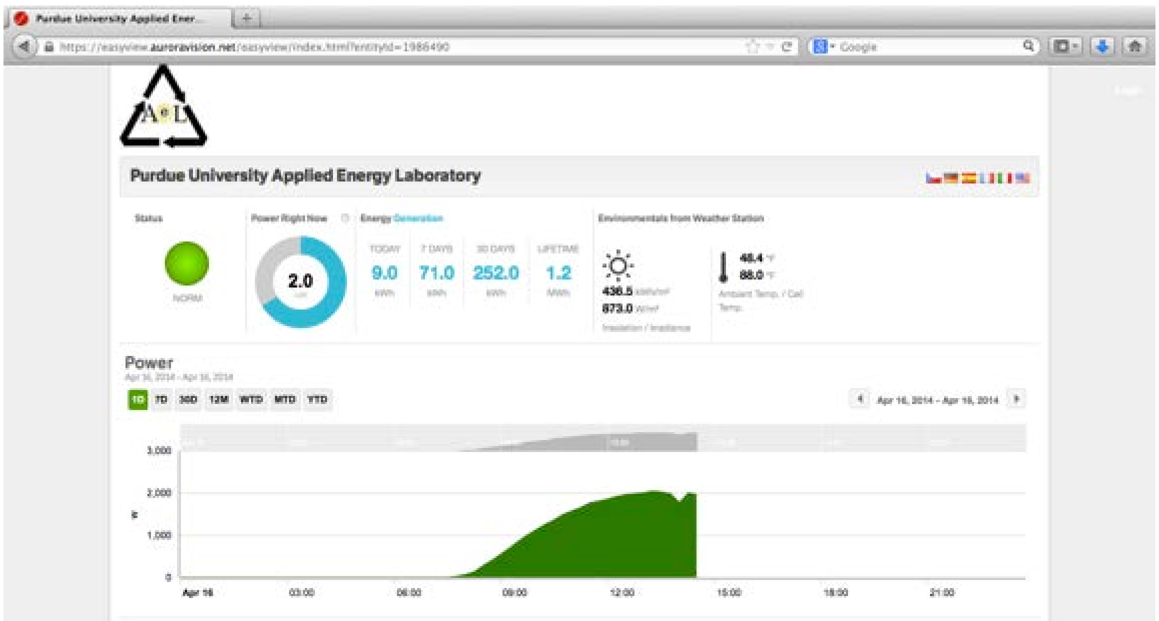

Figure H.18 Web-Based Monitoring of Solar PV Output in Power-One Management Dashboard

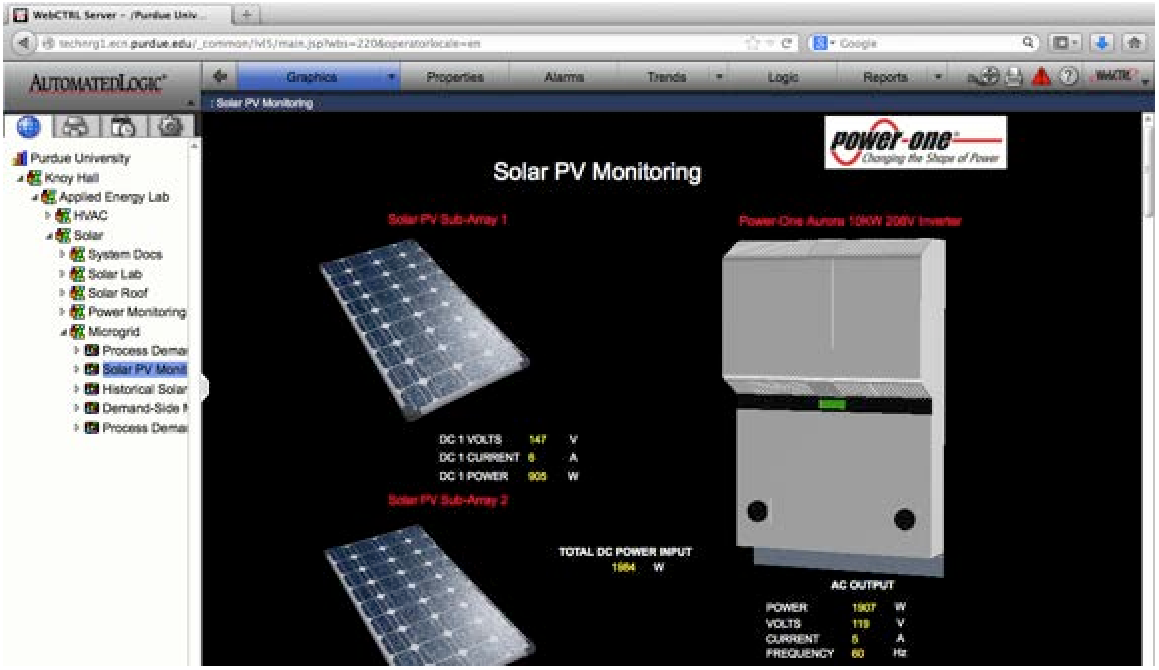

Figure H.19 Web-Based Monitoring of Solar PV Output within AutomatedLogic WebCTRL

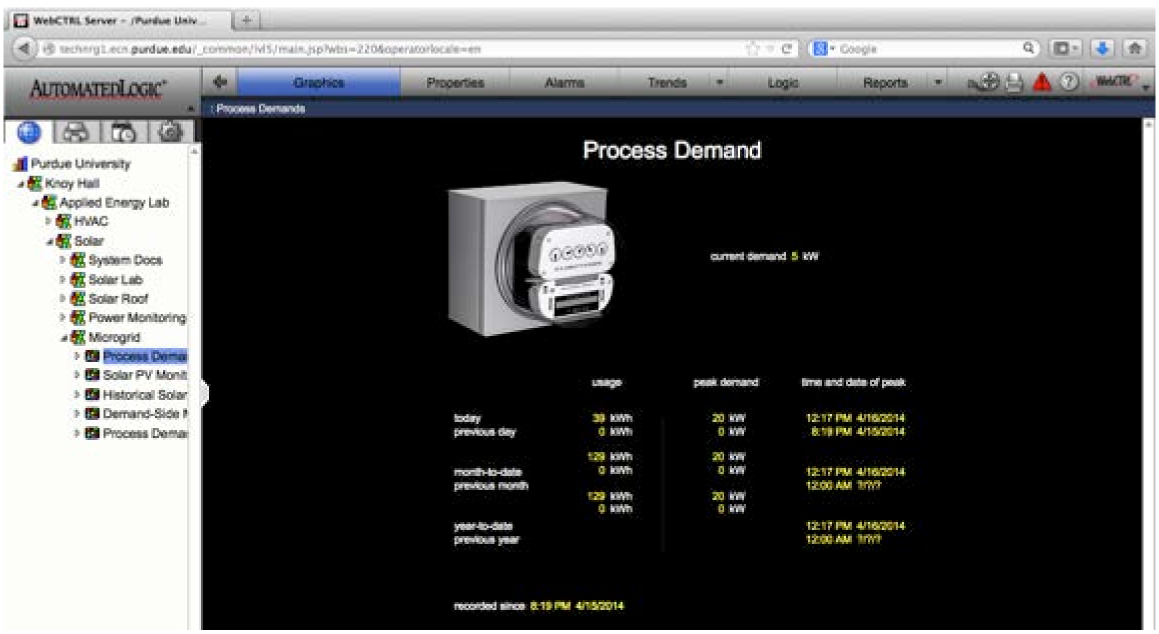

Figure H.20 Monitoring Interface for Process Demand within AutomatedLogic WebCTRL

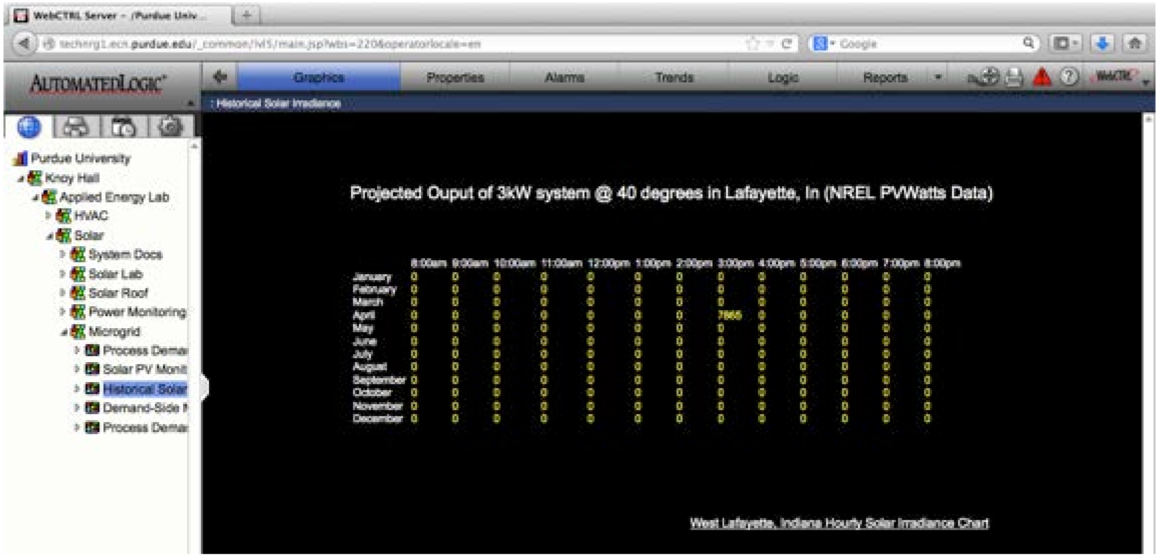

Figure H.21 Monitoring Interface of Historical Solar Data from NREL within AutomatedLogic WebCTRL

Appendix H: Compiled Raw Data

Table I.1 Compiled Raw Data

Date	Irradiance Levels	Consumption w/ DSM (kWh)	Consumption w/ Microgrid and DSM (kWh)	Solar Generation (kWh)
Baseline	*Any*	*66*	*0*	*N/A*
Solar Generation	*March Expected*	*N/A*	*N/A*	*9.7*
Solar Generation	*April Expected*	*N/A*	*N/A*	9.5
Solar Generation	*May Expected*	*N/A*	*N/A*	9
3/11/2014	**Good Condition**	45	36	9
3/12/2014	**Good Condition**	56	50	6
3/13/2014	**Good Condition**	54	45	9
3/14/2014	**Excellent Condition**	55	45	10
3/15/2014	**Excellent Condition**	60	44	16
3/16/2014	**Test Day**	60	56	4
3/17/2014	**Excellent Condition**	44	34	10
3/18/2014	**Excellent Condition**	56	46	10
3/19/2014	**Poor Condition**	28	27	1
3/20/2014	**Good Condition**	33	24	9
3/21/2014	**Excellent Condition**	48	35	13
3/22/2014	**Poor Condition**	28	25	3
3/23/2014	**Good Condition**	61	53	8
3/24/2014	**Excellent Condition**	48	37	11
3/25/2014	**Good Condition**	45	37	8
3/26/2014	**Excellent Condition**	58	44	14
3/27/2014	**Test Day**	31	31	0
3/28/2014	**Test Day**	61	57	4
3/29/2014	**Poor Condition**	25	24	1
3/30/2014	**Excellent Condition**	65	51	14
3/31/2014	**Excellent Condition**	51	40	11
4/4/2014	**Poor Condition**	28	26	2
4/5/2014	**Excellent Condition**	56	43	13
4/6/2014	**Excellent Condition**	44	34	10
4/7/2014	**Poor Condition**	63	61	2
4/9/2014	**Excellent Condition**	58	46	12
4/11/2014	**Excellent Condition**	57	44	13
4/12/2014	**Excellent Condition**	56	44	12
4/13/2014	**Poor Condition**	30	26	4
4/14/2014	**Poor Condition**	28	26	2
4/15/2014	**Good Condition**	45	38	7

4/16/2014	**Excellent Condition**	53	40	13
4/17/2014	**Excellent Condition**	55	43	12
4/18/2014	**Excellent Condition**	57	46	11
4/19/2014	**Excellent Condition**	58	45	13
4/20/2014	**Excellent Condition**	59	48	11
4/22/2014	**Excellent Condition**	58	45	13
4/23/2014	**Excellent Condition**	59	46	13
4/24/2014	**Good Condition**	49	40	9
4/25/2014	**Excellent Condition**	40	29	11
4/26/2014	**Excellent Condition**	50	38	12
4/27/2014	**Excellent Condition**	51	41	10
4/29/2014	**Excellent Condition**	56	45	11
4/30/2014	**Poor Condition**	39	34	5
5/1/2014	**Poor Condition**	62	60	2
5/2/2014	**Poor Condition**	36	32	4
5/3/2014	**Excellent Condition**	52	40	12
5/4/2014	**Excellent Condition**	50	40	10
5/5/2014	**Excellent Condition**	53	43	10
5/6/2014	**Excellent Condition**	57	45	12
5/7/2014	**Excellent Condition**	57	46	11
5/8/2014	**Excellent Condition**	62	50	12
5/9/2014	**Good Condition**	48	41	7
5/10/2014	**Excellent Condition**	59	47	12
5/11/2014	**Excellent Condition**	54	43	11
5/12/2014	**Good Condition**	41	34	7
5/13/2014	**Poor Condition**	66	63	3
5/14/2014	**Poor Condition**	32	30	2
5/15/2014	**Poor Condition**	66	63	3

Appendix I: Electrical Consumption ANOVA Test Raw Data

Table J.2 Raw Data for SAS Input for Electrical Consumption ANOVA Test

Date	Baseline Consumption (kWh)	DSM Consumption (kWh)	Microgrid Consumption (kWh)
3/11/2014	66	45	36
3/12/2014	66	56	50
3/13/2014	66	54	45
3/14/2014	66	55	45
3/15/2014	66	60	44
3/16/2014	66	60	56
3/17/2014	66	44	34
3/18/2014	66	56	46
3/19/2014	66	28	27
3/20/2014	66	33	24
3/21/2014	66	48	35
3/22/2014	66	28	25
3/23/2014	66	61	53
3/24/2014	66	48	37
3/25/2014	66	45	37
3/26/2014	66	58	44
3/27/2014	66	31	31
3/28/2014	66	61	57
3/29/2014	66	25	24
3/30/2014	66	65	51
3/31/2014	66	51	40
4/4/2014	66	28	26
4/5/2014	66	56	43
4/6/2014	66	44	34
4/7/2014	66	63	61
4/9/2014	66	58	46
4/11/2014	66	57	44
4/12/2014	66	56	44
4/13/2014	66	30	26
4/14/2014	66	28	26
4/15/2014	66	45	38
4/16/2014	66	53	40
4/17/2014	66	55	43
4/18/2014	66	57	46

4/19/2014	66	58	45
4/20/2014	66	59	48
4/22/2014	66	58	45
4/23/2014	66	59	46
4/24/2014	66	49	40
4/25/2014	66	40	29
4/26/2014	66	50	38
4/27/2014	66	51	41
4/29/2014	66	56	45
4/30/2014	66	39	34
5/1/2014	66	62	60
5/2/2014	66	36	32
5/3/2014	66	52	40
5/4/2014	66	50	40
5/5/2014	66	53	43
5/6/2014	66	57	45
5/7/2014	66	57	46
5/8/2014	66	62	50
5/9/2014	66	48	41
5/10/2014	66	59	47
5/11/2014	66	54	43
5/12/2014	66	41	34
5/13/2014	66	66	63
5/14/2014	66	32	30
5/15/2014	66	66	63

Appendix J: Peak Demand ANOVA Test Raw Data

Table K.3 Raw Data for SAS Input for Peak Demand ANOVA Test

Date	Baseline Peak Demand	DSM Peak Demand	Microgrid w/DSM Peak Demand
4/15/2014	20.2	19.5	19.3
4/18/2014	20.2	19.7	18.2
4/22/2014	20.2	19.8	19.1
4/23/2014	20.2	20.1	18.3
4/24/2014	20.2	19.9	19.5
4/25/2014	20.2	19.5	18.0
4/26/2014	20.2	19.7	19.0
4/27/2014	20.2	19.6	19.2
4/28/2014	20.2	19.3	19.1
4/29/2014	20.2	20.0	19.4
4/30/2014	20.2	19.4	19.3
5/1/2014	20.2	20.0	20.0
5/2/2014	20.2	20.0	19.9
5/3/2014	20.2	19.5	18.8
5/4/2014	20.2	19.5	18.9
5/5/2014	20.2	19.7	19.2
5/6/2014	20.2	19.9	18.5
5/7/2014	20.2	19.5	18.7
5/8/2014	20.2	19.5	18.4
5/9/2014	20.2	19.5	18.4
5/10/2014	20.2	19.8	18.0
5/11/2014	20.2	19.6	18.9
5/12/2014	20.2	18.9	17.9
5/13/2014	20.2	19.9	19.4
5/14/2014	20.2	19.1	19.1
5/15/2014	20.2	19.7	19.5

Appendix K: MI vs. MO Regression Test Raw Data

Table L.4 Raw Data for SAS Input for Regression Test

Date	Manufacturing Intensity	Microgrid Output
3/11/2014	68%	93%
3/12/2014	85%	62%
3/13/2014	82%	93%
3/14/2014	83%	103%
3/15/2014	91%	165%
3/16/2014	91%	85%
3/17/2014	67%	103%
3/18/2014	85%	103%
3/19/2014	42%	10%
3/20/2014	50%	93%
3/21/2014	73%	134%
3/22/2014	42%	31%
3/23/2014	92%	82%
3/24/2014	73%	113%
3/25/2014	68%	82%
3/26/2014	88%	144%
3/27/2014	47%	47%
3/28/2014	92%	86%
3/29/2014	38%	10%
3/30/2014	98%	144%
3/31/2014	77%	113%
4/4/2014	42%	21%
4/5/2014	85%	137%
4/6/2014	67%	105%
4/7/2014	95%	21%
4/9/2014	88%	126%
4/11/2014	86%	137%
4/12/2014	85%	126%
4/13/2014	45%	42%
4/14/2014	42%	21%
4/15/2014	68%	74%
4/16/2014	80%	137%
4/17/2014	83%	126%
4/18/2014	86%	116%
4/19/2014	88%	137%

4/20/2014	89%	116%
4/22/2014	88%	137%
4/23/2014	89%	137%
4/24/2014	74%	95%
4/25/2014	61%	116%
4/26/2014	76%	126%
4/27/2014	77%	105%
4/29/2014	85%	116%
4/30/2014	59%	53%
5/1/2014	94%	22%
5/2/2014	55%	44%
5/3/2014	79%	133%
5/4/2014	76%	111%
5/5/2014	80%	111%
5/6/2014	86%	133%
5/7/2014	86%	122%
5/8/2014	94%	133%
5/9/2014	73%	78%
5/10/2014	89%	133%
5/11/2014	82%	122%
5/12/2014	62%	78%
5/14/2014	48%	22%

PUBLICATIONS

1. Harper, Terance, Hutzel, William, Foreman, Christopher, Adams, Aaron, and Kulatunga, Athula, (2014), Microgrids for improving manufacturing energy efficiency, Proceedings of the 3rd International High Performance Buildings Conference at Purdue, West Lafayette, IN, July 14-17,10 p.
2. Harper, Terance, Hutzel, William, Foreman, Christopher, Adams, Aaron, and Kulatunga, Athula, (2014), A Novel Microgrid Demined-Side Management System for Manufacturing Faculties, *Proceedings of the Great Lakes Symposium on Smart Grid and the New Energy Economy, Chicago, IL*, September 22-25,10 p.